MECHANISMS OF ACTION FOR Ad5-TRAIL/CpG IMMUNOTHERAPY FOR THE TREATMENT OF ADVANCED RENAL CELL CARCINOMA

A Thesis
SUBMITTED TO THE FACULTY OF
UNIVERSITY OF MINNESOTA
BY

Britnie R. James

IN PARTIAL FULFILLMENT OF THE REQUIREMENTS
FOR THE DEGREE OF
DOCTOR OF PHILOSOPHY

Thomas S. Griffith

June 2014

Acknowledgements

I would first like to acknowledge my advisor, Dr. Thomas Griffith. He has taught me so much in my four years that I have worked with him. Most notably, he taught me how to be confident in my ideas and how to accurately and efficiently test those ideas. He has helped me develop into a competent scientist, critical thinker and writer. I also would like to thank my thesis committee: Dr. Christpher Pennell, Dr. Jaime Modiano, and Dr. Kaylee Shwertfeger for their continued support and scientific expertise. Additionally, I would like to thank Dr. Pennell for his guidance when I transferred to the University of Minnesota and for helping me integrate into the MICaB program. I must also thank Tammy Kucaba; I am confident that I would not have made it through without your continued encouragement and friendship. I also want to thank all of the people involved in both the Immunology Program at the University of Iowa and the MICaB program at the University of Minnesota for all of their support and guidance during my graduate career.

Dedication

This thesis is dedicated to my friends, family and husband, for all of your unconditional love and support. You have all, in your own ways, helped me get to where I am today and for that I am eternally grateful!

Abstract

Renal cell carcinoma (RCC) affects ~65,000 people in the U.S. annually. About 30% of RCC patients have multiple metastases at diagnosis, and an equal percentage will develop metastatic tumor recurrence after nephrectomy. Metastatic RCC is incurable, with a median survival time of only 18 months. Immune-based therapy for RCC provides the potential for long-lived protection against reoccurrence. However, even the most successful immunotherapy-based clinical trials only show objective response rates in <50% of the patients. Many factors may account for this limited clinical success, including pre-clinical use of young, normal weight ("lean") animals lacking immunomodulatory co-morbidities present in many cancer patients. Obesity is one of the main risk factors and co-morbidities for RCC. The reasons for this are likely complex and multifactorial, but generalized immune suppression during obesity may contribute to these findings. Due to the negative effects of obesity on the immune system, studies are needed to provide a framework from which novel immunotherapies can be developed for patients with metastatic RCC that is complicated by such co-morbidities.

In a subcutaneous RCC model we have demonstrated that Ad5-TRAIL/CpG immunotherapy could eradicate local tumors. However, the mechanisms by which this therapy worked in a metastatic model and the negative effects obesity may exert were not known. Using a model of metastatic RCC we found that lean mice required CD8αDC and pDC to mount an antitumor $CD8^+$ T cell response capable of clearing tumors, following Ad5-TRAIL/CpG treatment. Mice complicated with diet-induced obesity (DIO) presented with immune dysregulations in both the DC and $CD8^+$ T cell compartments. Additionally, Ad5-TRAIL/CpG therapy modulated the immunosuppressive MDSC population in lean mice, but not in DIO mice. These data correlated with the inability of DIO mice to respond to Ad5-TRAIL/CpG therapy and they ultimately succumbed to tumor burden. The research presented here highlights the immunosuppression evident in the obese environment and demonstrate the importance of examining co-morbidities, such as obesity, in pre-clinical studies for novel therapies.

Table of Contents

List of Figures

.

Chapter 1: General Introduction

Renal Cell Carcinoma and Current Therapies

Renal cell carcinoma (RCC) affects nearly 65,000 people in the U.S. annually, and is considered the third most common urogenital cancer worldwide. Localized, early stage RCC carries a fairly high 5-year survival rate of 91% of greater. However, a sizeable percentage of patients (about 33%) present with metastatic disease at the time of diagnosis and unfortunately a third of the patients who undergo a nephrectomy will eventually develop metastases. Metastatic RCC patients have a median survival of 7-11 months, and a 5-year survival rate of less than 10%; the poor survival is mainly attributed to the resistance to chemotherapy and radiotherapy in these patients[1].

Surgical resection of the tumor-bearing kidney and operable metastatic lesions can be beneficial to patients with locally metastatic RCC. However, patients with multiple, systemic metastatic sites usually do not benefit from nephrectomy, and require additional immunotherapy or small molecule inhibitor therapy. Though RCC evokes immune responses and can spontaneously regress in ~0.1% of patients with metastatic disease[2], the majority of patients need some sort of immune intervention. Two immunotherapies have shown efficacy for the treatment of advanced RCC treatment: interleukin (IL)-2 and interferon (IFN)-α[3]. The exact mechanisms by which these therapies work are not completely understood, but it is thought they both stimulate the endogenous immune response to attack the tumor[4-7]. IFN-α is also thought to have direct anti-proliferative effects on tumor cells and anti-angiogenic effects on the tumor microenvironment[8]. Though these agents have shown some efficacy, the effects have been minimal. IFN-α has been shown to increase the median survival of advanced RCC patients 7 months, with a response rate of less than 20%[9]. IL-2 has demonstrated slightly higher survival benefits, reaching 13-17 months; however the high dose needed to achieve these results can be extremely toxic to the patient[10].

Small molecule inhibitors for advanced RCC have more recently demonstrated efficacy in extending survival. Sunitnib, a small multi-kinase inhibitor, was able to prolonged survival when compared to IFN by 6 months in a percentage of patients (31%)[11, 12]. Another multi-kinase inhibitor, Sorafenib, approved for the treatment of RCC, can extend progression-free survival by an additional 3 months, with a 10% response rate[13]. While the above therapies have shown significant increases in response rate and progression-free survival compared to placebos and controls, it is obvious that there is a need for improvement for novel immunotherapies for the treatment of advanced RCC.

Renca Mouse Model to Study RCC

Multiple mouse models of RCC exist, including transgenic mice models, syngeneic mouse models and human xenograft mouse models. Transgenic mouse models can be very useful in studying initiation and mutations implemented in initiation of tumors (i.e. transgenic model of cancer of the kidney, TRACK mouse model[14]), but they are not ideal for treatment studies. Tumor initiation and progression can vary animal to animal in transgenic models, making an assessment of therapy response variable. Human xenograft models are advantageous because they utilize human RCC cell lines[15, 16] (i.e. ACHN and 786-O); however, xenograft model studies are carried out in immunocompromised mice making them not a feasible option to study responses to immunotherapy. For these reasons we have chosen a syngeneic model using the murine renal cell carcinoma cell line, Renca, which originated from a spontaneously arising tumor in Balb/c mice[17, 18].

We have developed an orthotopic model of RCC, in which Renca cells are directly implanted into the kidneys of mice through the intact peritoneum[19]. These cells give rise to local tumors within the kidney and spontaneous metastases in the lungs, mimicking advanced RCC in humans. The primary tumors that arise from Renca implantation are histologically similar to human tumors, and have a predictable growth rate that is similar to the clinical disease[18]. Renca cells are relatively silent to the immune system, making them a prime candidate to study the immune response following therapy, as any response would be due to therapy and not the tumor itself[20]. In our lab we have generated an immunotherapy for the treatment of murine RCC that includes an

adenovirus encoding the cDNA for TNF-related apoptotsis inducing ligand (TRAIL) and CpG-containing oligodinucleotides (CpG)[19, 20].

TNF-Related Apoptosis Inducing Ligand (TRAIL)

TRAIL as an anticancer therapy

Prior to the discovery of TRAIL, two other members of the TNF family - TNF and the closely related Fas Ligand (FasL) - had been identified to be potent inducers of tumor cell death. Unfortunately, significant toxicity (i.e. induction of normal cell/tissue death) was observed after systemic administration of TNF and FasL (or anti-Fas mAb). Later, TRAIL was identified and characterized as a Type II transmembrane protein that can be released as a soluble form following cleavage of the C-terminal extracellular domain. TRAIL was described as having similar homology to other TNF-related family members such as the previously described TNF and FasL [21]. Unlike TNF and FasL, early *in vitro* studies on TRAIL function revealed that it preferentially induced apoptosis in transformed cells, while leaving normal cells and tissues intact [22], and multiple *in vivo* studies have confirmed that the primary targets of TRAIL-induced apoptosis are malignant cells [23-27].

TRAIL is a biologic therapy that has shown great promise in pre-clinical studies, due to its ability to preferentially induce apoptotic cell death in transformed cells. However, further investigation into TRAIL function in tumor-free model systems has demonstrated that it can, in fact, induce apoptosis in specific populations of untransformed cells depending on the pathophysiological conditions [28-30]. Despite the fact that noncancerous cells can also be killed by TRAIL under certain circumstances, the development of TRAIL as an anti-cancer agent has continued and the vast majority of work with TRAIL has focused on its tumoricidal activity. Therapeutic TRAIL use has been investigated in many different formats. Initial approaches employed systemic or local administration of recombinant TRAIL protein to ligate the TRAIL receptors on cancer cells thereby activating the extrinsic cell death machinery [31]. As the cell surface receptors for TRAIL were identified, antibody-based therapies became an alternative to

specifically bind to the death-inducing TRAIL receptors on cancer cells and trigger apoptotic death [31]. However the use of recombinant proteins and antibodies in these early studies have proven to be suboptimal therapies to transition into humans, as large amounts and multiple doses of these therapies are needed to observe any therapeutic effect. We have therefore utilized a gene-transfer method to deliver TRAIL protein to the tumor microenvironment where it is able to induce apoptosis of tumor cells *in situ.*

TRAIL and TRAIL Signaling

In humans, TRAIL mRNA is present in a variety of tissues including the spleen, thymus, prostate, ovary, small intestine, colon and placenta [22]. Within the hematopoietic compartment, TRAIL is expressed on activated T lymphocytes, B cells, NK cells, monocytes, dendritic cells, and neutrophils [32-37]. Like other TNF-family member proteins, TRAIL monomers interact in a head-to-tail fashion to form a bell-shaped trimer [21]. This TNF-family protein hallmark of trimerization leads to much greater biologic activity than is observed for either the monomeric or dimeric forms [22]. TRAIL (either soluble or membrane-bound) can bind to one of several receptors. In humans, four membrane-bound TRAIL receptors have been identified: TRAIL receptor-1 (Death Receptor 5(DR4)) [38 39], TRAIL receptor-2 (Death Receptor 5 (DR5)) [40, 41], TRAIL receptor-3 (Decoy Receptor 1 (DcR1)/ TRAIL receptor without an intracellular domain (TRID)) [40, 42, 43], and TRAIL receptor-4 (Decoy Receptor 2 (DcR2)/TRAIL receptor with a truncated death domain (TRUNDD)) [43-46]. The cytoplasmic tails of DR4 and DR5 contain functional death domains that transduce apoptotic signals after receptor trimerization [46]. In contrast, neither TRAIL-R3 nor -R4 possess a functional intracellular death domain, and consequently have been referred to as "decoy receptors" because they bind TRAIL with similar affinity as DR4 and DR5 but cannot initiate apoptotic signaling. The decoy receptors can thus "compete" for binding of TRAIL and therefore diminish the net apoptotic activity of TRAIL protein [42]. In mice, TRAIL is thought to bind to three receptors: TRAIL-R/DR5, mDcTRAIL-R1, and mDcTRAIL-R2. Of these murine TRAIL receptors, only DR5 has been characterized at the functional level [47, 48].

Upon ligation of TRAIL trimers to DR4 or DR5 in humans, an apoptotic pathway is activated via a series of intracellular changes that culminate in the apoptotic death of the TRAIL receptor-bearing cell. Apoptosis is a tightly regulated cellular process, that proceeds by two main pathways, referred to as intrinsic, which is controlled by interactions of pro-apoptotic and anti-apoptotic members of the B-cell leukemia/lymphoma 2 (Bcl-2) protein family [49], and extrinsic, which is induced via ligation of apoptosis-inducing "death receptors" on the cell surface [50]. TRAIL-induced death activates the extrinsic apoptotic pathway as transformed cells have been documented to express the death receptors necessary for TRAIL-induced death.The TRAIL-induced signaling cascade begins with the formation of a multimeric protein structure called the death-inducing signaling complex (DISC). The functional DISC is comprised of several proteins, including the ligated death receptors, Fas-associated death domain protein (FADD), and procaspases 8 and 10 [51, 52]. Following DISC formation, the downstream signaling cascade is initiated via autocatalytic cleavage of procaspase 8 into its active form [52]. Active caspase 8 then amplifies the apoptotic signal by cleaving and activating the effector caspases 3, 6, and 7. Caspases 3, 6, and 7 actively promote cell death by cleaving multiple protein targets that are responsible for maintaining cellular integrity. Active caspase 8 can also cleave the pro-apoptotic Bcl-2 protein Bid, thereby simultaneously triggering the intrinsic apoptotic pathway [53].

Cells expressing functional TRAIL receptors can be classified as either Type I or Type II, depending on their differential requirements for involvement of the intrinsic pathway in triggering apoptosis. Type I cells undergo apoptosis in response to extrinsic signals that lead to caspase 8 cleavage. Type II cells do not undergo apoptosis upon activation of the extrinsic pathway alone; they also require activation of the intrinsic apoptotic pathway and inactivation of intracellular proteins that inhibit caspase signaling cascades, such as X-linked Inhibitor of Apoptosis Protein (XIAP) [54]. Initiation of the intrinsic apoptotic pathway leads to a loss of mitochondrial membrane potential. This allows cytochrome c to escape from the mitochondria into the cytosol, and also releases Second Mitochondria-derived Activator of Caspases/Direct Inhibitor of Apoptosis

Protein Binding Protein with Low Isoelectric Point (Smac/DIABLO), which blocks the function of caspase inhibitors such as XIAP [55, 56]. Cytosolic cytochrome c promotes apoptosis by contributing to the formation of the apoptosome, which also includes ATP and Apoptotic Peptidase-Activating Factor 1 (APAF-1), and results in activation of caspase 9 [57, 58]. Thus, induction of the intrinsic apoptotic pathway results in greater overall caspase activity, and a stronger pro-apoptotic signal that robustly promotes cell death.

Adenovirus 5(Ad5)-TRAIL Gene Therapy

Depending on the disease, gene therapy has become a viable therapeutic alternative for patients over the last decade because this technology can be used to express proteins with the intent of stimulating anti-tumor immunity (i.e. immunization), and/or to introduce genes that encode cytotoxic proteins. Viruses act as natural vehicles for delivering genes as they readily transfer their genetic material to infected host cells [59, 60]. For use as a therapeutic agent, viral vectors are frequently genetically modified to circumvent productive infection and toxicity, while allowing for transgene insertion and subsequent expression in host cells. A number of viral vectors have been described; among the most frequently studied viral vectors are adenoviruses (Ad) [59-61]. Ad- based vectors have been used in a number of pre-clinical studies examining the potential of viral vector-mediated TRAIL administration via gene therapy.

Ad is a non-enveloped virus with a double stranded 26-45 kb DNA genome [62]. There are 51 identified human serotypes of Ad, with types 2 (Ad2) and 5 (Ad5) being the best characterized [59, 60]. Ad2 and Ad5 have high tropism for numerous cell types, do not cause extensive disease in humans, and were the first established vectors for gene therapy [63, 64]. Ad vectors can be engineered to remain replication-sufficient, conditionally replication-sufficient, or replication-deficient in the host. Ad vectors traditionally contain a deletion in the of the early gene 1 region (*E1),* which is activated upon entry into the host cell and is vital for transcription and function of the other early genes [65]. Deletion of *E1* region renders the Ad vector replication-deficient and allows space within the genome for transgene insertion. For entry into a cell by receptor-mediated endocytosis, Group C

adenovirus (e.g. Ad5) requires interaction between the viral fiber capsid protein with the coxsackievirus and adenovirus receptor (CAR), and the viral penton base binding to α_v integrins [66-68]. Thus, the success of any Ad-based therapy is primarily dictated by CAR recognition [69]. CAR is ubiquitously expressed in most benign epithelial tissues, yet marked variations in CAR levels have been demonstrated using different cancer cell lines of the same tissue origin [70]. Ad viral vectors are also ideal for gene-transfer therapy due to the transient nature of gene expression by Ad viruses because they do not integrate into the host genome[59]. A main drawback to utilizing Ad vectors is the presence of neutralizing antibody in the host. Many people are exposed to Ad viruses and therefore would have neutralizing antibodies. However, the intratumoral route of injection (discussed below) for the Ad vector will presumably help to overcome this obstacle.

We were the first to describe the in vitro and in vivo tumoricidal activity of a replication-deficient (by deletion of the E1 genes) Ad5-TRAIL viral vector[71, 72]. These initial studies were designed to only examine the Ad5-TRAIL-induced tumor cell death, and a number of other investigators have evaluated similar TRAIL-encoding Ad vectors in a variety of tumor models [27, 73, 74]. Our more recent studies have examined the impact of Ad5-TRAIL-induced tumor cell death on the subsequent induction of systemic anti-tumor immunity. Using a murine model of RCC, we demonstrated that combinatorial therapy with Ad5-TRAIL and an immune adjuvant, CpG, increased tumor regression and prolonged animal survival [20]. Data from this report also showed that Ad5-TRAIL/CpG therapy led to the generation of immunological memory, since mice that went on to clear the primary tumor after treatment were also able to resist a second tumor challenge. These initial studies paved the way for subsequent studies aimed at investigating the mechanisms of the therapy, and the efficacy of the therapy when faced with immunosuppressive factors.

CpG Oligodinucleotides (CpG)

Optimal activation of the immune system is the prime goal of an immunotherapy for the treatment of cancer; therefore, an immune adjuvant of some kind is typically necessary.

One of the most commonly used immune adjuvants is synthetic CpG. Unmethylated CpG motifs are commonly found in the genomes of bacteria and DNA viruses which stimulate immune cells via the Toll-like receptor (TLR) 9[75, 76]. TLRs are a class of pattern recognition receptors (PRR) that are sensors of either pathogen-associated molecular patterns (PAMPs) or damage-associated molecular patterns (DAMPs)[77, 78]. Recognition of CpG, by TLR9 leads to downstream signaling and subsequent activation of the cell expressing the TLR. There are multiple classes of CpG: A, B, and C. The different classes correspond to the CpG backbone and ability to form higher-order structures and subsequent ability to activate different immune cells[79]. With respect to the work performed in this thesis, our immunotherapy utilizes a class B CpG (1826) that has a phosphorothioate backbone and typically cannot form higher order structures[79]. Class B CpGs potently activate both B cells and dendritic cells (DC)[80, 81].

DC are one of the main cells of the immune system that expresses TLR9, which is important as DC are one of the first line defenses the immune system has against pathogens[82, 83]. Targeting of CpG to DC for activation and ensuing immune system activation is the main goal of using CpG as an immune adjuvant, and the reason it is used in combination immunotherapies[84-87]. CpG has previously been used in FDA approved human trials for numerous vaccination protocols; we therefore would be able to expand upon the already approved uses [88, 89].

Dendritic Cell Biology

DC are a heterogeneous cell population of hematopoietic origin that can be detected in all tissues of the body. DC sample their surrounding environment and are specialized in the capture, processing and presentation of antigens, resulting in their common reference as professional antigen-presenting cells (APC). DC present antigen as peptide fragments in major histocompatibility complex (MHC) molecule complexes to T cells, resulting in the induction of cellular immunity. Typically, DC in peripheral tissues and circulation capture antigen and migrate into draining lymph nodes where they then present antigen to naïve T cells. Alternatively, antigens can also reach the lymph node-resident DC through

the lymphatic system. Upon DC-mediated antigen presentation and costimulation, naïve T cells can then differentiate into effector cells. However, it is important to understand that different forms of immune response can be elicited depending on the type of DC and its activation state.

Development and Subsets

DC are comprised of multiple distinct subsets and all DC have the capacity to take up antigen, process and present it to naïve T cells[90-93]. However, DC subsets differ in development[94-96], location, inflammatory stimuli[97-99], cytokine production[100], and optimal ability to cross-present antigen to CD8 T cells[90], specifically. The two main DC populations that exist in humans and mice are plasmacytoid DC (pDC) and conventional DC (cDC, also known as 'classical' DC, defined by $MHCII^{hi}CD11c^{hi}$ phenotype). It is believed that all DC populations can arise from either lymphoid-restricted or myeloid-restricted progenitors (DC development reviewed in [101]). Studies have shown that under certain conditions common lymphoid progenitors (CLP) can give rise to different DC populations; however, it is thought the majority of DC arise from the common myeloid progenitor (CMP). Downstream of the CMP is the macrophage-dendritic progenitor (MDP), the first precursor that has the ability to give rise to pDC and cDC, as well as other myeloid cells such as monocytes and macrophage. A common DC progenitor (CDP) has been identified that is a restricted precursor for only pDC and cDC[102]. The CDP is the immediate precursor for the pre-cDC, and while the CDP can give rise to both cDC and pDC, the pre-cDC is restricted to cDC development. Pre-cDC are immature cDC that are present in the blood and lymphoid and non-lymphoid peripheral tissues and will differentiate and mature into varying subsets of cDC. In contrast, pDC mature from CDP in the bone marrow and emigrate through the blood to secondary lymphoid tissues. The development, differentiation and maintenance of DC are primarily dependent on a receptor tyrosine kinase, fms-like tyrosine kinse 3 (Flt3)[103, 104]. Flt3 is expressed on all CLP and a subset of CMP. It is also maintained on MDP, CDP and pre-cDC, and is lost on precursor cells as they commit to non-DC lineages[104]. The ligand for Flt3, Flt3L, drives the generation, expansion and mobilization of DC[105]. Flt3L also acts in a positive

feedback loop, where low numbers of DC drives upregulation of Flt3L, which in turn drives generation of DC[104].

As mentioned previously, location is another determinant for subsetting DC. cDC can further be broken down into migratory and lymphoid DC. Migratory DC can migrate from peripheral tissues, such as skin, liver and kidneys, to lymphoid tissues. Lymphoid DC are resident to lymphoid tissues and do not migrate. Lymphoid DC include DC found in spleen, lymph nodes and thymus, and can be further divided by $CD4^+$ and $CD8\alpha^+$ expression. The non-conventional DC, such as pDC, can be found in both lymphoid and non-lymphoid organs. Other subsetting determinants, like necessary transcription factors, stimuli, cytokine production and T cell activation can vary extensively between the DC subsets that exist. Two of these subsets that are arguably the most important for induction of a cellular immunity are the pDC and CD8αDC. Data suggests that it is the concomitant and cooperative activity of these different DC subsets that is necessary for the induction of an effective immune response from antigen sensing, early cytokine production and antigen presentation to T cells.

CD8αDC are a subset of cDC, and data suggests that while spleen and lymph node resident CD8αDC are derived from pre-cDC, thymic resident CD8αDC may be derived from lymphoid progenitors (reviewed in [101]). CD8αDC express the same phenotypic markers as cDC (MHCII and CD11c) and the defining CD8α molecule[106]. Originally it was thought that CD8αDC expressed the CD8αβ heterodimer molecule, similar to CD8 T cells; however, they express only CD8αα homodimers[106]. While CD8α is a distinguishing marker for CD8αDC, no physiological function has been attributed to CD8α on these DC[100]. Other distinguishing markers for CD8αDC are DEC205, Clec9A, and CD24. Of note, CD8αDC do not exist in humans as they do in mice. The human equivalent is the $CD141^+$ DC subset. Developmentally, CD8αDC require the expression of a multitude of transcription factors, but most notably interferon regulatory factor 8 (IRF8)[107], and the AP-1 transcription factor, Batf3. IRF8 is required for CDP generation from MDP and is therefore required for other DC lineages, but Batf3 is specific to the generation of CD8αDC[96]. CD8αDC are key regulators of adaptive immunity for viral and

intracellular pathogen infections and for antitumor immunity, due to their ability to process exogenous antigen and cross-present it to CD8 T cells (discussed below). Among the lymphoid DC subsets, CD8αDC are the main producers of type I IFN and IL-12 cytokines, further enabling them to induce cellular immunity[108]. An additional, indispensable DC subset for activation of adaptive immunity is the non-conventional pDC subset.

pDc are a distinct lineage from cDC based on their gene expression, morphology and cytokine production (reviewed in [101]). Developmentally, pDC are similar to CD8αDC in regard to their dependence on the IRF8 transcription factor. pDC also specifically rely on the expression of the E2-2, Spi-B and Bcl-11a transcription factors for generation. Morphologically, immature pDC are distinct from other DC as they exhibit a circular shape absent of the "dendrite" appendages that are characteristic of DC; however, upon activation, pDC do acquire this morphological feature[98, 102, 109]. In contrast to cDC and CD8αDC, pDC express low levels of MHCII and CD11c, while expressing high levels of the pDC differentiation antigen (PDCA1) and during stages of maturation will concomitantly upregulate Ly6C[110]. Other distinguishing markers for pDC are their unique differential expression of $CD19^-$ and $B220^+$[110]. The most defining characteristic of pDC is arguably their ability to secrete large amounts of type I IFN following viral infection[82, 109]. This is attributed to their high expression of TLR7 and TLR9 that are triggered by intracellular nucleic acids, poising them as optimal detectors of viral pathogens. This unique ability of pDC, makes them key players in the activation of adaptive immunity.

Activation and Cross-presentation of Tumor Antigens

The main function of DC is to act as sentinel cells to sample the environment for foreign invaders. Thus, DC express a plethora of "sensing" molecules. These molecules include PRRs that detect PAMPs. One of the main PRR classes that are primarily associated with DC are TLR family members[77]. Ten TLRs exist in humans, while at least 12 have been described in mice[78]. Many of the TLRs are expressed by both murine CD8αDC and pDC, with a few exceptions: CD8αDC do not express TLR5 or TLR7[111], while pDC

specifically do not express TLR3[111]. Each TLR is specific for different PAMPs, and differential expression of TLRs correlates to the ability/efficacy of the different DC subsets to respond to different stimuli (reviewed in [83, 112]). As pDC are especially important in viral infections, it is not surprising that pDC express the highest levels of TLR7 (ssRNA) and TLR9 (CpG-containing dsDNA). CD8αDC also express high levels of TLR9 allowing them to also respond to dsDNA. Activation of pDC and CD8αDC via TLR stimulation leads to upregulation of costimulatory molecules CD40, CD80 and CD86. Though both DC subsets express MHCII at basal levels, MHCII expression increases with DC activation. Following activation via TLR-stimulation, both pDC and CDαDC are capable of making type I IFN, albeit to varying degrees, and CD8αDC can also go onto produce the IL-12 and IL-15 cytokines, all of which are essential for optimal antitumor immunity[100, 108, 113-116].

Type I IFN is not only important to activate the adaptive immune response, it is also important for activation of function of DC[81, 91]. Data suggest that for DC, specifically CD8αDC, type I IFN is important for optimal functionality, such as uptake, processing and retention of antigens[117]. The efficiency of these functions by CD8αDC is essential for the cross-presentation and priming of $CD8^+$ T cells. Cross-presentation is a mechanism by which the APC takes up exogenous antigen (i.e. tumor cell debris), processes the antigen and loads it onto MHC I to be presented to naive $CD8^+$ T cells (reviewed in [90]). The process of antigen uptake is complex and can happen in a variety of ways; however, uptake of dead tumor cell-associated antigens is thought to be receptor mediated. As cells die, they undergo a number of morphological and biochemical changes, most notably the externalization of phosphatidylserine (PS) to the surface of the dying cells. PS is recognized by multiple bridging molecules that then bind to their cognate receptor expressed on the APC[118]. The multiple bridging molecules and receptors that can trigger receptor-mediated phagocytosis of dead cells by APC are necessary to trigger differential downstream mechanisms. For the purpose of cross-presentation, DEC205 receptor-mediated phagocytosis of dead cells by CD8αDC has been shown to be the optimal receptor[119]. While CD8αDC are by far the most efficient DC subset at taking up cellular

material via the classical receptor-mediated pathway for cross-presentation, pDC can also do this, although to a lesser degree[92].

Once cellular debris/dying cells are endocytosed, they can be found in the early phagosome within the cell (reviewed in [90]). The phagosome transitions into a phagolysosome by a maturation process of merging the endosome with a lysosome. Typically, acidification and degredation of the cargo in the phagolysosome would then ensue; however, for the purpose of cross-presentation, acidification seems to be staved off to allow for antigen persistence within the DC[120, 121]. For antigen processing, two pathways have been proposed, the vacuolar and cytosolic pathways, though the latter is the favored for cross-presentation[122]. This pathway calls for antigen escape from endosomes to the cytosol (by not fully understood mechanisms) where they are further processed by the proteasome to generate small antigenic peptides which are then shuttled into the lumen of the ER, cleaved to appropriate length and loaded on to MHCI molecules, via TAP (transporter associated with antigen processing)[122]. With costimulation molecules expressed and a peptide-loaded MHC I complex, these cross-presenting DC are now poised and capable to activate naïve $CD8^+$ T cells into antitumor effector cells.

Antitumor $CD8^+$ T cell Immune Response

Eliciting an antitumor immune response for therapeutic benefit in cancer has been a long standing goal in immunology. While chemotherapeutics and radiation can confer some initial benefit, induction of effective antitumor immunity that can clear tumor and establish memory to inhibit tumor reoccurrence has really become the goal of current cancer therapy research. These immunotherapies are ideally designed to elicit an effector $CD8^+$ T cell response against the tumors, using the host's own immune system. However, activation of a specific robust antitumor $CD8^+$ T cell response is a multifaceted process that has multiple checkpoints that must be met. Additionally, tumors have evolved to escape and/or suppress the antitumor immune response, and therapies must not only

activate tumor-specific $CD8^+$ T cells but also inhibit immunosuppression exerted by the tumor.

$CD8^+$ T cell Activation and Effector Function

Activation and subsequent development of effector and memory $CD8^+$ T cells (reviewed in [123]) requires a three hit system: T cells must first come in contact with their cognate peptide bound to MHC I on an APC, followed by costimulation (via the APC) and finally T cells must be stimulated via cytokines which can also be provided by the APC. T cells bind their cognate peptide via the T cell receptor (TCR), which consists of the hypervariable α/β chains that dictate antigen specificity, as well as the invariant receptor-associated CD3 and ζ accessory chain proteins. $CD8^+$ T cells express the co-receptor transmembrane glycoprotein, CD8. Co-binding of the TCR and CD8 to peptide-bound MHC I on an APC is necessary for optimal downstream signaling and subsequent activation of the T cell. Typically, the activation of antitumor $CD8^+$ T cells will result from cross-presentation of tumor cell-derived antigens by APC, as described previously.

Concomitantly, as $CD8^+$ T cells are binding their cognate peptide, they must also encounter costimulatory molecules on the APC[124]. This activation typically occurs via ligation of CD28/CD40L on the T cell to CD80 /CD86 and CD40, respectively, on the APC. Ligation of CD28 by CD80/86 leads to increased cytokine gene expression, promotion of T cell survival and maintenance of T cell responsiveness[124]. Lack of costimulation can result in T cells becoming hyporesponsive (anergic)[125]. Following TCR/CD8 activation and costimulation, T cells must be exposed to cytokines, such as type I IFN and IL-12 for optimal activation, proliferation/survival and subsequent effector function[123, 125, 126]. Together, the presentation of tumor-derived peptides in the context of MHC I on an APC, combined with costimulation and cytokines provided via activated APC are all necessary for the induction of a robust antitumor $CD8^+$ T cell effector response.

Once $CD8^+$ T cells have been primed and activated via antigen-loaded DC and cytokine stimulation, clonal expansion of the tumor antigen-specific T cells will follow. These $CD8^+$ T cells will acquire “effector” function and homing capabilities to traffic to

the tumor bed where they will again see their cognate antigen (presumably being expressed by the tumor) and subsequently carryout destruction of the tumor[123, 125-127]. These effector functions include the ability to directly kill tumor cells via TRAIL[128] or FasL mechanisms[129], or to secrete cytolytic molecules such as IFN-γ, TNF-α, perforin and granzymeB[129], all of which can play a role in direct tumor cell death; these "killer" cells are termed cytolytic T lymphocytes (CTL)[130, 131]. IFN-γ and TNF-α can also have cytolytic effects on the tumor stroma and vasculature[132], as well as activating effects on other immune cells that can offer help in the antitumor response. IFN-γ is also crucial in the activation of $CD4^+$ T cells and subsequent induction of a humoral response. Ideally, once the tumor has been eradicated, the $CD8^+$ T cells will eventually die off, leaving behind a small but effective memory population (both central and effector)[123]. Unfortunately for the antitumor response, many mechanisms of suppression are at play within the tumor microenvironment that can lead escape of the tumor from the immune response, or directly suppress the immune response.

Tumor-mediated Immune Suppression

Immune escape and immune suppression are two of the main obstacles that need to be considered when thinking about therapies to induce an antitumor immune response[133]. Tumors can directly escape the immune system by downregulating their MHC I molecules, thus the CTL will not be able to recognize the tumor cell and subsequently kill it[134]. Tumors can also induce anergy of resident naïve T cells by presenting tumor-associated antigens in the absence of co-stimulation or by secreting suppressive molecules[135]. Engagement of inhibitory receptors, such as CTLA-4 and PD-1, on T cells is an additional direct mechanism that tumor cells employ to suppress T cells[136]. CTLA-4 and PD-1 are members of the CD28 family, but instead of activating the T cells, they can induce anergy, and tumor cells or cells within the tumor milieu can express the ligands for these receptors[135].

Tumors cells can also secrete immunosuppressive molecules such as IL-10 and TGF-β, which can inhibit proliferation and development of CTLs. These molecules also have the ability to recruit immunosuppressive cell populations into the tumor

microenvironment. Regulatory T cells that accumulate systemically in tumor-bearing hosts can directly and indirectly inhibit the antitumor $CD8^+$ T cell response. Similarly, a population of myeloid derived suppressor cells (MDSC) accumulates and expands in tumor-bearing hosts that very potently induce immune suppression both in the tumor microenvironment and in the periphery.

Myeloid Derived Suppressor Cells (MDSC)

Extramedullary hematopoiesis and neutrophilia were first described as characteristics of tumor progression in the early 1900's[137]. These events were associated with atypical myeloid progenitor generation and differentiation resulting in abnormal myeloid cells that lacked conventional B, T cell and macrophage markers and were capable of decreasing CTL generation and function[138]. In recent years these "tumor induced" cells have been identified as myeloid derived suppressor cells (MDSC), which are present in high numbers and correlate with poor prognosis, and tumor evasion of host immunity[139].

Identification and Phenotype

MDSC expanded during a tumor challenge are not a specific, defined population of cells; rather they are a heterogeneous population of immature myeloid cells (reviewed in [140]). MDSC are not fully differentiated, and lack differentiation markers that are seen on other myeloid cells, such as DC and macrophages. Data suggests that under certain circumstances MDSC can be terminally differentiated into DC or macrophages, and upregulate the respective markers and acquire the respective functionality[141-143]. Historically MDSC were characterized as $CD11b^+$ (an αM integrin) and Gr-1 (a granulocyte marker); however it is now well appreciated that the Gr-1 antibodies used to identify MDSC bind to two epitopes from two different GPI-anchored cell surface glycoproteins, Ly6G and Ly6C[144]. Using differential antibodies to each Ly6G and Ly6C, two sub-populations of MDSC have been identified: $CD11b^+Ly6C^{+/lo}Ly6G^{hi}$ granulocytic MDSC, and $CD11b^+Ly6C^{hi}Ly6G^-$ monocytic MDSC[145-147]. While other markers have been identified on MDSC, such as F4/80, IL-4α receptor and CD115, these markers can be tumor model specific, and therefore are not always as faithfully expressed on MDSC.

The phenotype and morphology of MDSC are very similar to other monocyte and granulocyte cell lineages resulting in the necessity to further identify these cells via function. Neutrophils and macrophage can express some of the same phenotypic markers as MDSC, but MDSC specifically expand during a tumor challenge, and when isolated by $CD11b^{+}Ly6C^{+/lo}Ly6G^{hi}$ and $CD11b^{+}Ly6C^{hi}Ly6G^{-}$, demonstrate immunosuppressive capacities via a variety of mechanisms (discussed below). Consequently, it is essential to not only phenotype MDSC but also assess their function.

Expansion and Activation of MDSC

MDSC are readily induced by inflammation and the presence of tumors[147-150]. In the context of tumors, expansion and activation of MDSC can be induced by multiple factors made primarily by two groups of cells: tumor/stromal cells and activated immune cells within the tumor microenvironment. These secreted factors can promote expansion by stimulating myelopoiesis and inhibit differentiation of mature myeloid cells, and direct activation of MDSC. Granulocyte-macrophage colony-stimulating factor (GM-CSF), prostaglandin E2 (PGE_2)[151], and S100A[152-154] proteins are some of the main molecules produced by tumor cells that induce the expansion and activation of MDSC both in the periphery (bone marrow, secondary lymphoid organs) and in the tumor. Molecules expressed by immune cells, such as activated T cells and myeloid cells, that can induce MDSC include IFN-γ[147], IL-6[150], IL-1β and cyclooxygenase (COX)-2/PGE_2.

Many of these factors have cognate receptors that are expressed on the surface of MDSC[155], and upon ligation activate JAK/STAT pathways. The main STATs that are triggered and have been shown to play a role in activation of MDSC are STATs 1/3/6. The activation of STAT3 regulates expansion by stimulating myelopoiesis and inhibiting differentiation in committed lineages, such as DC[156]. STAT3 also leads to upregulation of MYC and BCL-XL, which leads to increased survival of MDSC[157]. Induction of STAT1 and STAT6 leads to activation of MDSC by inducing production of reactive oxygen species (ROS), arginase 1 (Arg1), and inducible nitric oxide synthase (iNOS), which all play a role in the functional immunosuppressive capacity of MDSC[147, 158-160].

Suppression Mechanisms of MDSC

Suppressive function is the main denominator that distinguishes MDSC from other myeloid cells, such as neutrophils and macrophage. MDSC have a multitude of mechanisms to inhibit the antitumor immune response, two of which are significant upregulation and activity of the Arg1 and iNOS enzymes[158, 161-163]. These mechanisms induce non-specific T cell inhibition by catabolism of L-arginine from the surrounding environment and converting it into urea (Arg1) and nitric oxide (NO, by iNOS). Both the depletion of the essential amino acid, L-arginine, and the production of the byproducts leads to inhibition of T cell proliferation. ROS are produced by MDSC in response to cytokines, and have also been implemented in immunosuppression, and more recently peroxynitrite has been shown to inhibit T cell activation by making them unresponsive to antigen stimulation. Many of these byproducts have direct effects on T cells by altering the CD3 and CD8 molecules on the surface of the T cell.

MDSC heterogeneity is seen not only in phenotypic differences between subsets but also in function. The granulocytic population of MDSC are thought to be activated more potently through STAT3 which leads to ROS production, while the monocytic population is more commonly activated via STAT1 leading to increased iNOS activity. Both subsets utilize Arg1 as a suppression mechanism. Multiple MDSC subsets exist, and they have all been linked to tumor outgrowth and poor prognosis in cancer patients. For these reasons, targeted therapy to deplete or modulate MDSC is currently the focus of many antitumor therapies.

Modulation and Targeting of MDSC for cancer therapy

Over the last few years, therapeutic targeting of MDSC to reduce immune suppression for the purpose of mounting a robust antitumor immune response has become increasingly more common. Interestingly, many approved treatments for cancer have been identified to decrease or modulate the MDSC population in tumor-bearing hosts. Such chemotherapies as Gemcitabine and 5-Fluoruricil selectively deplete MDSC[152, 164]. Small molecule inhibitors for the treatment of RCC, Sorafenib and Sunitnib, have recently

demonstrate the ability to decrease the suppressive capacity of MDSC in RCC patients[165, 166]. Though these agents are capable of reducing immune suppression through altering the MDSC populations, they can have off target effects, toxicities, and even have negative effects on subsequent immune responses. Therefore, immunotherapy strategies for overcoming MDSC immunosuppression that do not negatively affect the immune response are of utmost importance.

Obesity and Cancer

Obesity is defined by the World Health Organization (WHO) as having a body mass index (BMI, kg/m^2) over 30, and as of 2011 the Center for Disease Control estimated that about one-third (37%) of the U.S. adult population was considered obese. This is concerning as obesity has long been associated is one of the main risk factors and co-morbidities associated with RCC, which is concerning given the fast rate at which the obesity epidemic is growing. Though RCC only accounts for about ~4% of all adult cancers, it is the third most correlated cancer with obesity, just after endometrial and esophageal. A study in 2008 demonstrated that 40% of RCC cases in the U.S. were in fact directly related to excessive body weight, and about 15-20% of cancer deaths can be attributed to obesity[167]. Reasons for this are likely complex and multifactorial, but generalized inflammation and immune suppression during obesity may factor into these findings.

Adipose tissue is an abundant tissue in the body and it had previously been thought to be an inert tissue used solely has an energy depot. However, it has become increasingly clear that adipose tissue acts an important regulator of immunological and pathological functions, especially in the context of increased adiposity seen in obese hosts (reviewed in [167-170]). Adipose tissue is a major endocrine and metabolic organ that produces adipokines that have far-reaching effects on other organs and cells of the body. Adipose tissue is made up of adipocytes (the producers of the adipokines) that become dysregulated in the context of obesity that results in the over-production and circulation of proinflammatory cytokines and fatty acids. Adipokines have been implemented in the

link between obesity and the low-grade chronic inflammation that obese individuals present with (reviewed in [167-170]).

Chronic inflammation as a precursor to cancer was first observed over a 100 years ago by Randolph Virchow, when he observed an abundance of leukocytes in neoplastic tissue[171]. Inflammation has been implemented in both cancer initiation and tumor progression. This increased inflammation can induce the infiltration of myeloid cells into the adipose tissue, which in turn will further produce proinflammatory cytokines[172-175]. Interestingly, many of the proinflammatory cytokines that are over expressed in the context of obesity, are the same cytokines capable of inducing and activating MDSC. Multiple groups have made the connection between obesity and MDSC accumulation, such that as hosts become obese they also have aberrant systemic accumulation of immunosuppressive MDSC[176, 177]. As MDSC are known to promote tumors and metastasis, it is therefore not surprising that there has been increasing evidence to link obesity-induced inflammation and cancer.

The chronic inflammation in obese hosts can also lead to immune dysregulations, Obese individuals are more susceptible to infections (specifically viral influenza infection), bacteremia and demonstrate poor wound healing and antibody responses[178-180]. Though the specific mechanisms at play are not wholly understood, data suggest that the inflammatory milieu can have negative effects on the immune system. Diets high in mono- and poly-unsaturated (MUFAs, PUFAs) fats have been reported to inhibit lymphocyte trafficking and proliferation, respectively. Additionally, PUFAs can inhibit APC function, diminish IL-2 and IFN-γ responses and increase iNOS production[181, 182]. Mouse models of obesity have demonstrated overall decreases in numbers of T and B cell populations, and decreased responsiveness of lymphocytes. Many of the negative effects obesity has on the immune response are directly related to the adipokines and inflammatory cytokines that are overtly produced in obese hosts. The adipokine, leptin, promotes proinflammatory cytokine secretion and can directly induce proliferation of immunosuppressive regulatory T cells[183, 184]. Adiponectin, another adipokine, can directly inhibit costimulatory molecule upregulation on APCs while simultaneously increasing

suppressive molecules on the surface of the APC, both of which can lead to poor activation of T cells[184]. Based on these findings, immunotherapy for the treatment of cancer in obese patients will most likely be insufficient. Understanding the mechanisms by which a therapy works and how obesity affects the therapy will be imperative for making novel therapies to treat both lean and obese patients in the clinic.

Hypothesis

The endogenous immune system is incapable of clearing orthotopic RCC tumors. Local treatment of RCC tumors with Ad5-TRAIL/CpG therapy, leads to eradication of both local and metastatic tumor burden in lean mice but not in mice complicated with diet-induced obesity. In lean mice, $CD8^+$ T cells are necessary and dendritic cells are thought to play a role in the antitumor immune response following Ad5-TRAIL/CpG. The research outlined in this thesis explored the specific mechanisms by which Ad5-TRAIL/CpG therapy works to induce an efficacious $CD8^+$ T cell response in both lean and obese hosts. The overall hypothesis for this thesis is that Ad5-TRAIL/CpG therapy is dependent on the function of CD8α and plasmacytoid dendritic cells and the modulation of myeloid derived suppressor cells to mount a $CD8^+$ T cell response capable of clearing RCC tumors.

Chapter 2: Both plasmacytoid DC and CD8α DC are necessary for an effective antitumor immune response following Ad5-TRAIL/CpG Therapy

Introduction

Immune-based therapy for solid tumors provides the potential for long-lived protection against cancers of various stages – including metastatic cancer [185]. The development of successful cancer immunotherapeutic protocols depends on identifying the mechanisms that efficiently prime and activate effector cells within the immune system. One goal of many immunotherapeutic protocols is the generation of a systemic antitumor T cell response, which largely depends on the proper function of antigen presenting cells (APC). Dendritic cells (DC) are the most potent APC population that capture, process, and present tumor-derived Ag to T cells via MHC I or II [186, 187]. When presented with tumor-derived Ag in combination with co-stimulation and immunostimulatory cytokines, tumor-specific T cells differentiate into effectors that can directly kill tumor cells [186, 188, 189]. Because DC are essential for initiating antitumor T cell responses, understanding the roles played by specific DC subsets becomes paramount for optimizing immunotherapeutic protocols. Plasmacytoid DC (pDC) and CD8α DC are two DC subsets crucial in the generation of robust antitumor responses [188, 190]. pDC are recognized as the primary producers of type I interferon (IFN) after stimulation with various proteins or molecules containing pathogen- or damage-associated molecular patterns [190, 191], while CD8α DC cross-present Ag from exogenous sources (e.g., apoptotic tumor cells) in MHC I to CD8 T cells [192, 193].

The tumor necrosis factor (TNF) superfamily member TNF-related apoptosis-inducing ligand (TRAIL) is best known for its ability to selectively induce apoptosis in tumor cells [194, 195]. Moreover, systemically-administered recombinant TRAIL protein and TRAIL death receptor-specific agonistic mAb have been evaluated preclinically and in clinical trials for direct tumoricidal potential [196]. Our laboratory was the first to describe

the utility of a recombinant replication-defective adenovirus encoding TRAIL (Ad5-TRAIL) delivered locally into a tumor [197, 198]. When combined with immunostimulatory CpG-containing oligodeoxynucleotides (CpG), Ad5-TRAIL induces a systemic antitumor T cell response in mice bearing localized subcutaneous Renca tumors and in a mouse model of advanced renal cell carcinoma where an orthotopic primary Renca tumor gives rise to lung metastases [19, 199].

CD8 T cells are required for the complete eradication of the tumors in these models, suggesting the need for DC to cross-present tumor-derived Ag. In addition, one expected function of the CpG is to stimulate DC maturation for enhanced MHC/costimulatory molecule expression and inflammatory cytokine production. To address the specific necessity and function of pDC in the efficacy of the Ad5-TRAIL/CpG therapy, mice orthotopically challenged with Renca tumors were depleted of pDC using a mAb against PDCA1 [200]. We also examined the necessity and function of CD8α DC by examining the efficacy of Ad5-TRAIL/CpG immunotherapy in Renca-bearing *Batf3*$^{-/-}$ BALB/c mice [96]. We hypothesized that both pDC and CD8α DC would be required for the induction of antitumor immunity and the subsequent clearance of tumor. Data is presented to support this hypothesis, and the implications of these findings in regard to the development of current and future immunotherapeutic protocols are discussed.

Materials and Methods

Animals

Female wild-type BALB/c mice (7-8 wk old) and *Batf3*$^{-/-}$ BALB/c breeder mice were purchased from the National Cancer Institute (Frederick, MD) and Jackson Laboratories (Bar Harbor, ME), respectively. *Batf3*$^{-/-}$ BALB/c mice were housed and bred under pathogen-free conditions at the AALAC-accredited University of Minnesota Animal Care Facility. All animal procedures were approved by the University of Minnesota Institutional Animal Care and Use Committee.

Cell lines

The murine renal adenocarcinoma cell line, Renca [201], was obtained from Dr. Robert Wiltrout (National Cancer Institute, Frederick, MD). Renca cells were maintained in RPMI supplemented with 10% FBS, penicillin, streptomycin, sodium pyruvate, non-essential amino acids, 2-mercaptoethanol, and HEPES (a.k.a. complete RPMI) [19, 199]. Renca-GLE stably expresses firefly Luciferase and green fluorescent protein (GFP), and was obtained from Dr. Andrew Wilber (Southern Illinois University School of Medicine, Springfield, IL). Renca-GLE cells were maintained in complete RPMI supplemented with 0.3 μg/ml puromycin and 300 μg/ml zeosin.

Tumor challenge

For intrarenal (IR) tumor challenge, mice were anesthetized, a skin incision was made on the left flank, and 2 x 10^5 Renca or Renca-GLE cells were injected through the intact peritoneum into the left kidney in a 100 μl volume of HBSS [19, 202]. pDC depletion was accomplished with 2 consecutive doses of anti-PDCA1 mAb (clone 120G8 [203]) at 500 μg/mouse [200] in 100 μl PBS i.p. on d 5 and 6 after tumor challenge. Mice treated with rat IgG1 anti-βGAL mAb (clone GL113) served as controls for pDC-depleted mice. On d 7, mice were re-injected in the same kidney with sterile PBS, Ad5-TRAIL (10^9 pfu), and/or the nonmethylated CpG ODN 1826 (5'-tccatgacgttcctgacgtt-3', 100 μg; IDT, Coralville, IA) in a 100 μl volume. Renal and metastatic tumor burden was measured via bioluminescence imaging using a Xenogen IVIS Spectrum [19, 202]. Renca-GLE generated radiance (photons/second/cm^2) was calculated within a defined region of interest using Living Image software (Version 2.5). For end time-point experiments, renal tumor burden was measured via weight (g) between d 18-21 when mice became moribund.

Flow cytometry

Spleens, tumor-bearing kidneys, and contralateral kidneys were harvested, homogenized into a single cell suspension via gentleMACS Dissociator (Miltenyi BioTeck Inc., Auburn, CA), and then digested for 15-30 min in HBSS containing 0.56 Wuensch units/ml Liberase Blendzyme 3 (Roche, Branford, CT) and 0.15 mg/ml DNAse I (Sigma,

St. Louis, MO). Cells were then blocked with anti-CD16/32 and normal mouse serum prior to staining with the following mAb (eBioscience (San Diego, CA) or BioLegend (San Diego, CA)) and analyzed on a BD LSR II (BD Biosciences, San Diego, CA) and FlowJo software (TreeStar Inc., Ashland, OR): DC – anti-CD11c-APC/Cy7 or -PE/Cy7, I-A^d-PacBlue or -PE, CD45R/B220-APC/Cy7 or -PacBlue, CD317-APC or -FITC, CD8-PE-Cy7, CD40-PE, CD86-PE/Cy5, CD80-BV605; T cells – anti-CD3-PerCP/Cy5.5, CD4-PE/Cy7, CD8-PacBlue, CD44-PE or -AF700, KI-67-AF647, CD62L-PE, CD45.2-PE and -BV650. Intracellular staining for Foxp3 was done, as a dump gate, using a Foxp3 staining kit (eBioscience). For intracellular IFN-γ staining, cells from tumor-bearing kidneys were plated at $1x10^6$ cells/well in a 96-well plate with 5ng/ml PMA and 500ng/ml ionomycin with 10μg/ml BFA for 6 hrs prior to staining as stated above.

Intravascular staining

To specifically identify leukocytes within the tumor-bearing kidney tissue or kidney vasculature, intravascular (i.v.) staining was done [204]. Briefly, mice were injected i.v. with 3 μg of PE-conjugated anti-CD45.2 mAb 3 min before death and prepping the organs for flow cytometric analysis as described above. Additionally, cells were stained *ex vivo* with BV650-conjugated anti-CD45.2 mAb. Duel staining of CD45.2 discriminates cells within the vasculature (CD45.2 PE^+ and $BV650^+$) or the tissue (CD45.2 PE^- and $BV650^+$) at the time of harvest. Blood and inguinal lymph nodes served as positive and negative controls for i.v. staining, respectively

Quantitative PCR (qPCR)

Tumor-bearing kidneys were harvested 4 h after treatment, and homogenized via gentleMACS Dissociator. Total RNA was isolated using TRIzol reagent (Invitrogen, Carlsbad, CA), and 1 μg was reverse-transcribed using Superscript III. Resulting cDNA was used as a template for qPCR using TaqMan primer/probe sets for *Cxcl10, Ifit, Irf7, Isg15, Mda5, Mx1, Ifnβ* and 18s rRNA (PE Applied Biosystems, Foster City, CA). qPCR using SYBR Green 1 Master Mix (Roche) and the following primer sets were used to

quantify *Ifnα4* mRNA message (forward 5'-TGA TGA GCT ACT GGT CAG C-3', and reverse, 5'-GAT CTC TTA GCACAA GGA TGG C-3).

IL15/IL15R ELISA

Tumor-bearing kidneys were harvested 24 h after treatment and homogenized in Cell Extraction Buffer (Invitrogen, Grand Island NY) supplemented with Complete Mini protease inhibitor (Roche Applied Science, Indianapolis, IN) and 1 mM PMSF (Cell Signaling Technologies, Danvers, MA). Samples were incubated on ice for 30 min, spun at 3000*g* at 4^{o}C for 10 min, and resulting supernatants were frozen at -80^{o}C until use. The amount of IL-15/IL-15R complex was determined via ELISA (eBioscience).

Statistical analysis

Statistical analysis between groups was determined by 1-way ANOVA with a Tukey post hoc test or unpaired Student's *t*-test, where appropriate. Statistical analyses of tumor growth kinetics and survival between groups were performed via 2-way ANOVA, and Log-rank tests, respectively. Data was analyzed with Prism4 GraphPad software and statistical significance is indicated in figure legends (*** $p \leq 0.0001$; ** $p \leq 0.001$; * $p \leq 0.05$; not significant (n. s.)).

Results

DC-depletion models

Different DC populations play synergistic and mutually exclusive roles during the initiation of an antitumor immune response [186, 200, 205, 206]. To determine the *in vivo* significance of pDC and CD8α DC in the efficacy of Ad5-TRAIL/CpG therapy in a model of advanced RCC, we treated WT BALB/c mice with anti-PDCA1 mAb (clone 120G8 [200]), which depletes pDC, and utilized *Batf3*$^{-/-}$ BALB/c mice, which are deficient in CD8α DC [96]. Renca is derived from a spontaneously arising renal adenocarcinoma in BALB/c mice[207], and is widely used to model RCC. The H-2K/D^{d} restriction of this model consequently limited us to using *Batf3*$^{-/-}$ BALB/c mice; to our knowledge there are no mice on the BALB/c background genetically engineered to be deficient in pDC.

Tumor-free WT replete, anti-PDCA1-treated, and *Batf3*$^{-/-}$ BALB/c mice showed normal development of splenic conventional DC (CD11c^{+} MHC II^{+}) and CD8^{+} T cells, while having the expected reduction in frequency and number of pDC and CD8α DC (Figure 2-1). Both pDC-depleted mice and *Batf3*$^{-/-}$ mice also showed normal development and maintenance of the converse DC subset, and we did not detect any major shifts in the major immune populations (i.e., B cells [208-210]) shown to express PDCA-1 (CD317) in the steady-state in the anti-PDCA1-treated mice (Figure 2-2) although smaller effects on such subsets cannot be completely excluded. The degree of pDC and CD8α DC depletion observed in tumor-free mice was also obtained in tumor-bearing mice (Figure 2-3). The use of *Batf3*$^{-/-}$ BALB/c mice proved to be superior to administering a depleting anti-CD8α mAb, as mice given this mAb had significant reductions in both CD8α DC and CD8 T cells. Together, these mice and reagents gave us the ability to examine the therapeutic efficacy of Ad5-TRAIL/CpG in Renca-bearing mice missing either pDC or CD8α DC, while maintaining an intact CD8 T cell compartment.

DC-depleted mice succumb to tumor despite receiving Ad5-TRAIL/CpG therapy

Ad5-TRAIL/CpG therapy induces a systemic antitumor T cell response in RCC-bearing mice capable of clearing local and metastatic tumors and prolonging survival [19, 199]. Use of Ad5-TRAIL or CpG individually can slightly decrease tumor burden, but only the Ad5-TRAIL/CpG combination significant reduces tumor burden and enhances survival [19, 199]. These data suggested that Ad5-TRAIL-induced death creates the necessary tumor Ag debris that is taken up by DC and presented to tumor-specific T cells, while CpG serves to activate the DC for optimal Ag presentation and T cell stimulation [199]. As our previous study did not specifically investigate the importance of pDC and CD8α DC in the Ad5-TRAIL/CpG-induced tumor eradication, we compared tumor outgrowth and survival of WT replete, pDC-depleted, or *Batf3*$^{-/-}$ BALB/c mice following treatment with PBS or Ad5-TRAIL/CpG therapy. (Note – we did not treat mice with Ad5-TRAIL or CpG alone as they proved to be suboptimal therapy in our previous studies.) As before,

WT replete mice given Ad5-TRAIL/CpG displayed significantly suppressed tumor outgrowth, decreased frequency of mice with lung metastases, and prolonged survival compared to mice given PBS (Figure 2-4). In contrast, mice devoid of either pDC or CD8α DC displayed significant primary and metastatic tumor outgrowth and these groups had no survival benefit after Ad5-TRAIL/CpG therapy. Together, these data demonstrate the necessity of both pDC and CD8α DC in the efficacy of Ad5-TRAIL/CpG therapy in this model of advanced RCC.

pDC and CD8αDC have an alter activation phenotype in *Batf3-/-* and anti-PDCA1-treated mice, respectively

Given the lack of efficacy of Ad5-TRAIL/CpG therapy in the anti-PDCA1-treated and *Batf3*$^{-/-}$ mice, we initially investigated the phenotype of pDC from *Batf3*$^{-/-}$ BALB/c and CD8α DC from anti-PDCA1-treated mice after Ad5-TRAIL/CpG therapy. A number of reports have described the importance for pDC/CD8α DC crosstalk during an immune response, suggesting that one DC subset can "license" another DC subset [189, 205, 206]. Most notably, pDC can specifically license myeloid DC and CD8α DC to process and present Ag to CD8 T cells. With this in mind, we hypothesized that the absence of pDC would lead to decreased activation status in the CD8α DC compartment. However, there is little-to-no published data describing alterations in pDC activation as a result of a lack in CD8α DC. Splenocytes from tumor-bearing WT replete, anti-PDCA1-treated, and *Batf3*$^{-/-}$ BALB/c mice were analyzed via flow cytometry 24 h after PBS or Ad5-TRAIL/CpG treatment to examine the activation status of the remaining endogenous DC populations. Interestingly, pDC from *Batf3*$^{-/-}$ Balb/c mice exhibited a blunted activation phenotype 24 h after Ad5-TRAIL/CpG administration, as seen by significantly decreased CD40, CD80, and CD86 expression (Figure 2-5). Expression of these same proteins on CD8α DC in pDC-depleted mice was unchanged compared to WT replete mice. These results suggest that pDC maturation after Ad5-TRAIL/CpG therapy is dependent on cellular and/or soluble cues from CD8α DC, but the phenotypic maturation of CD8α DC does not require the presence of pDC.

pDC-depleted and *Batf3-/-* mice have an altered Type I-interferon response after Ad5-TRAIL/CpG therapy

An early hallmark of both adenovirus type 5 (Ad5) infection and CpG stimulation is the induction of type I IFN cytokines, and both pDC and CD8α DC can make type I IFN after Ad5 and CpG stimulation [211-213]. Quantitation of type I IFN (be it IFNα or IFNβ) can be difficult from tissue or serum samples in some settings because the cytokines are quickly sequestered by the interferon αβ receptor (IFNAR), reducing the amount a free cytokine below the level of detection of commonly used assays (such as ELISA). As an alternative, quantitative real-time PCR (qPCR) can be used to measure IFN transcripts directly. However, 14 isoforms of IFNα and one isoform of IFNβ exist, making it difficult to measure the entire type I IFN response without measuring all of the isoforms (Figure 2-6). To overcome this obstacle we utilized qPCR to measure a panel of type I IFN-stimulated genes (*Cxcl10, Ifit, Irf7, Isg15, Mda5, and Mx1*) as a proxy for the response. Tumor-bearing kidneys from WT replete, pDC depleted and *Batf3*$^{-/-}$ BALB/c mice were harvested 4 h after injection of PBS, Ad5-TRAIL, and/or CpG. WT-replete mice treated with both Ad5-TRAIL/CpG had the greatest increase in type I IFN-stimulated gene mRNA expression compared to mice injected with PBS, Ad5-TRAIL alone, or CpG alone (Figure 2-7). These results support our previous data demonstrating the superior therapeutic efficacy of Ad5-TRAIL/CpG over either component alone. We then examined the expression of the 6 type I IFN-stimulated genes in WT replete, pDC-depleted, and *Batf3*$^{-/-}$ BALB/c mice 4 h after PBS or Ad5-TRAIL/CpG injection. Tumor-bearing WT replete mice that received Ad5-TRAIL/CpG had substantial mRNA upregulation of the 6 type I IFN-stimulated genes when normalized to tumor-free controls (Figure 2-8). By comparison, Ad5-TRAIL/CpG-treated *Batf3*$^{-/-}$ BALB/c mice had significantly reduced induction of mRNA for these genes, and there was a decreased trend in mRNA expression in similarly treated pDC-depleted mice. The data in Figure 8 suggest alterations in the type I IFN response after Ad5-TRAIL/CpG injection contribute to the reduced efficacy of therapy.

pDC-depleted and *Batf3-/-* mice have reduced production of IL-15/IL-15R following Ad5-TRAIL/CpG therapy

Type I IFNs can induce DC production of IL-15, and DC production of proinflammatory cytokines (including IFN) after CpG-stimulation is dependent on IL-15 [206, 214]. Further, the presence of endogenous or exogenous IL-15 during a tumor challenge promotes an antitumor CD8 T cell response capable of eradicating established tumors [215]. When we measured the amount of IL-15/IL-15R complex within tumor-bearing kidneys of WT replete, anti-PDCA1-treated, and *Batf3*$^{-/-}$ BALB/c mice after Ad5-TRAIL/CpG administration, we found a significant increase in the amount of IL-15/IL-15R complex within the kidneys of WT replete mice over PBS-treated mice and when compared to anti-PDCA1-treated or *Batf3*$^{-/-}$ BALB/c mice (Figure 2-9). Collectively, the data in Figures 8 and 9 suggest both pDC and CD8α DC are required for the Ad5-TRAIL/CpG-induced production of proinflammatory cytokines important for stimulating antitumor T cell responses.

pDC-depleted and *Batf3-/-* mice have a decreased CD8$^+$ T cells response following Ad5-TRAIL/CpG therapy

pDC and CD8α DC have been implicated in the activation and expansion of tumor-specific CD8 T cells, and a CD8 T cell response is induced with Ad5-TRAIL/CpG therapy [19, 199]. The inability of Ad5-TRAIL/CpG therapy to control tumor outgrowth in pDC- and CD8α DC-deficient mice along with the decreased production of proinflammatory cytokines and DC maturation prompted us to evaluate CD8 T cell infiltration into tumor-bearing kidneys following therapy. As no Renca-specific tumor Ag have been identified to our knowledge, we determined the frequency of "effector phenotype" CD8 T cells ($CD3^+CD8^+CD44^{hi}$) in the tumor-bearing kidneys of WT replete, anti-PDCA1-treated, or *Batf3*$^{-/-}$ BALB/c mice 5 d after receiving Ad5-TRAIL/CpG therapy. It is important to note that though T cells have been documented to upregulate PDCA-1 under inflammatory conditions, we did not observe any loss of the T cell population in the spleens of DC-depleted groups following therapy (i.e. inflammation,

Figure 2-10). There was a however a significant increase in the frequency of $CD3^+CD8^+CD44^{hi}$ cells in kidneys from Ad5-TRAIL/CpG-treated WT replete tumor-bearing mice compared to PBS-treated mice when calculated from total live cells or from total $CD45.2^+$ leukocytes (Figure 2-11). Similar increases in frequency in $CD3^+CD8^+CD44^{hi}$ cells were not seen within the tumor-bearing kidneys from Ad5-TRAIL/CpG-treated pDC-depleted or *Batf3*$^{-/-}$ BALB/c mice. It is important to note that the CD8 T cell expansion seen in the WT replete mice was not in response to adenovirus, as mice treated with Ad5-TRAIL alone did not display this increase in CD8 T cell infiltration. The diminished infiltration of CD8 T cells into the kidneys of tumor-bearing anti-PDCA1-treated mice after Ad5-TRAIL/CpG therapy was also not due to anti-PDCA1-mediated depletion of activated (IFN-stimulated) CD8 T cell (Figure 2-10) as suggested by fact that this mAb can deplete stromal cells and IFN-stimulated hematopoietic cells [208].

Our orthotopic RCC model is based on injection of Renca cells into the kidney to form the primary tumor. Kidneys are highly vascular organs, making it likely that evaluation of leukocytes from tumor-bearing kidneys would include T cells "localized" within the kidney tissue and present in the kidney vasculature (i.e., in the circulating blood) at the time of organ harvest. Thus, we used an intravascular staining technique [204], in which PE-conjugated anti-CD45.2 mAb was injected i.v. immediately prior to tumor-bearing kidney harvest to label cells within the vasculature of the kidney at the time of harvest. The cells were then stained *ex vivo* with a BV650-conjugated anti-CD45.2 mAb, allowing for the clear distinction between tissue ($BV650^+PE^-$) vs. blood ($BV650^+PE^+$) T cells. Using this method, it was determined that ~90% or more of the $CD45.2^+CD3^+CD8^+CD44^{hi}$ T cells were localized within the kidney tissue at the time of harvest – regardless of the experimental group (Figure 2-11). Subsequent analysis of the $CD45.2^+CD3^+CD8^+CD44^{hi}$ T cells localized within the kidney at the time of harvest revealed a significant reduction in the frequency of Ki-67^+ cells from Ad5-TRAIL/CpG-treated pDC-depleted or *Batf3*$^{-/-}$ BALB/c mice. CD11a is upregulated on Ag-experienced CD8 T cells [216] and is also crucial for CD8 T cell-mediated killing of Renca cells [129].

There was a significant reduction in CD11a expression on the tumor-infiltrating $CD45.2^{+}CD3^{+}CD8^{+}CD44^{hi}$ T cells from Ad5-TRAIL/CpG-treated pDC-depleted and *Batf3*$^{-/-}$ BALB/c mice compared to WT replete mice. Stimulation of CD8 T cells from tumor-bearing WT replete, pDC depleted, and *Batf3*$^{-/-}$ mice treated with Ad5-TRAIL/CpG cell *in vitro,* demonstrated that CD8 T cells from DC depleted mice retained the ability to secrete effector cytokine, but were far fewer in numbers compared to WT replete controls (Figure 2-12). Collectively, these data demonstrate that the absence of pDC or CD8α DC results in the abrogation of the Ad5-TRAIL/CpG therapy-induced CD8 T cell immune response essential for the eradication of tumor cells in this model of advanced RCC.

Discussion

The ability to stimulate antitumor immunity is the primary goal of many active clinical trials [185]. The generation of T cell-mediated antitumor immunity should be (in theory) relatively straightforward, since a variety of Ag expressed by tumors (including overexpressed tissue-differentiation Ag, mutant proteins, and/or viral Ag) can be recognized by the immune system. However, there are many aspects unique to T cells and other components of the immune system that inhibit optimal T cell activation. Among the cells needed to generate antitumor T cell immunity, the importance of DC cannot be underemphasized. DC engulf fragments of dying tumor cells, and process the numerous proteins into antigenic peptides for presentation via MHC I/II to T cells. A variety of methods can be employed to kill tumor cells *in vivo* (e.g., chemotherapy, radiation, or cryotherapy), but these methods frequently lack the specificity to safely and selectively target tumor cells and not harm normal, healthy cells. The immune system also has a wide arsenal of molecules that can induce cell death, some of which possess discrete tumoricidal activity. TRAIL and agonistic mAb against TRAIL death receptors kill tumor cells, but have little-to-no toxicity to normal cells [217]. Our laboratory developed an immunotherapy that utilizes TRAIL-mediated tumor cell death *in vivo* that induces a robust systemic antitumor immune response mediated by tumor-specific CD8 T

cells [19, 197, 199]. To further understand the mechanism by which this immunotherapeutic approach is successful, we performed a series of experiments that demonstrated the importance of two distinct DC populations, pDC and CD8α, in the generation of the antitumor CD8 T cell response.

The development of immunotherapies that specifically use or target DC is a major area of interest in the treatment of cancer [218]. While the potential for DC-mediated tumoricidal activity has been reported [219-221], the intended role of DC in tumor immunotherapy is to generate an antitumor T cell response with the potential to deal with disseminated and/or recurrent disease. While the data presented suggest the key role of pDC and CD8α DC in the success of Ad5-TRAIL/CpG therapy in a model of advanced RCC, it is also important to note that the roles played by these DC populations are partially dependent on the successful induction of TRAIL-mediated apoptotic tumor cell death. It is reasonable to think that any agent that induces tumor cell apoptosis would achieve similar effects, but there are many factors that can influence whether apoptotic cell death leads to an immunogenic or tolerogenic outcome [222]. TRAIL is unique in the sense that it selectively induces apoptosis in tumor cells [194], but there is still much to learn in regard to how tumor cells killed by TRAIL are perceived by DC and other cells of the immune system.

We focused our investigation to pDC and CD8α DC, as these DC subsets are classically defined by being able to respond to CpG (and producing proinflammatory cytokines) and cross-present tumor Ag from the apoptotic tumor cells. The CpG ODN used in our studies is thought to function as an adjuvant to activate the immune system to more efficiently respond to the tumor [223]. Unmethylated CpG-containing motifs are specifically recognized by TLR9, and murine pDC, Mϕ, B cells, and all myeloid DC subsets identified to date express TLR9 and respond to CpG [224, 225]. Thus, the inability of pDC-depleted mice to eliminate tumor after Ad5-TRAIL/CpG therapy cannot be explained simply by a failure to respond to CpG. TLR-activated pDC have increased MHC and costimulatory molecule expression giving them the ability to stimulate T cells [226]. Activated pDC also undergo a differentiation process that features production of

proinflammatory cytokines and other molecules that act on other cells of the immune system. In our hands, anti-PDCA1-treated tumor-bearing mice had reduced proinflammatory cytokine production (based on IFN-stimulated gene expression and IL-15/IL-15R production) and effector CD8 T cell infiltration into the tumor-bearing kidney after Ad5-TRAIL/CpG therapy compared to WT replete mice, which together likely contributed to the increased tumor growth and decreased survival.

In vivo depletion of CD8α DC can be achieved a number of ways. For us *Batf3*$^{-/-}$ BALB/c mice proved to be ideal, as these mice are devoid of CD8α DC while still having CD8 T cells [96]. *Batf3* encodes a transcription factor highly expressed in conventional CD11c^{+} DC, and splenic CD11c^{+} conventional DC from *Batf3*$^{-/-}$ mice lack the ability to cross-present Ag to CD8 T cells [96]. Thus, the lack of significant effector CD8 T cell infiltration into the tumor-bearing kidneys of *Batf3*$^{-/-}$ BALB/c mice and absence of a therapeutic benefit after Ad5-TRAIL/CpG administration was expected. It was unexpected to see, however, the minimal response by the *Batf3*$^{-/-}$ BALB/c mice in regard to IFN-responsive gene expression and IL-15/IL-15R production after Ad5-TRAIL/CpG therapy – especially since the *Batf3*$^{-/-}$ BALB/c mice still have pDC (Fig 1). In addition, there was minimal upregulation of costimulatory molecules on the pDC from *Batf3*$^{-/-}$ BALB/c mice after Ad5-TRAIL/CpG therapy. These data suggest that of the two DC populations investigated, CD8α DC may play a more important role in the successful treatment of advanced RCC with Ad5-TRAIL/CpG than pDC.

There is increasing evidence suggesting the necessity for DC subset interaction for the development of optimal T cell responses. Lou *et al.* showed that a mixture of CpG-stimulated pDC plus CD11c^{hi}CD11b^{+} B220^{-} myeloid DC synergized to induce increased Ag-specific CD8 T cell responses and antitumor immunity compared to either DC subset alone [205]. Similarly, Kuwajima *et al.* found pDC were required for the production of IL-12 by CpG-stimulated conventional DC [206]. The role for pDC being essential to license CD8α DC function has been shown in multiple models [205, 227], and data presented herein suggests the possibility for pDC/CD8α DC crosstalk is important in the success of Ad5-TRAIL/CpG immunotherapy. Both cell-to-cell contact and soluble

factors have been suggested to be the molecular mechanism behind DC subset communication [189, 205, 206, 227, 228], but our experiments were not designed to define which of these previously defined (or perhaps some other) mechanisms were being used by the pDC and CD8α DC to communicate with one another, as this would have significantly broadened the scope of the study beyond its initial intention. Future studies are planned to specifically address this aspect, as it will be important to understand the signaling methods that allow pDC and CD8α DC to talk with one another for the generation of a successful antitumor immune response after Ad5-TRAIL/CpG therapy and apply this knowledge to scenarios where the therapy is ineffective.

For years (and still today), metastatic or unresectable cancers of many types have been treated by systemic administration of a drug that directly or indirectly (via modification of the tumor microenvironment) leads to tumor cell death. This approach required careful dosing to demonstrate a reduction in tumor growth without inducing toxic side effects. The refinement of powerful imaging and minimally invasive techniques have improved the identification and access to tumors *in situ,* as well as increasing the types of therapies that can be performed to treat cancer in patients that may have previously had limited therapeutic options [229]. Thus, it seems logical to envision a setting where cancer immunotherapies designed to activate DC would benefit from local injection of the therapeutic molecules directly into the tumor microenvironment. A number of CpG oligonucleotides have been tested in clinical trials, mostly in combination with tumor vaccines and given subcutaneously (perhaps for convenience), and have shown evidence of antitumor activity [230]. However, it is not unreasonable to consider a protocol consisting of CpG delivered directly into the tumor – alone or in combination with another drug with tumoricidal activity. For example, we have examined the tolerability of direct intratumoral injection of Ad5-TRAIL in a phase I clinical trial in men with locally-confined prostate cancer [231], or the systemic administration of TRAIL death receptor agonists [232], which could easily be combined with local CpG therapy. Other drug regimens are feasible, but the potential benefit of intralesional administration of cancer therapies, like CpG, in human remains to be determined.

The findings presented herein are important to the basic biological understanding of how Ad5-TRAIL/CpG therapy for cancer works, as well as being essential for understanding how to modify the use of Ad5-TRAIL/CpG when immunomodulatory co-morbidities are present. For example, Renca-bearing diet-induced obese (DIO) mice do not respond to Ad5-TRAIL/CpG therapy and ultimately succumb to tumor burden, unlike lean controls [202]. I-$A^{d+}$$CD11c^{hi}$ $CD11b^{+}$ splenic DC from the DIO mice had decreased T cell stimulatory capacity compared to the same population of cells from lean mice. However, these markers identify a unique "immunosuppressive" DC population [202] that is mutually exclusive from pDC and CD8α DC (based on the markers used in this study). It is tempting to speculate that in addition to the immunosuppressive I-$A^{d+}$$CD11c^{hi}$ $CD11b^{+}$ DC in DIO mice, altered function of pDC and/or CD8α DC (be it cytokine production, Ag uptake/processing/presentation, or communication needed for DC licensing) also contribute to the failure of Ad5-TRAIL/CpG therapy in tumor-bearing obese mice. Regardless of the different DC populations (pDC, CD8α DC, or immunosuppressive $CD11b^{+}$ DC) examined, knowing which specific DC populations and their functional characteristics are essential for the success of Ad5-TRAIL/CpG therapy.

Figure 2-1: Validation of DC depletion models

Spleens were harvested from WT replete, anti-CD8α-treated, anti-PDCA1-treated, or *Batf3*$^{-/-}$ BALB/c mice. Anti-CD8α or -PDCA1-treated mice were given 250μg and 500μg mAb i.p., respectfully, on 2 consecutive days, after which spleens were harvested and processed for flow cytometry. (**A**) Representative flow plots showing the gating for conventional DC (cDC, MHCII^{+}CD11c^{+}), CD8α DC (gated from MHCII^{+}CD11c^{+}), pDC (gated from MHCII^{lo}CD11c^{lo}B220^{+}) and CD8 T cells (gated from CD3^{+}). Samples from *Batf3*$^{-/-}$ mice were run independently of the other groups, resulting in slight changes in the gating. (**B**) Mean (+ SEM) frequency of DC and T cell populations. (**C**) Mean (+ SEM) total number of DC and T cell populations. Cumulative data from two independent experiments, n=3-4 mice/group/experiment. ns = not significant, * $p \leq 0.05$, *** $p \leq 0.01$, *** $p \leq 0.001$ using 1-way ANOVA with Tukey post hoc test.

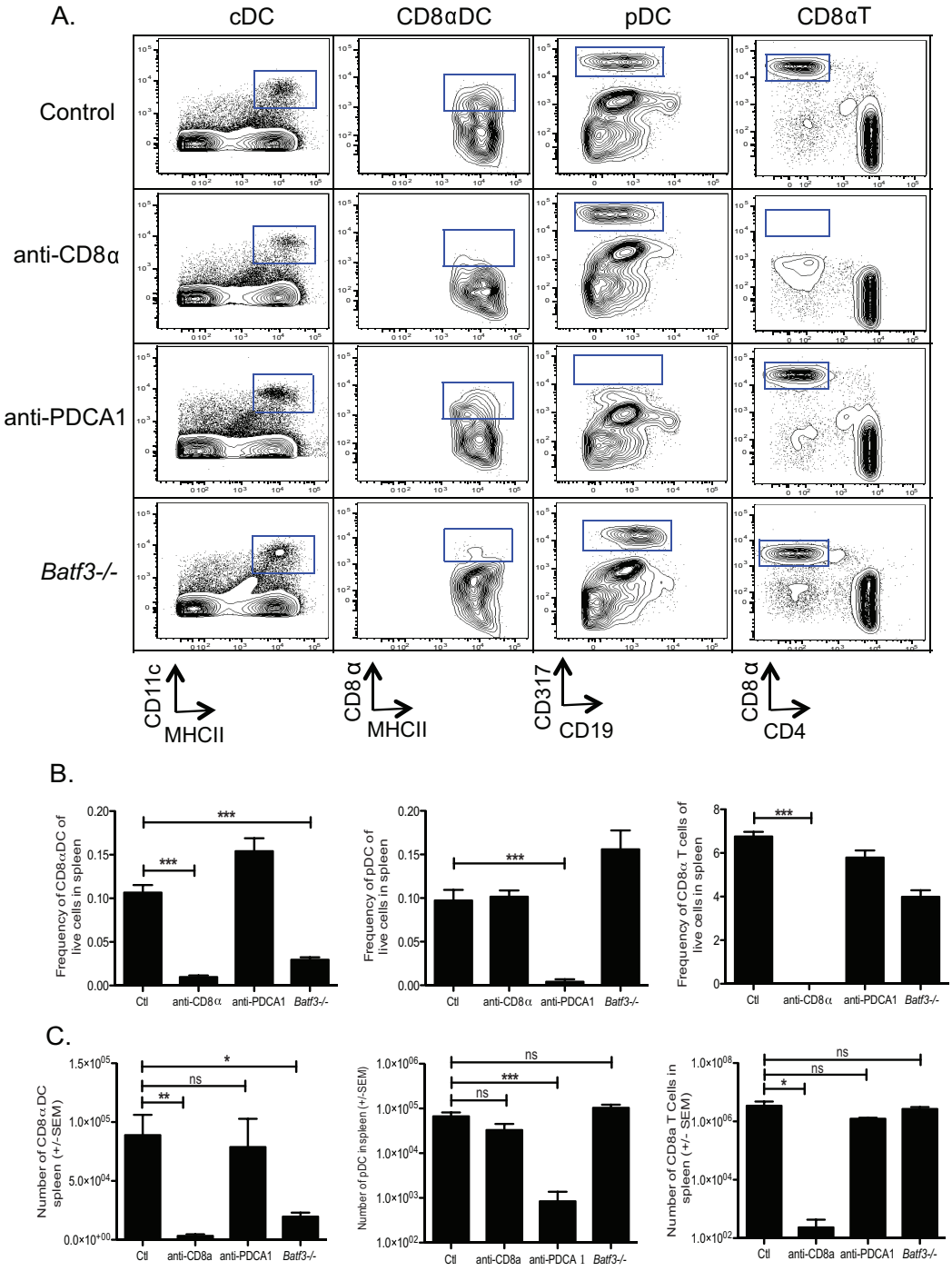

Figure 2-1: Validation of DC depletion models

Figure 2-2: Anti-PDCA1 Ab does not deplete resting B cells

Spleens were harvested from WT replete, anti-PDCA1-treated, or *Batf3*$^{-/-}$ BALB/c mice. Anti-PDCA1-treated mice were given 250μg and 500μg mAb i.p., respectfully, on 2 consecutive days, after which spleens were harvested and processed for flow cytometry. (**A**) Representative flow plots showing the gating for conventional B cells ($B220^{+}CD19^{+}$). Samples from *Batf3*$^{-/-}$ mice were run independently of the other groups, resulting in slight changes in the gating. (**B**) Mean (+ SEM) frequency of B cell.

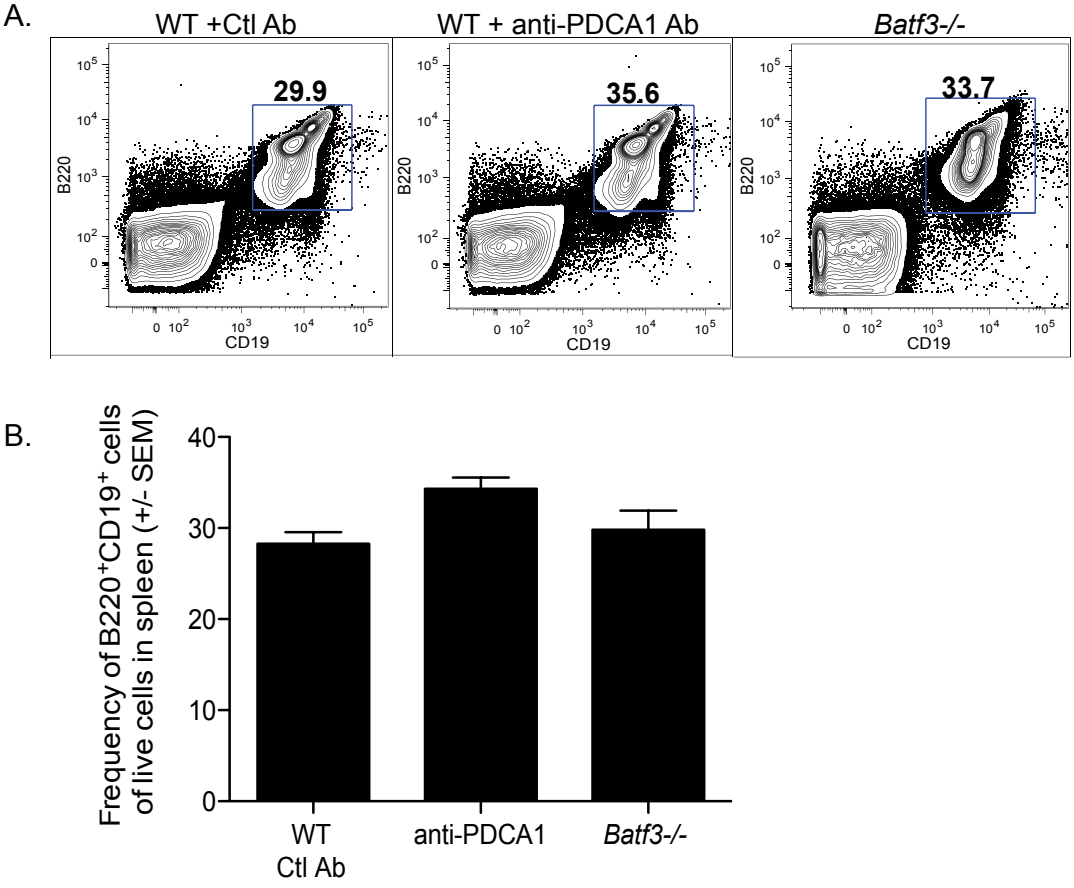

Figure 2-2: Anti-PDCA1 Ab does not deplete resting B cells

Figure 2-3: The presence of tumor does not alter DC depletion in anti-PDCA1-treated or *Batf3-/-* mice

WT replete and *Batf3*$^{-/-}$ BALB/c mice were implanted IR with 2 x 10^5 Renca. On days 5 and 6 some mice were treated with anti-PDCA1 (500μg) mAb i.p after which spleens were harvested and processed for flow cytometry. (**A**) Experimental scheme. (**B**) Mean (+ SEM) frequency of DC populations: pDC (gated from MHCII^{lo}CD11c^{lo}B220^{+}) and CD8αDC (CD11c^{+}MHCII^{+}CD8α^{+}).

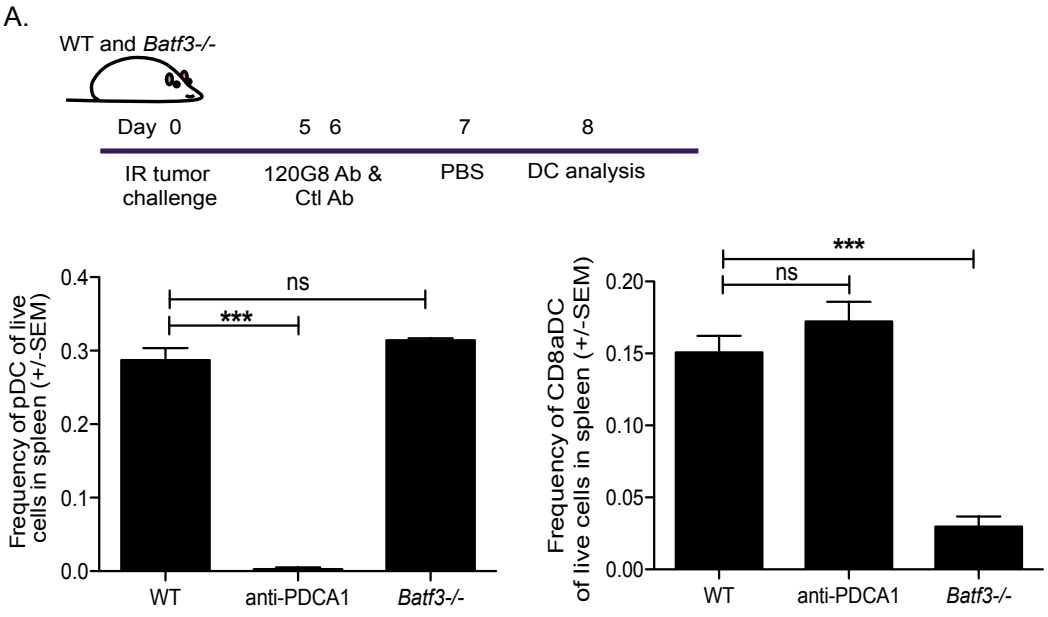

Figure 2-3: The presence of tumor does not alter DC depletion in anti-PDCA1-treated or *Batf3-/-* mice

Figure 2-4: DC depleted mice do not respond to Ad5-TRAIL/CpG therapy

WT replete, anti-PDCA1-treated, and *Batf3*$^{-/-}$ BALB/c mice were implanted IR with 2 x 10^5 Renca or Renca-GLE cells, and then treated with either PBS or Ad5-TRAIL/CpG (Rx) on d 7. (**A**) Mean + SEM tumor-bearing kidney mass (g) for mice harvested when they became moribund (18-21 days, cumulative data from 3 independent experiments, n for each group: tumor-free ctl= 5, WT PBS= 9, WT Rx= 18, ctl Ab= 8, anti-PDCA1= 8, *Batf3*$^{-/-}$ = 7). (**B**) Mean +/- SEM orthotopic tumor burden in mice monitored via bioluminescence. Excised lungs were imaged on d 17 via bioluminescence, for the presence of metastatic tumor burden (cumulative data of multiple independent experiments, n=3-5 mice/group/experiment). (**C-D**) Overall survival for WT replete vs. (**C**) anti-PDCA1-treated mice and (**D**) *Batf3*$^{-/-}$ BALB/c mice that received PBS or Ad5-TRAIL/CpG therapy. All test groups were compared to Ad5-TRAIL/CpG-treated WT replete mice (cumulative data from 3 independent experiments; n= 3-5 mice/group/experiment). * $p \leq 0.05$, ** $p \leq 0.01$, *** $p \leq 0.001$ using 1-way ANOVA with Tukey post hoc test in *A* and 2-way ANOVA in *B*. Log-rank tests were performed in *C-D*.

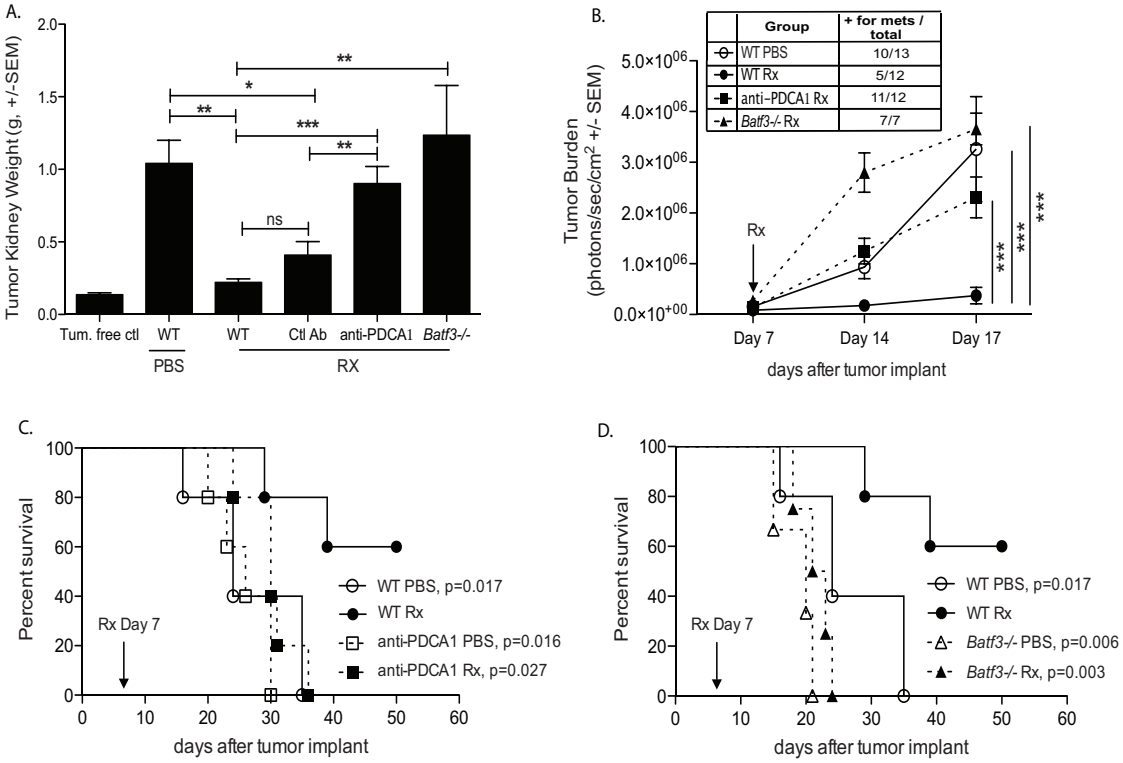

Figure 2-4: DC depleted mice do not respond to Ad5-TRAIL/CpG therapy

Figure 2-5: The absence of CD8αDC results in decreased pDC activation following Ad5-TRAIL/CpG therapy

WT replete, anti-PDCA1-treated, and *Batf3*$^{-/-}$ BALB/c mice were implanted IR with $2x10^5$ Renca cells, and then treated with either PBS or Ad5-TRAIL/CpG (Rx) on d 7. Spleens were harvested 24 h later, made into single cell suspensions, and stained for flow cytometric analysis. Mean + SEM geometric MFI for CD40, CD80, and CD86 expression on (**A**) pDC in *Batf3*$^{-/-}$ mice and (**B**) CD8α DC in anti-PDCA1-treated mice. Data are representative of two independent experiments, n= 4-5 mice/group/experiment. * $p \leq 0.05$, ** $p \leq 0.01$, *** $p \leq 0.001$ using 1-way ANOVA with Tukey post hoc test.

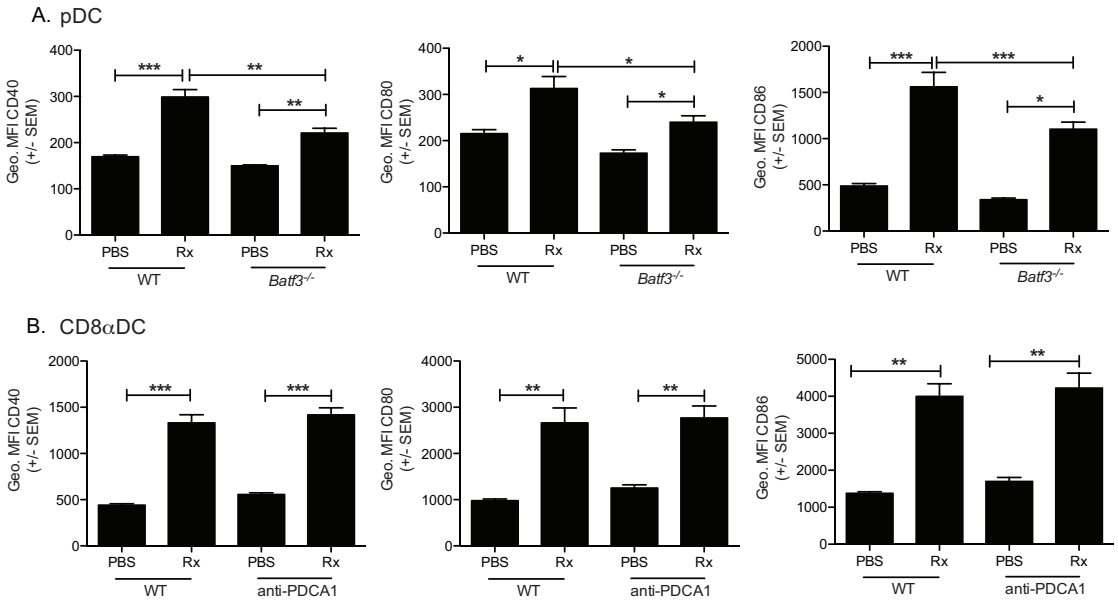

Figure 2-5: The absence of CD8αDC results in decreased pDC activation following Ad5-TRAIL/CpG therapy

Figure 2-6: Ad5-TRAIL alone, CpG alone, and full therapy induce different type I-IFN sub type responses in tumor-bearing kidneys

(**A-B**) WT replete BALB/c mice were implanted IR with $2x10^5$ Renca cells, treated with PBS, Ad5-TRAIL alone, CpG alone, or Ad5-TRAIL/CpG on d 7, and tumor-bearing kidneys were harvested 4 h later. Total RNA was isolated from tumor-bearing kidneys, reverse transcribed into cDNA, and analyzed by qPCR for the abundance of the type I IFN genes. Mean fold change of type I IFN genes was determined relative to tumor-free kidneys. n= 3-5 mice/ group

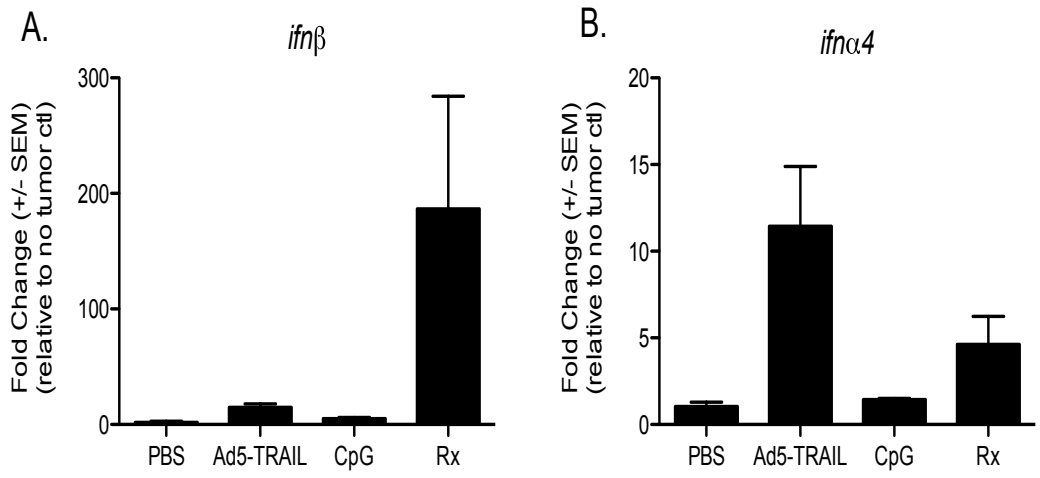

Figure 2-6: Ad5-TRAIL alone, CpG alone, and full therapy induce different type I- IFN sub type responses in tumor-bearing kidneys

Figure 2-7: Ad5-TRAIL/CpG therapy elicits a more robust Type I-IFN response than Ad5-TRAIL or CpG alone

(**A-F**) WT replete BALB/c mice were implanted IR with $2x10^5$ Renca cells, treated with PBS, Ad5-TRAIL alone, CpG alone, or Ad5-TRAIL/CpG on d 7, and tumor-bearing kidneys were harvested 4 h later. Total RNA was isolated from tumor-bearing kidneys, reverse transcribed into cDNA, and analyzed by qPCR for the abundance of the type I IFN-stimulated genes. Mean fold change of type I IFN-stimulated genes was determined relative to tumor-free kidneys. n= 3-5 mice/ group

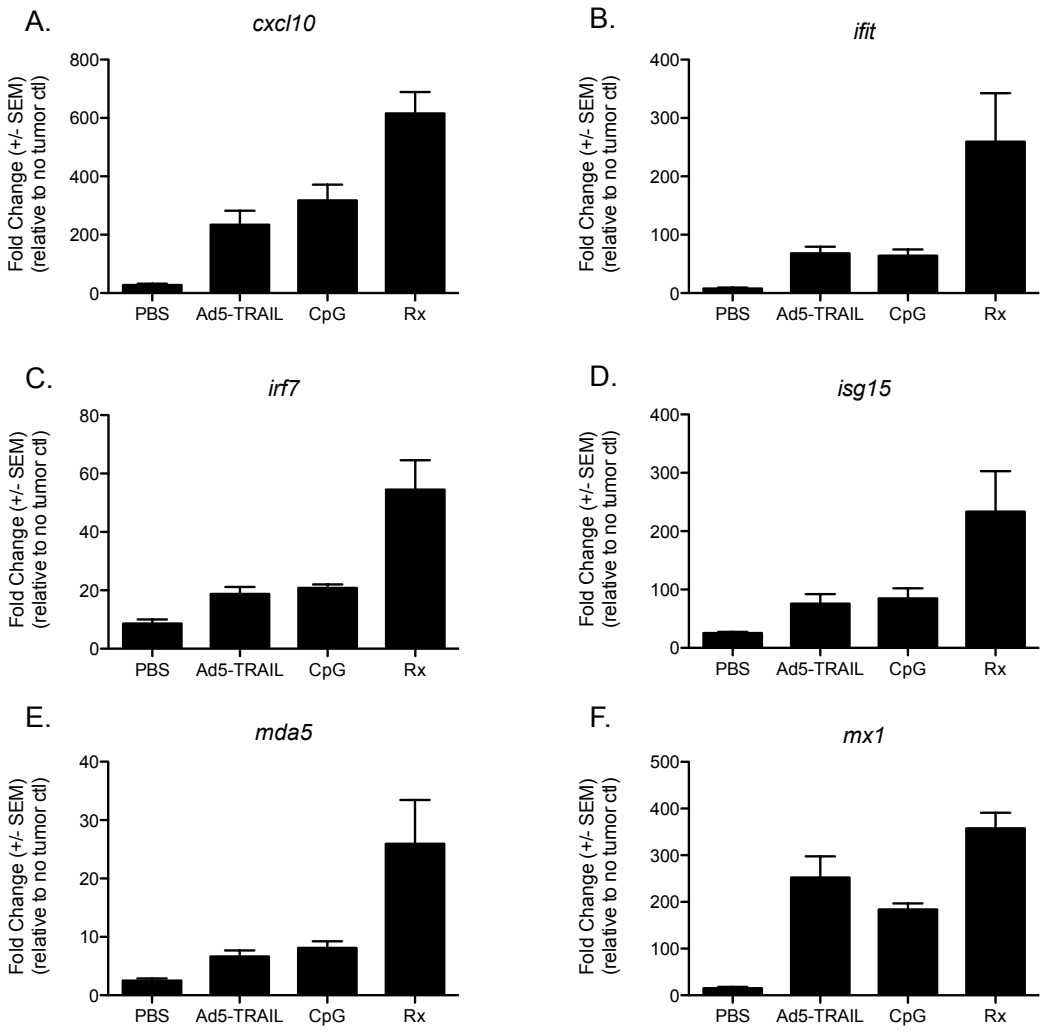

Figure 2-7: Ad5-TRAIL/CpG therapy elicits a more robust Type I-IFN response than Ad5-TRAIL or CpG alone

Figure 2-8: The absence of CD8αDC results in a decreased type I IFN signature within tumor-bearing kidney

(**A-F**) WT replete, pDC-depleted, and *Batf3*$^{-/-}$ BALB/c mice were implanted IR with Renca cells, treated with either PBS or Ad5-TRAIL/CpG (Rx) on d 7, and tumor-bearing kidneys were harvested 4 h later. Total RNA was isolated from tumor-bearing kidneys, reverse transcribed into cDNA, and analyzed by qPCR for the abundance of the type I IFN-stimulated genes. Mean fold change of type I IFN-stimulated genes was determined relative to tumor-free kidneys. Data are representative of three independent experiments, n = 3-5 mice/group/experiment. ns = not significant, * $p \leq 0.05$, ** $p \leq 0.01$, *** $p \leq 0.001$ using 1-way ANOVA with Tukey post hoc test.

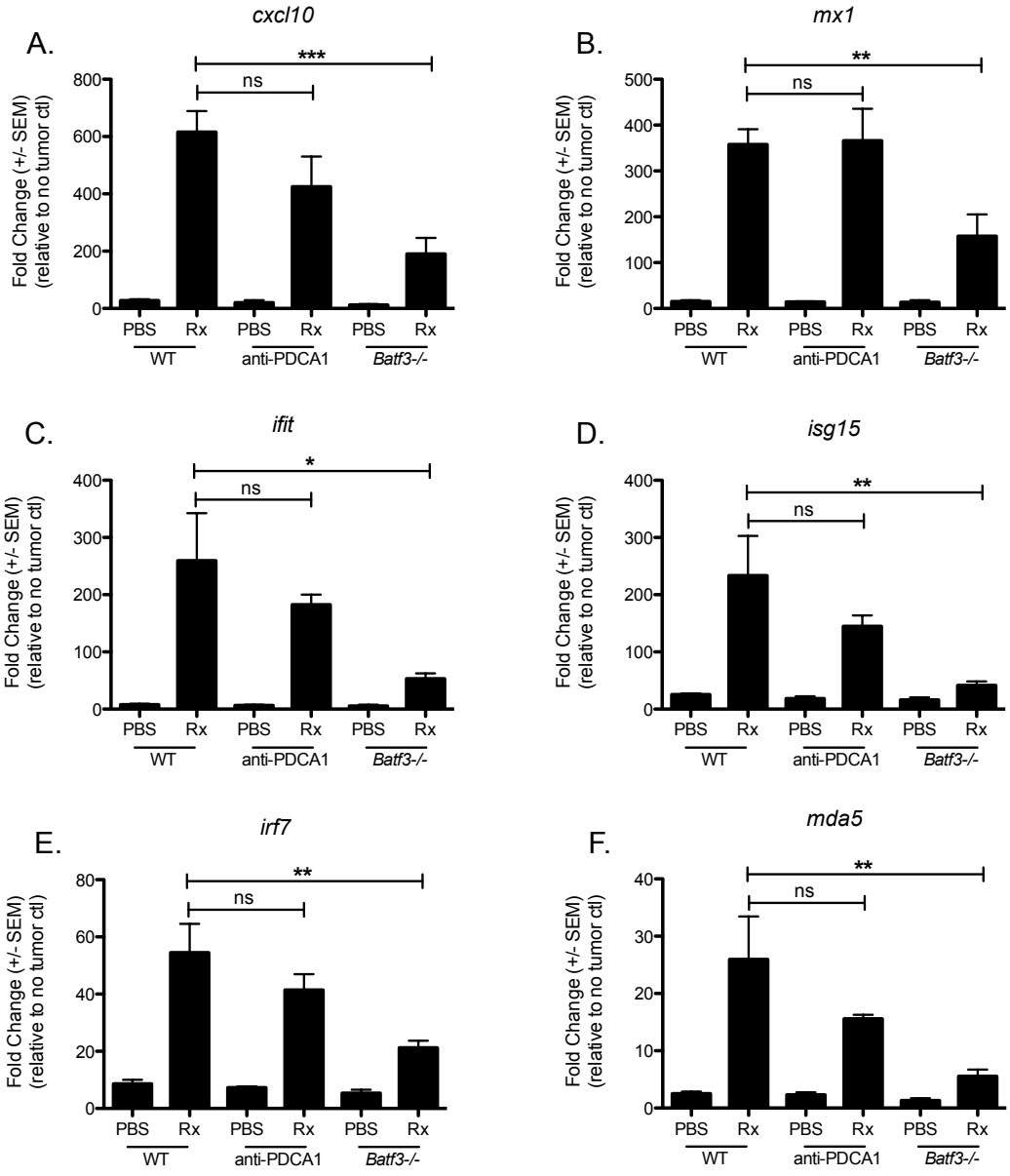

Figure 2-8: The absence of CD8αDC results in a decreased type I IFN signature within tumor-bearing kidney

Figure 2-9: Mice deficient in pDC or CD8αDC have decreased IL-15/IL-15R productions in tumor-bearing kidneys after therapy

WT replete, anti-PDCA1-treated, and *Batf3*$^{-/-}$ BALB/c mice were implanted IR with $2x10^5$ Renca cells, and then treated with PBS or Ad5-TRAIL/CpG (Rx) on d 7. Tumor-bearing kidneys were harvested 24 h later, homogenized, and supernatants were analyzed in duplicate by ELISA for IL-15/IL-15R complexes. n = 4 mice/group/experiment. * $p \leq 0.05$, ** $p \leq 0.01$ using 1-way ANOVA with Tukey post hoc test.

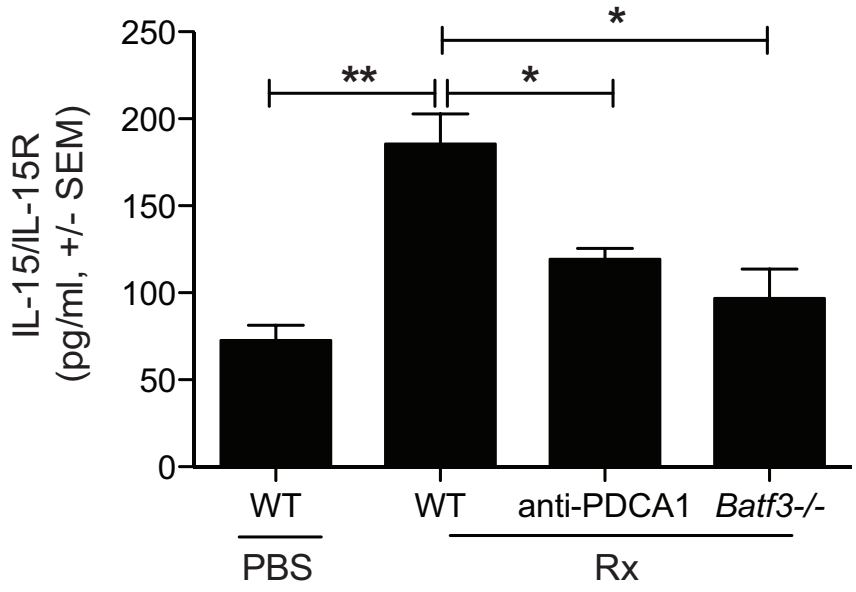

Figure 2-9: Mice deficient in pDC or CD8αDC have decreased IL-15/IL-15R productions in tumor-bearing kidneys after therapy

Figure 2-10: Therapy does not alter specificity of anti-PDCA1 mAb, or *Batf3-/-* phenotype

WT replete, anti-PDCA1-treated, and *Batf3*$^{-/-}$ BALB/c mice were implanted IR with $2x10^5$ Renca cells, treated with either PBS or Ad5-TRAIL/CpG (Rx) on d 7, and spleens were harvested on d 12. Single cell suspensions of spleens were prepared, and stained for flow cytometric analyses to assess immune cell frequency. (**A)** Experiment scheme**. (B-D**) Mean + SEM frequency of pDC, CD8aDC and $CD3^+CD8^+CD44^{hi}$ T cells among total live cells in spleens. n = 4 mice/group. * $p \leq 0.05$, ** $p \leq 0.01$, *** $p \leq 0.001$ using 1-way ANOVA with Tukey post hoc test.

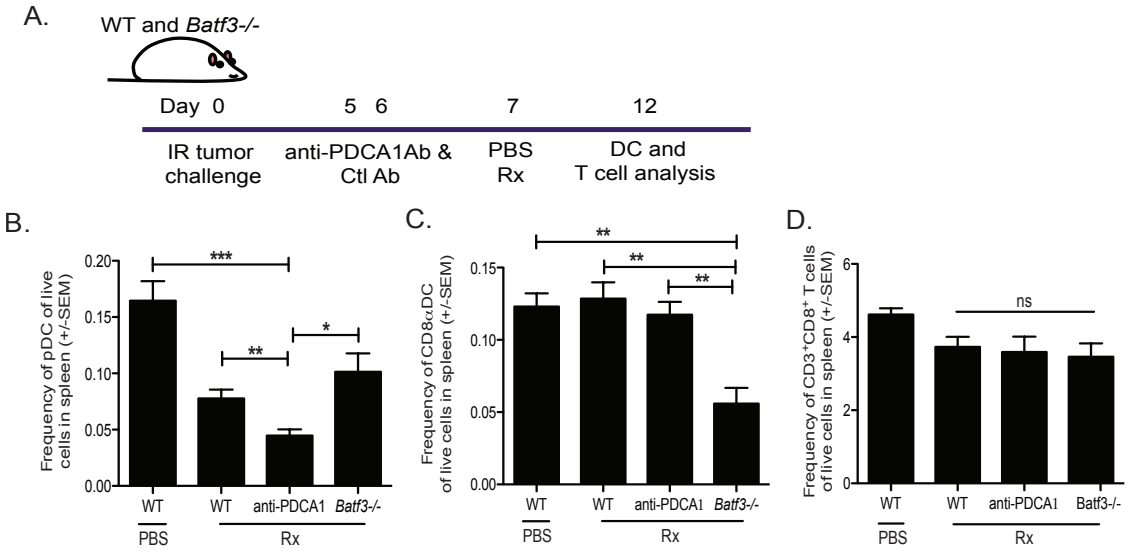

Figure 2-10: Therapy does not alter specificity of anti-PDCA1 mAb, or *Batf3-/-* phenotype

Figure 2-11: DC depleted mice have a blunted CD8 T cell antitumor response compared to WT-replete mice following Ad5-TRAIL/CpG therapy

Absence of pDC or CD8α DC results in a blunted effector CD8 T cell infiltration into the tumor after Ad5-TRAIL/CpG. WT replete, anti-PDCA1-treated, and *Batf3*$^{-/-}$ BALB/c mice were implanted IR with 2x10^5 Renca cells, treated with either PBS or Ad5-TRAIL/CpG (Rx) on d 7, and kidneys were harvested on d 12. Prior to harvest, all mice were injected i.v. with PE-conjugated anti-CD45.2 mAb (3 μg) in PBS and sacrificed 3 min later. Single cell suspensions of tumor-bearing kidneys were prepared, and stained for flow cytometric analyses to assess immune cell infiltration. (**A-B**) Mean + SEM frequency of CD3$^+$CD8$^+$CD44^{hi} T cells among (**A**) total live cells or (**B**) CD45.2$^+$ cells within tumor-bearing kidneys. (**C-D**) Intravascular staining reveals that the majority of CD3$^+$CD8$^+$CD44^{hi} T cells within tumor-bearing kidneys, regardless of receiving PBS or Ad5-TRAIL/CpG, are located within the tissue. Representative gating from each group are presented in (**C**), and mean + SEM data are in **(**D). (**E**) Mean + SEM frequency of KI67$^+$ cells within the CD3$^+$CD8$^+$CD44^{hi} effector phenotype CD8 T cell gate. (**F**) Mean + SEM geometric MFI for CD11a expression on the CD3$^+$CD8$^+$CD44^{hi} effector phenotype CD8 T cells. Cumulative data from two independent experiments shown, n= 5 mice/group/experiment. * $p \leq 0.05$, ** $p \leq 0.01$, *** $p \leq 0.001$ using 1-way ANOVA with Tukey post hoc test.

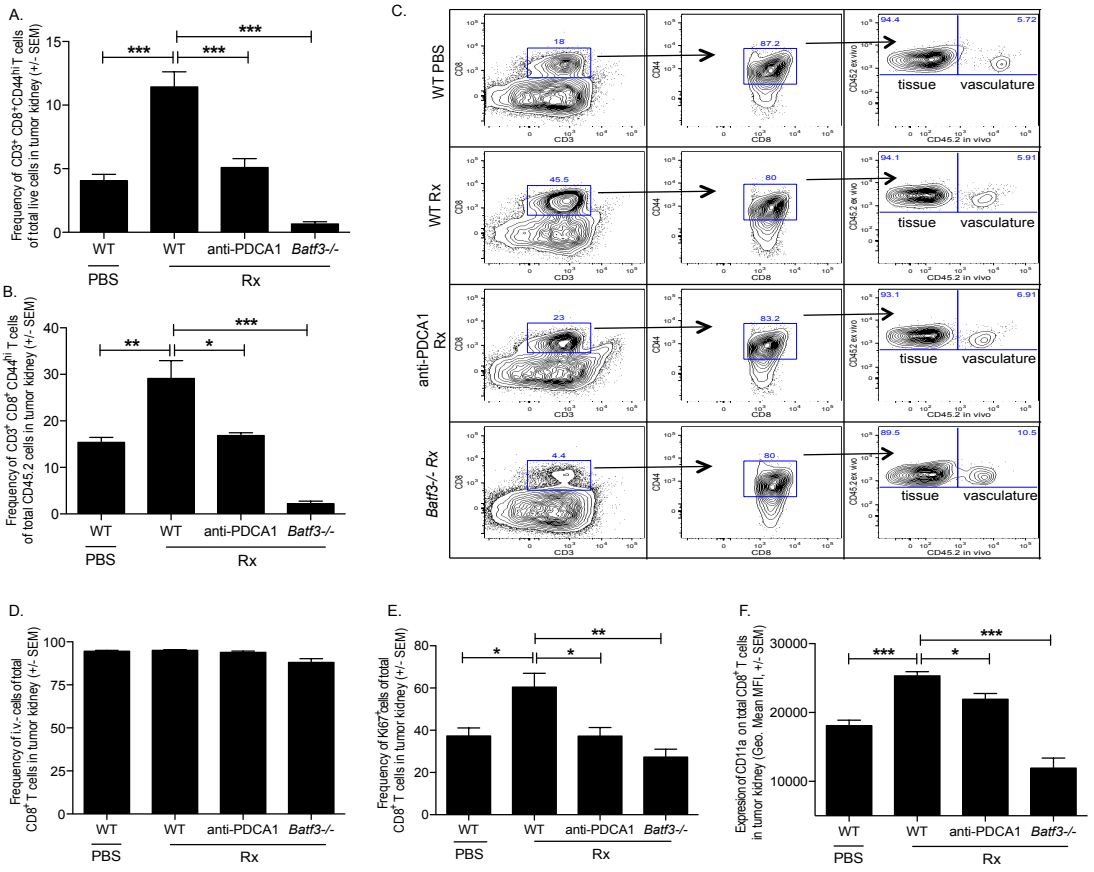

Figure 2-11: DC depleted mice have a blunted CD8 T cell antitumor response compared to WT-replete mice following Ad5-TRAIL/CpG therapy

Figure 2-12: DC-depleted mice have a decreased number of effector CD8 T compared to WT-replete mice after Ad5-TRAIL/CpG

Absence of pDC or CD8α DC results in a blunted effector CD8 T cell response after Ad5-TRAIL/CpG. WT replete, anti-PDCA1-treated, and *Batf3*$^{-/-}$ BALB/c mice were implanted IR with 2x10^5 Renca cells, treated with either PBS or Ad5-TRAIL/CpG (Rx) on d 7, and kidneys were harvested on d 12 and processed for either surface staining or plated and cultured for intracellular staining to assess T cell functions. For the T cell assay whole tumor cells were plated with PMA and ionomycin in the presence of BFA for 6 hrs. Cells were then harvested and stained for intracellular cytokine production from CD8 T cells. (**A**) Mean + SEM total number of $CD3^+CD8^+CD44^{hi}$ T cells in tumor bearing kidneys. **(B)** Mean + SEM total number of IFN-γ producing T cell s based on the mean number of CD8 T cells present in the tumor-bearing kidney. Cumulative data from two independent experiments shown, n= 5 mice/group/experiment. * $p \leq 0.05$, ** $p \leq 0.01$ using student's t-test.

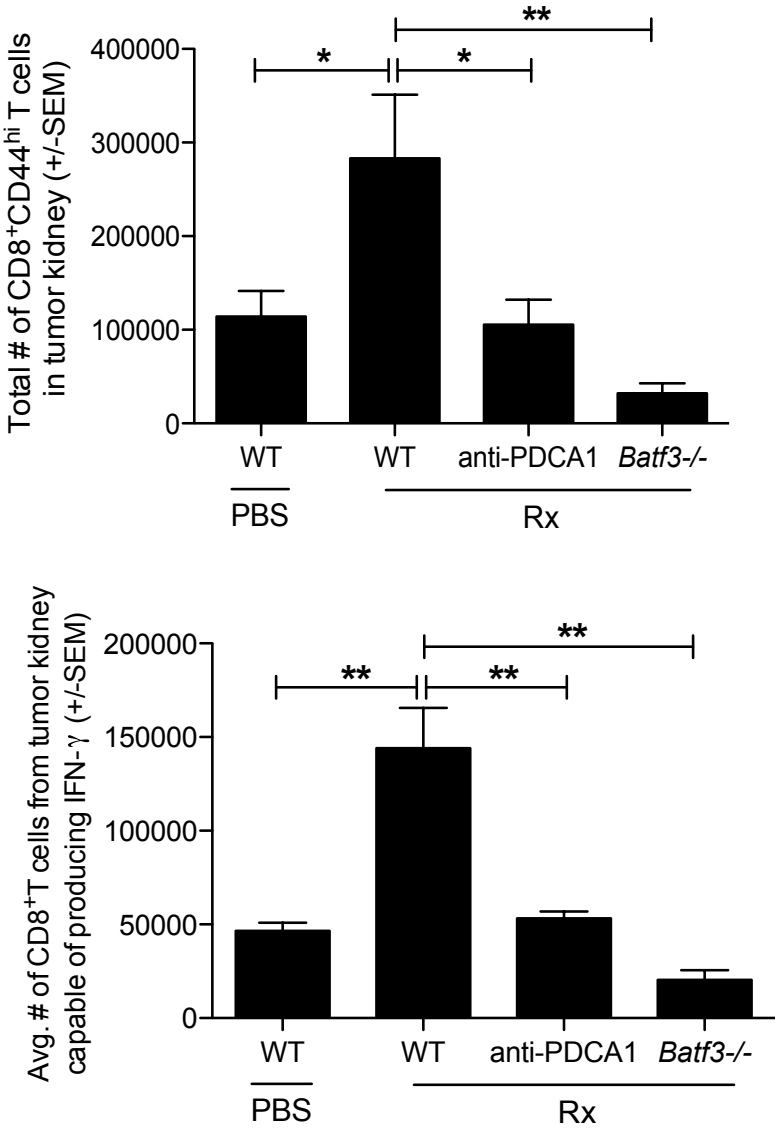

Figure 2-12: DC-depleted mice have a decreased number of effector CD8 T compared to WT-replete mice after Ad5-TRAIL/CpG

Acknowledgement: The work in this chapter was modified from "Effective TRAIL-based immunotherapy requires both plasmacytoid and CD8α dendritic cells" published in *Cancer Immunology, Immunotherapy.* PMID: 24711083

Chapter 3: Diet-induced obesity alters dendritic cell function in the presence and absence of tumor growth

Introduction

Immune-based therapy for solid tumors provides the potential for long-lived protection against cancers of various stages – including metastatic cancer. However, even the most successful immunotherapy-based clinical trials only show objective response rates in <50% of the patients[1]. Many factors may account for this limited clinical success, including preclinical use of young, normal weight ("lean") animals lacking immunomodulatory co-morbidities present in many cancer patients. Obesity is one of the most critical health care concerns in the U.S. today, as a large majority of adults are considered overweight or obese. Obese individuals face an increased risk of developing cancer, including RCC[233, 234]. Morbidity and mortality associated with cancer are also greater in obese persons. The reasons for this are unclear but may include such factors as increased rates of tumorigenesis, accelerated tumor outgrowth, and diminished antitumor immunity. Currently, the confounding effects of obesity on immunotherapeutic efficacy in cancer patients are unknown, and given the number of adults affected by obesity, more research in this area is needed.

Obesity is characterized by numerous physiological changes that may directly or indirectly influence the immune system. In the obese, visceral adipocytes secrete high levels of proinflammatory cytokines such as TNF-a, and IL-6, triggering a chronic, low-grade systemic inflammation[174, 235-238]. In mice, obesity can be induced through genetic means or prolonged feeding of high-fat feed (HFF). Genetically modified mice rapidly develop obesity, but diet-induced obesity represents a clinically relevant model with slower progression, characterized by increased leptin (an immunomodulatory protein produced by fat cells) production and systemic inflammation[239-241]. Studies using tumor-free diet-induced obese (DIO) mice have defined a number of alterations and defects in immune cell function, including altered differentiation of adipose tissue macrophages,

diminished dendritic cell antigen presentation during infection, decreased stimulatory capacity in bulk splenic antigen presenting cells, reduced secondary expansion of CD8+ T cells, and reduced IFNγ production by memory T cells [178-180, 242, 243]. Due to the negative effects of obesity on the immune system, studies are needed to provide a framework from which novel immunotherapies can be developed for patients with metastatic RCC that is complicated by such co-morbidities.

At this time, a thorough evaluation of highly purified, steady-state DC from DIO mice has not been performed, and the DIO DC response to tumor outgrowth is unclear. The aforementioned findings suggest that DC-dependent antitumor immunotherapies would be less effective in the obese, but this has not yet been demonstrated. DC are key regulators of T cell immunity, therefore normal DC function is essential for achieving T cell-mediated tumor clearance[86, 244]. Given the importance of understanding how obesity and tumor outgrowth collectively impact immune function, we examined how obesity influences DC function in the presence and absence of tumor growth. For tumor studies, we used an orthotopic RCC model, in which parental or luciferase-expressing Renca tumor cells were injected directly into murine kidneys and then measured renal tumor growth via bioluminescent imaging (BLI). We then administered a DC-dependent immunotherapy and found that its efficacy was greatly reduced in DIO mice. Our findings suggest that preclinical murine studies evaluating the efficacy of novel immunotherapies should examine host responsiveness in not only lean mice but also in obese mice, because results in the latter may differ substantially. Doing so may speed the development of immunotherapeutic regimens that show efficacy in obese cancer patients.

Materials and Methods

Animals and diets

Female wild-type BALB/c mice (7-8 wk old) were purchased from the National Cancer Institute (Frederick, MD), and *Batf3*$^{-/-}$ BALB/c breeder mice were purchased from Jackson Laboratories (Bar Harbor, ME). For diet-induced obesity (DIO) studies, mice were randomly assigned to either standard chow or high fat feed (HFF; Research Diets

#12492, 60% kcal from fat [202]). After 20 weeks, mice in the HFF group were defined as obese if their body weight was >3 S.D. above the mean of the mice fed standard chow ("lean"). All mice were housed under pathogen-free conditions at the University of Minnesota Animal Care Facility, which is fully accredited by the Association for Accreditation of Laboratory Animal Care. All animal procedures were approved by the Institutional Animal Care and Use Committee at The University of Minnesota.

Cell lines and tumor challenge

The murine renal adenocarcinoma cell line, Renca [201], was obtained from Dr. Robert Wiltrout (National Cancer Institute, Frederick, MD), and was authenticated in 2010 by microsatellite marker analysis (Research Animal Diagnostic Laboratory, Columbia, MO). Renca cells were maintained in RPMI supplemented with 10% fetal bovine serum, penicillin, streptomycin, sodium pyruvate, non-essential amino acids, 2-mercaptoethanol, and HEPES (hereafter referred to as complete RPMI), as previously described [19].
For intrarenal (IR) tumor challenge, mice were anesthetized, a skin incision was made on the left flank, and $2x10^5$ Renca cells were injected through the intact peritoneum into the left kidney in a 100 μl volume of HBSS [19, 202]. On d 7, mice were injected in the tumor-bearing kidney with sterile PBS alone, Ad5-TRAIL (10^9 pfu) [199], and/or the nonmethylated CpG ODN 1826 (5'-tccatgacgttcctgacgtt-3', 100 μg; IDT, Coralville, IA) with a phosphorothioate-modified backbone for nuclease resistance in a 100 μl volume.

DC enrichment and isolation from tumor-bearing mice

DC were harvested from spleens or tumor-bearing kidneys, as indicated. Organs were removed, manually disrupted, and then digested for 15–30 min in HBSS containing 0.56 Wuensch U/ml Liberase Blendzyme 3 (Roche, Branford, CT) and 0.15 mg/ml DNAse I (Sigma-Aldrich, St. Louis, MO). Single-cell suspensions were prepared as described previously[245]. DC were enriched using Miltenyi Biotec anti-CD11c microbeads and then sort-purified on a BD Aria II or FACSDiva based on expression of the following markers: $CD45^+/CD11c^{high}/CD11b^+/Gr\text{-}1^-$ after gating on live cells via Hoechst 33258 exclusion.

T cell proliferation and inhibition assays

T cells were harvested from naïve DUC18 TCR transgenic mice [246], incubated with Miltenyi anti-CD8α microbeads and purified over two sequential columns, collecting the bound fractions. The percentage of CD8 T cells was determined via flow cytometry, based on surface co-expression of CD8α and Vβ8.3. T cell proliferation was assessed by culturing naive DUC18 T cells ($5x10^4$ cells/well) with tERK peptide-pulsed splenic DC (spDC, $5x10^3$ cells/well) from either lean or DIO tumor-free BALB/c mice in a flat-bottom 96-well plate. [^{3}H] Thymidine was added to co-cultures during the final 18 h of 72 h incubation. DC inhibition of T cells proliferation was assessed culturing the DUC18 T cells and tERk peptide-pulsed spDC from control tumor-free BALB/c mice as stated above, with sort purified renal DC from tumor bearing mice ($5x10^3$ cells/well). T cell inhibition was calculated as the percent decrease in T cell proliferation with renal DC present relative to that seen for DUC18 T cells cultured with control, peptide-pulsed spDC alone.

Flow cytometry

Single cell suspensions of tumor-bearing or contralateral kidneys, and spleens were prepared using a gentleMACS Dissociator (Miltenyi BioTeck Inc., Auburn, CA), and then digested for 15-30 min in HBSS containing 0.56 Wuensch units/ml of Liberase Blendzyme 3 (Roche, Branford, CT) and 0.15 mg/ml DNAse I (Sigma, St. Louis, MO). Cells were then blocked using a cocktail of anti-CD16/32 and normal mouse serum before surface staining. Cells were stained with combinations of the following mAb (eBioscience (San Diego, CA) or BioLegend (San Diego, CA)) and analyzed using multi-parameter flow cytometry on a BD LSR II (BD Biosciences, San Diego, CA) and FlowJo software (TreeStar Inc., Ashland, OR): For DC: CD11c biotin, streptavidin-APC/Cy7, CD11b-PE/Cy7, Gr1-APC, I-A_d-PE, CD4-FITC, CD8-PerCP-Cy5.5, CD83-A488, CD86-APC, H-2K_d-FITC, CD40-APC, and Hoechst; for T cells: CD3-PE, CD8-APC, CD4-PE/Cy7, CD11a-FITC, IFNg-PerCP-Cy5.5, and Hoechst.

Cytokine and chemokine evaluation by BioPlex

Splenocytes from lean and DIO mice were cultured overnight at $1x10^6$cells/well in complete medium in the presence or absence of 5μg CpG. Supernatants were harvested and frozen at -80°C until use. Supernatant concentrations of 32-analytes including cytokines and chemokines were determined via Multiplex analysis (Milliplex MAP kits; Millipore) on a Bio-Rad BioPlex

In vivo CTL assay

The mouse-adapted A/PuertoRico/8/34 (PR8; H1N1) IAV strain was obtained from Dr. Kevin Legge (University of Iowa, Iowa City, IA). Lean and DIO mice were anesthetized by isoflurane and infected intranasally with a $0.1LD^{50}$ dose of PR8 in 50 ul Iscove's media on d0. For the in vivo CTL assay, naive BALB/c splenocytes were pulsed with 10μM IAV $HA_{518-526}$ peptide (Anaspec, Fremont, CA). Non-pulsed (reference) and peptide-pulsed (target) cells were labeled with 0.5μM CFSE (target) obtained from Dr. Ross Fulton (University of Minnesota, Minneapolis, MN) and reference cells were labeled with 5.0μM CFSE. Equal numbers of reference and target cells were mixed and $1\text{-}2x10^7$ total cells were transferred i.v. into naive mice or lean and DIO mice that had been infected with IAV 10 days earlier. Lungs were harvested 8 hrs post-transfer and the relative frequencies of reference and target cells were examined via flow cytometry. The reduction in the number of recovered peptide-pulsed target cells in the IAV-infected versus naive mice was considered the percent specific lysis.

Statistical analysis

Statistical analysis between groups was determined by unpaired Student's *t*-test, where appropriate. Statistical analyses of tumor growth kinetics and survival between groups were performed via 2-way ANOVA, and Log-rank tests, respectively. Data was analyzed with Prism4 GraphPad software and statistical significance is indicated in figure legends (*** $p \leq 0.0001$; ** $p \leq 0.001$; * $p \leq 0.05$; not significant (n. s.))

Results

DIO mice exhibit classic signs of obesity

The majority of prior studies on murine DIO used the C57BL/6 strain, because these mice rapidly become obese after being placed on HFF[239, 241]. Because our goal was to determine the combined effects of renal tumor outgrowth and obesity on DC function, our experimental model necessitated using the BALB/c strain for Renca RCC tumor challenge. To examine the role obesity plays in RCC tumor progression and response to therapy we developed a DIO model where BALB/c mice were fed HFF for 20 wk and characterized for classic signs of obesity including weight, visceral body fat content, and serum leptin levels[172]. We observed that 45–55% of BALB/c mice on HFF showed increased weight gain relative to age-matched mice fed standard chow over the same period of time (Figure 3-1). Therefore, we defined DIO mice as those having a final weight of greater than the mean weight + 3 SD of age-matched lean mice that had been fed standard chow for 20 wk. Compared with lean mice, DIO mice had increased percentages of visceral body fat and increased concentrations of serum leptin (Figure 3-1).

DIO mice have an increased frequency of splenic cDC

As a prior report had shown increased percentages of $CD11c^+$/MHC II^+ spDC in leptin deficient ob/ob C57BL/6 mice [242], we examined the percentages of steady-state spDC in BALB/c DIO mice to determine whether these mice also had increased percentages of spDC. Conventional spDC are identified by high CD11c expression, which differentiates them from other cell populations that can express intermediate to low levels of this integrin [101, 102]. We observed increased percentages of $CD11c^{high}$ spDC in DIO mice (Figure 3-2). An analysis of $CD11c^{high}$ DC subsets revealed equivalent percentages of $CD8a^+$ DC, $CD4^+$ DC, $CD11b^+$ DC, and $CD8^-$/$CD4^-$ double-negative DC in the spleens of lean and DIO mice (Figure 3-2). Of note, total live splenocyte counts were nearly identical in lean and DIO mice, indicating that the obesity-associated inflammation had not resulted in overall increases in splenic cellularity. Thus, our findings in BALB/c DIO

mice support those reported earlier by Macia et al. during their study of leptin deficient obese mice.

Leukocytes from naïve DIO have an altered functional capacity

Previous investigations into the effects of obesity on DC stimulatory capacity produced conflicting results. Studies on naive animals had found that bulk splenic APCs from DIO mice and bone marrow derived DC from leptin-deficient ob/ob mice were less able to stimulate naive T cell proliferation than were cellular counterparts from lean mice [242, 243]. In contrast, another report found that during influenza infection, lung DC from DIO mice retained the ability to induce IFN-γ production in T cells[179]. Therefore, our next set of experiments addressed whether DIO impacted the steady-state stimulatory capacity of highly purified spDC. For these experiments, spDC were sort purified from lean or DIO mice by gating on $CD45^+/Gr\text{-}1^{neg}/CD11c^{high}/CD11b^+$ cells. We focused on $CD11b^+$ DC, because it had been determined previously that this subpopulation accumulated within murine fibrosarcomas and mammary carcinomas [245], we therefore wanted to determine whether baseline differences were present in the stimulatory capacity of this DC subset in tumor-free DIO versus lean mice. Following purification, spDC were pulsed with tERK peptide and used to stimulate $CD8^+$ TCR-transgenic DUC18 T cells in vitro. The data illustrated that spDC from DIO mice induced less T cell proliferation than their lean counterparts (Figure 3-3). Overall, mean T cell proliferation in the presence of DIO spDC was 58% of that seen with lean spDC.

We next wanted to examine what functional difference may be present between lean and DIO spDC that would account for decreased T cell proliferation and presumed function. A main function of APC, specifically to activate and aid in proliferation of T cells, is robust cytokine/chemokine production. To assess the cytokine/chemokine production by splenocytes, spleens were harvested from both DIO and lean mice and stimulated overnight with CpG (the immune adjuvant present in our immunotherapy). Supernatants were then tested for concentrations of 32 different chemokines and cytokines. We found that supernatants from DIO and lean stimulated splenocytes differed significantly (Figure 3-4). DIO splenocytes produced elevated levels of multiple pro-

tumorigenic chemokines/cytokines such as IL-17[247], CXCL-5 [248], and MIP-2 [249], while producing lower levels of several anti-tumorigenic chemokines/cytokines (IP-10[116] and IL-15[250]). These data, along with the data in figure 3 suggest that the splenocytes from DIO mice have an altered functional capacity.

Decreased T cell function in mice fed HFF has also been reported in the literature[180, 243]. To assess if the T cells in our DIO mice were functional, we utilized an influenza-priming model to test for T cell cytolytic (CTL) function. To determine whether the cytolytic activity of DIO effector $CD8^+$ T cells was also diminished, we performed an in vivo CTL assay using lean and DIO influenza-infected mice, because this model system allowed us to readily evaluate site-specific cytolytic activity in vivo. Mice were infected with influenza A virus (IAV) and injected with duel CFSE labeled DC that had either been HA-pulsed (target) or not (reference) 10 days later. CTL activity was determined 8hrs later by loss of the target population relative to the reference population. DIO mice exhibited a significant decrease in the their ability to specifically lyse target calls, indicative of a decreased CTL response, compared to lean controls (Figure 3-5). These data, combined with figured 3 and 4 suggest that leukocytes in non-tumor bearing DIO animals are significantly altered.

DIO mice have accelerated tumor growth

Once a baseline examination of steady-state leukocyte function had been performed in tumor-free DIO versus lean mice, we examined the combined effects of tumor outgrowth and obesity on DC function. Previously seen was that tumor-infiltrating $CD11c^+$ /$CD11b^+$/Gr-1^{neg} DC (TIDC) from lean mice acted as regulatory cells that suppressed T cell proliferation *ex vivo* and impeded antitumor immunity *in vivo*, leading to enhanced tumor outgrowth[245]. Currently, the impact of obesity on antitumor immunity is unclear, and it is not known how or whether obesity and tumor growth interact to further alter DC function. Our experiments made use of an orthotopic RCC model, in which luciferase-expressing Renca tumor cells were injected directly into the left kidney of DIO or lean mice after 20 wk of feeding either HFF (DIO) or standard chow (lean). This system allowed us to measure renal tumor burdens over time in live mice via BLI. BLI revealed

that early tumor growth through day 7 was more rapid in DIO mice as compared with lean counterparts; however tumor-bearing kidney masses remained comparable at day 7 (Figure 3-6).

DIO mice have increased frequency of regulatory TIDC

We then evaluated DC infiltration after renal tumor growth had continued unchecked for more than 3 wk. Advanced tumor outgrowth was accompanied by increased percentages of DC in the tumor-bearing kidneys of DIO mice (Figure 3-7). On the basis of our prior work showing that TIDC from multiple tumor types functioned as suppressor cells, we evaluated the inhibitory capacity of renal TIDC from DIO and lean mice. To accomplish this, $CD11c^{+}/CD11b^{+}/Gr\text{-}1^{neg}$ DC were sort purified from the kidneys of mice with advanced renal tumor growth, as evidenced by BLI. Performing DC isolations in this manner allowed us to control for variations in tumor outgrowth rates and to isolate DC when tumor burdens were similar. Following sort purification, renal DC from tumor-bearing kidneys were put into culture with naive DUC18 T cells and stimulatory tERK peptide-pulsed spDC from young, lean tumor-free mice. We then determined DC-suppressive capacity by measuring decreases in T cell proliferation, relative to control wells that contained only T cells and stimulatory spDC. Mean results from three independent experiments showed a significantly stronger inhibitory capacity in DC from tumor-bearing kidneys of DIO mice, as compared with counterparts from lean mice (Figure 3-7). Although the suppressive capacity of DIO TIDC was moderate on a per cell basis, increased frequencies of these cells were present in the tumor-bearing kidneys of DIO mice. This raised the possibility that the net effect might be a noticeable inhibition of tumor clearance in vivo.

We next examined the degree of DC infiltration into tumor-bearing kidneys following therapy, to see if therapy would alter the accumulation. We found that tumor bearing kidneys from DIO mice treated with Ad5TRAIL/CpG had increased percentages of DC: ~14-fold higher than what was seen in Ad5TRAIL/CpG -treated lean mice (Figure 3-8). Of note, Ad5TRAIL/CpG in lean mice decreased the percentage of DC compared to untreated lean tumor-bearing mice. In Ad5TRAIL/CpG -treated DIO mice,

the increased percentage of renal DC was again specific to the tumor site, because increased DC percentages were not evident in non–tumor-bearing contralateral kidneys. The spleens of Ad5TRAIL/CpG -treated DIO mice did trend toward having an increased percentage of DC relative to similarly treated lean spleens, but this difference was not significant (Figure 3-8).

We next assessed DC function from DIO tumor-bearing kidneys to determine whether administration of immunotherapy had diminished the suppressive capacity of these cells. Experiments similar to those described above were performed, this time using sort-purified renal DC from DIO Ad5TRAIL/CpG -treated mice. Even in the presence of immunotherapy, renal DC from tumor-bearing DIO mice inhibited T cell proliferation (Figure 3-8). Suppressive function was specific to DC from tumor-bearing kidneys, because DC isolated from the spleens of Ad5TRAIL/CpG -treated tumor-bearing DIO mice showed no inhibition of T cell proliferation. Cumulatively these data suggest that the DIO environment elicits a robust accumulation of a TIDC population that is unchanged in the context of immunotherapy.

DIO mice do not respond to Ad5-TRAIL/CpG therapy

The endogenous immune response to Renca tumors is not protective, but we had determined previously that administration of immunotherapy could induce DC- and T cell-dependent Renca eradication in lean mice[19, 251]. Successful Ad5-TRAIL/CpG therapy relies upon DC presentation of Ag derived from apoptotic tumor cells to CD8 T cells, which then become the main effectors of tumor clearance. Given the elevated percentages of suppressive DC in tumor-bearing kidneys from DIO mice, we predicted that DIO mice would have a reduced ability to clear Renca tumors following administration of Ad5-TRAIL/CpG immunotherapy. DIO and lean mice were challenged s.c. with Renca tumor cells on day 0, followed by either Ad5-TRAIL/CpG therapy or PBS on day 7 (directly into tumors). Lean mice that had received Ad5-TRAIL/ CpG on day 7 showed a substantial reduction in tumor growth as compared with PBS-treated lean mice (Figure 3-9). In contrast, DIO mice that received Ad5-TRAIL/ CpG on day 7 showed no decrease in tumor burden relative to PBS-treated DIO mice. An examination of survival in s.c.-

challenged DIO versus lean mice revealed that whereas 80% of lean mice survived long-term after Ad5-TRAIL/ CpG therapy, all treated DIO mice succumbed to their tumors (Figure 3-9). Thus, an immunotherapy that was able to reverse tumor outgrowth in lean mice was ineffective in DIO mice.

DIO mice have a blunted CD8 T cell response following Ad5-TRAIL/CpG therapy

The inability of Ad5-TRAIL/CpG therapy to control tumor outgrowth in DIO mice prompted us to evaluate CD8 T cell infiltration into tumor-bearing kidneys following therapy. We have previously seen that an increase of CD8 T cells into the tumors of Ad5-TRAIL/ CpG-treated mice accompanies tumor regression[251]. As no Renca-specific tumor Ag have been identified to our knowledge, we determined the frequency of "effector phenotype" CD8 T cells ($CD3^+CD8^+CD44^{hi}$) in the tumor-bearing kidneys of lean and DIO mice 5 d after receiving Ad5-TRAIL/CpG therapy. Using an i.v. staining technique[252] to discern leukocytes in the tissue and vasculature at the time of harvest, it was determined that DIO had a significant reduction in frequency and number of $CD45.2^+CD3^+CD8^+CD44^{hi}$ T cells localized within the kidney tissue at the time of harvest compared to lean mice (Figure 3-10). Collectively, these data demonstrate that the obese environment resulted in the abrogation of the Ad5-TRAIL/CpG therapy-induced CD8 T cell immune response essential for the eradication of tumor cells in this model of advanced RCC.

Discussion

Understanding the influence of obesity on immune function, tumor outgrowth, and the efficacy of administered antitumor immunotherapies is of critical importance, given the widespread prevalence of obesity in the United States today. In the current study, we used a mouse model of DIO to identify DC and T cell functional alterations, both in the absence and presence of orthotopic RCC, a cancer for which obesity is a major risk factor. We found that a DC-based immunotherapy was largely ineffective in DIO mice with RCC, although the same therapy was able to control RCC outgrowth in lean mice.

Increased percentages of suppressive DC in tumor-bearing kidneys of DIO mice and a decreased influx of CD8 T cells accompanied this loss of efficacy into the tumor site. We identified several obesity-related alterations in DC function in DIO mice. During steady-state conditions, we found that spDC from DIO mice had a reduced ability to stimulate naive T cell proliferation, an observation that could have contributed to the decreased T cell response we observed in tumor-bearing kidneys of DIO mice receiving immunotherapy. Our study illustrated that the combination of obesity and tumor outgrowth leads to a markedly impaired DC response to RCC in this orthotopic murine model. We observed increased infiltration of DC into tumor-bearing kidneys of DIO mice in the presence and absence of immunotherapy. Rather than inducing T cell proliferation, the DC that infiltrated tumor-bearing kidneys in DIO mice inhibited T cell expansion. This was in contrast to the DC from tumor-bearing kidneys in lean mice, which did not show any ability to suppress T cell proliferation. In DIO mice, suppression of T cell expansion occurred even after administration of a combinatorial therapy that contained CpG. These results highlight the necessity of examining immunotherapeutic efficacy in both lean and obese mice, because the altered physiology of the latter may negatively impact results.

It was previously shown using two murine breast cancer models and a fibrosarcoma model that TIDC from young lean mice were able to inhibit T cell expansion ex vivo. Although the degree of inhibition varied according to the tumor model being examined, all TIDC showed some ability to suppress T cell expansion[245]. Because of this, we were initially surprised to find that DC from RCC-bearing kidneys in lean mice did not inhibit T cell proliferation. Several factors may account for this finding. First, there were low percentages of DC present in tumor-bearing kidneys from lean mice. Second, it was impossible for us to determine whether those low numbers of renal DC were actually infiltrating tumor masses within kidneys or were located in normal tissue adjacent to malignant areas. The use of BLI allowed us to monitor tumor growth in live mice, so we were able to objectively determine that all mice used for experiments had progressively growing tumors by day 7. However, even after several weeks of tumor

growth, when most DC experiments were performed, it was frequently impossible to identify distinct tumor masses upon gross examination of excised kidneys. Consequently, we could not determine the relative ratios of true "TIDC" versus the broader population of renal DC. It is possible that many of the renal DC from tumor-bearing lean mice had resided in healthy kidney tissue, rather than in the developing tumor mass.

In our study, BLI analyses revealed that early RCC outgrowth was more rapid in DIO mice than in lean counterparts, but these differences were not sustained. Although accelerated tumor outgrowth has been reported in other models of murine obesity, this trend is not universally observed[253, 254]. The variable responses of tumor growth to ongoing obesity likely stem from the unique responses of each tumor cell type to the cytokine/chemokine environment present in the host. Leptin is known to promote angiogenesis through increased expression of VEGF, to promote tumor cell proliferation in vitro, and to increase tumor cell resistance to apoptosis[184, 255]. These actions could have promoted the increased early tumor growth we observed and could also have contributed to the decreased efficacy of Ad5-TRAIL/ CpG therapy in DIO mice. It is also likely that the low-grade inflammation seen in DIO mice influenced the rapid, early tumor outgrowth in DIO mice, as it is well established that inflammation can lead to cancer[256-258]. It is possible that blocking inflammatory pathways might have benefits in terms of reducing tumor burdens and/or normalizing antitumor immunity in obese individuals, an idea that could be addressed in future experiments.

DC responses to tumor outgrowth are critical factors that impact the success or failure of many immunotherapeutic strategies being used or developed today. New treatment options are illustrating the potential for DC-based immunotherapies to prolong the lives of cancer patients[259, 260]. The confounding effects of obesity on these and other DC-based cancer immunotherapies are not known. We found that baseline DC stimulatory capacity was diminished in DIO mice and that DC from DIO tumor-bearing kidneys suppressed T cell expansion ex vivo. Ultimately, administration of a DC-dependent anticancer therapy was found to be ineffective in DIO mice with RCC. Our results suggest that both preclinical studies in mice and clinical trials in cancer patients

may benefit from examining the efficacy of DC-based immunotherapies in the presence of obesity and its associated inflammation.

Figure 3-1: DIO mice exhibit classic signs of obesity

(A) Final body weights for individual mice are shown after being on either standard chow (lean) or HFF for 20 wk. The dashed line indicates 3 SD above the lean mean. (B) Mean (+/- SEM) final body weights for 13 lean and 13 DIO HFF mice are shown. (C) Mean (+/- SEM) visceral body fat, as a percentage of total body weight, for the same mice used in (B). (D) Individual serum leptin concentrations as determined by ELISA for n = 7 lean and 7 DIO.**$p \leq 0.01$ using student's t-test.

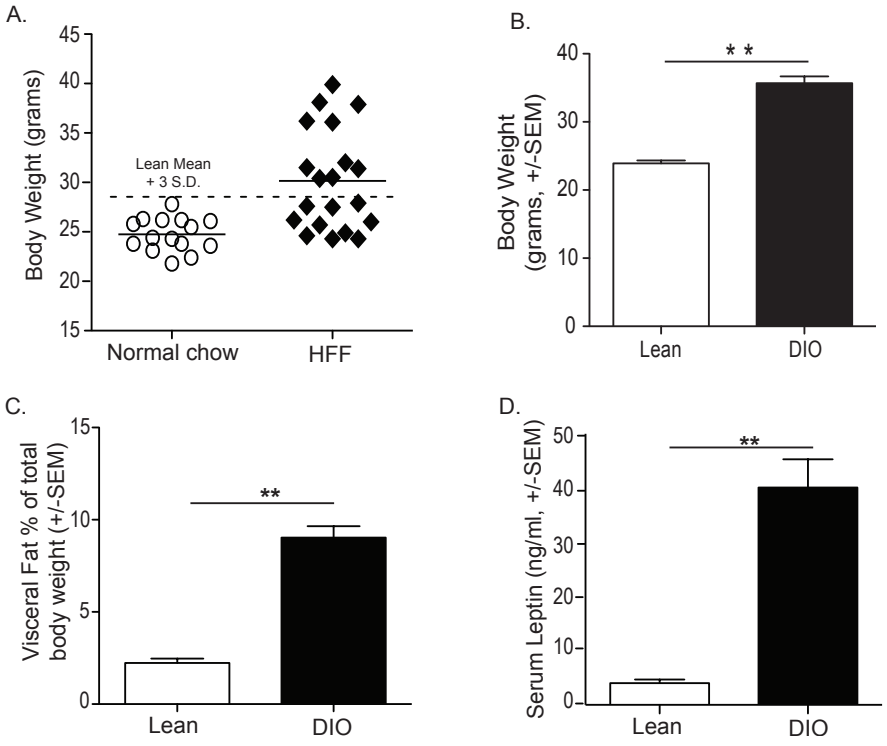

Figure 3-1: DIO mice exhibit classic signs of obesity

Figure 3-2: DIO mice have an increased frequency and number of total spDC

(A) Flow cytometric analysis of spDC populations from lean and DIO mice. Dot plots from individual mice are shown, representative of data from 13 lean and 13 DIO mice. (B) Mean (+/- SEM) percentages of $CD11c^{high}/I\text{-}A^{d}{}_{+}$ spDC are shown for the mice used in (A). (C) Mean (+/- SEM) live splenocyte counts are shown for 11 lean and 9 DIO mice. (D-E) Gating and mean percentage (+/- SEM) of indicated spDC subsets is shown, where n=3-4 individual mice per group, pooled from 2 independent experiments. No statistical differences were observed between lean and DIO percentages for any spDC subset examined. **$p \leq 0.01$ using student's t-test.

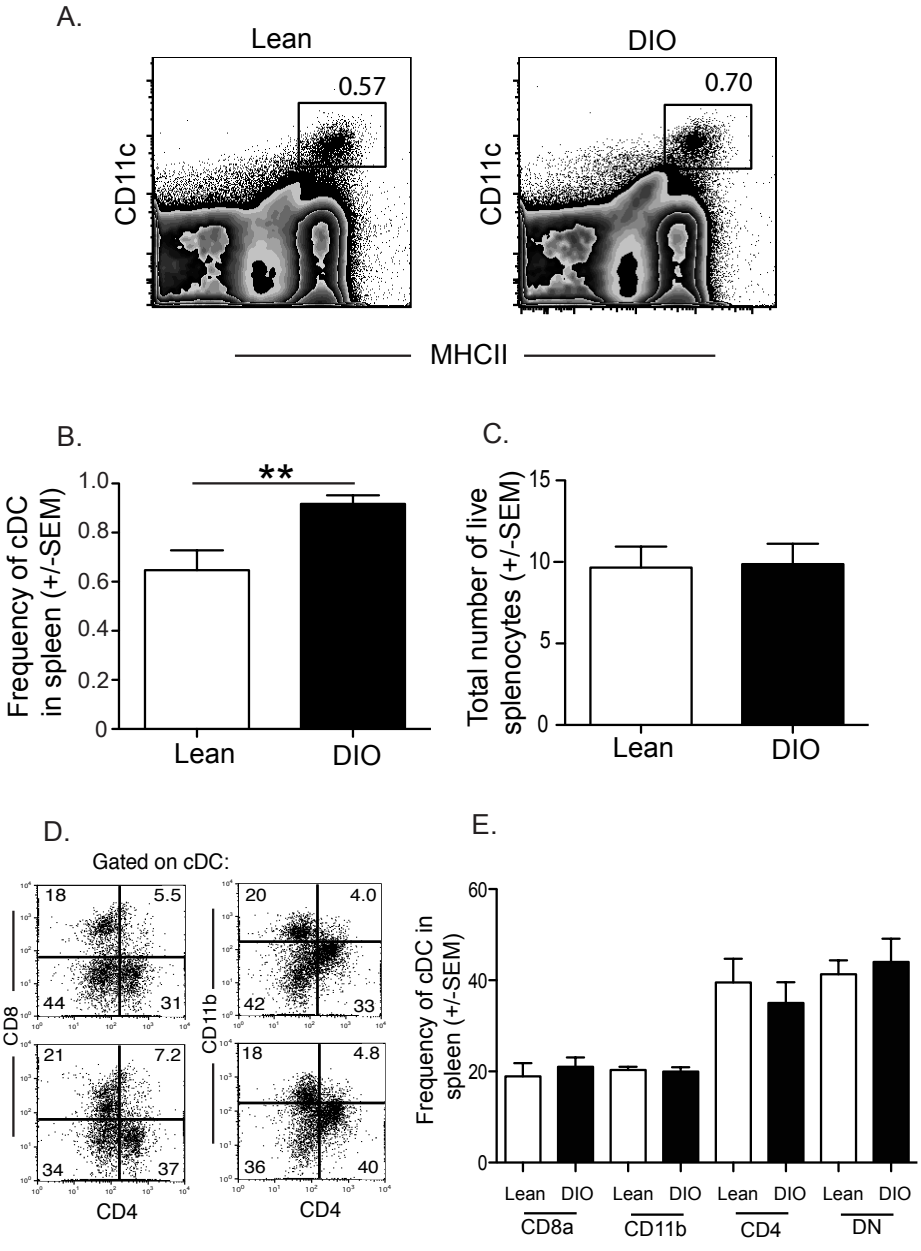

Figure 3-2: DIO mice have an increased frequency and number of total spDC

Figure 3-3: Myeloid DC from DIO mice have a decreased functional capacity

(A) Individual results from one independent T cell proliferation assay using sort-purified, tERK-pulsed spDC and enriched $CD8^+$ DUC18 T cells. The mean (+/- SEM) for triplicate wells is shown. (B) Individual results from four independent T cell proliferation assays, performed as in (A), are shown. Bars indicate the mean T cell proliferation calculated. The DIO mean is 58% of the LEAN mean. ** $p \leq 0.001$ using student's t-test.

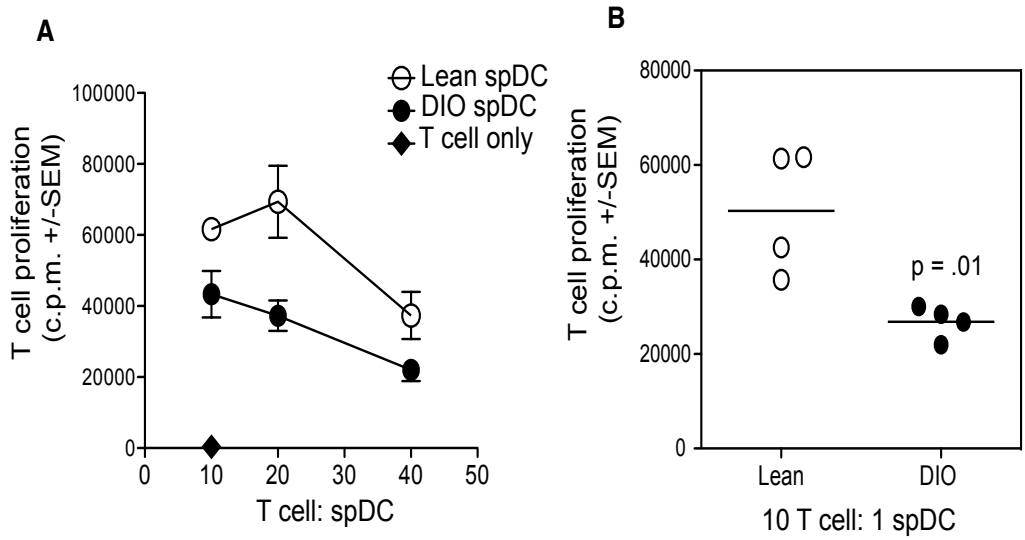

Figure 3-3: Myeloid DC from DIO mice have a decreased functional capacity

Figure 3-4: DIO splenocytes have an altered cytokine/chemokine profile following CpG stimulation

Splenocytes were harvest from lean and DIO mice and plated at $1x10^6$ cells/well and stimulated with 5ug CpG overnight. Supernatants were run on a BioPlex using Millipore 32-analyte MILLIPLEX Map Kit. Samples run by the Cytokine Reference Lab, University of Minnesota, Minneapolis, MN. One representative experiment shown where n=3 mice/group/experiment * $p \leq 0.05$, *** $p \leq 0.001$ using student's t-test.

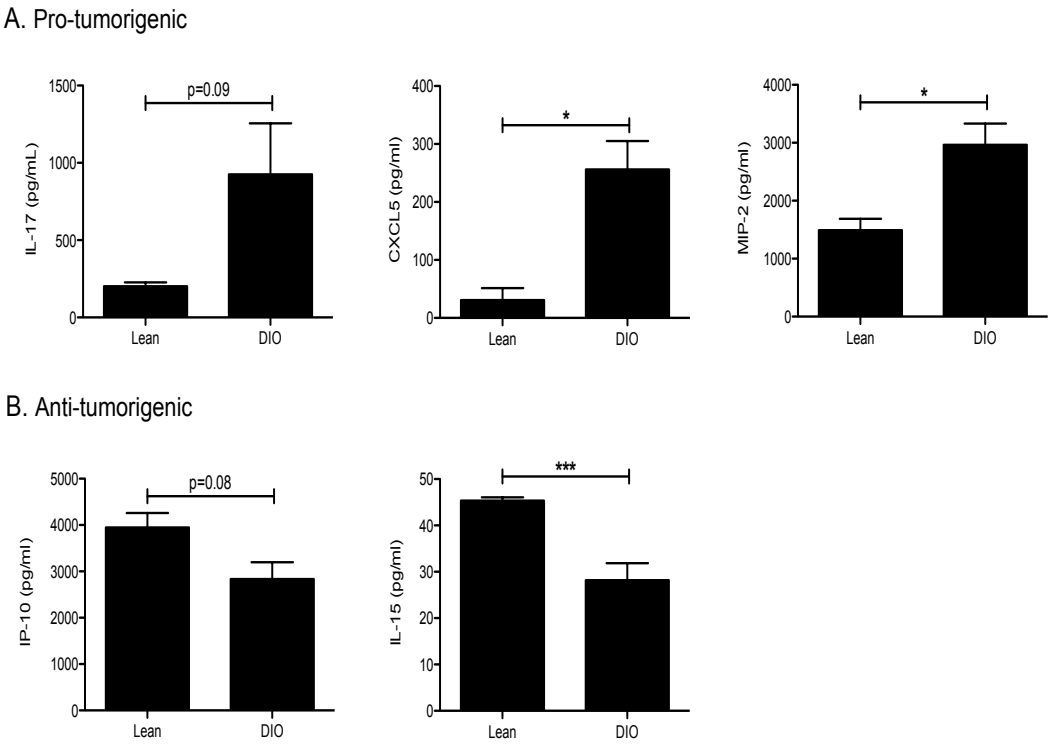

Figure 3-4: DIO splenocytes have an altered cytokine/chemokine profile following CpG stimulation (data generated in collaboration with Dr. Erik L. Brincks)

Figure 3-5: CD8 T cells from DIO mice have a decreased cytolytic capacity

The mouse-adapted A/PuertoRico/8/34 (PR8; H1N1) IAV strain was obtained from Dr. Kevin Legge (University of Iowa, Iowa City, IA). LEAN and DIO mice were anesthetized by isoflurane and infected intranasally with a $0.1LD^{50}$ dose of PR8 in 50 ul Iscove's media on d0. For the in vivo CTL assay, naive BALB/c splenocytes were pulsed with 10_M IAV $HA_{518\text{-}526}$ peptide (Anaspec, Fremont, CA). Non-pulsed (reference) and peptide-pulsed (target) cells were labeled with 0.5μM CFSE (target) obtained from Dr. Ross Fulton (University of Minnesota, Minneapolis, MN) and reference cells were labeled with 5.0μM CFSE. Equal numbers of reference and target cells were mixed and $1\text{-}2x10^7$ total cells were transferred i.v. into naive mice or lean and DIO mice that had been infected with IAV 10 days earlier. Lungs were harvested 8 hrs post-transfer and the relative frequencies of reference and target cells were examined via flow cytometry. The reduction in the number of recovered peptide-pulsed target cells in the IAV-infected versus naive mice was considered the percent specific lysis. Data are cumulative of two independent experiments where n=3 mice/group/experiment. * $p \leq 0.05$ using student's t-test.

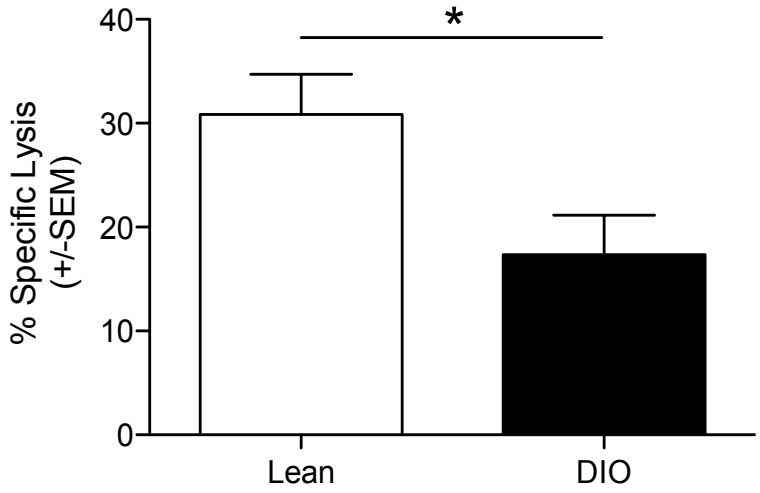

Figure 3-5: CD8 T cells from DIO mice have a decreased cytolytic capacity

Figure 3-6: DIO mice have accelerated tumor growth

(A) Mice were challenged IR with Renca-Luc cells on day 0. At day 7, relative tumor burdens were evaluated via BLI of live mice after i.p. injection of luciferin substrate. Total flux indicates light emitted by luciferase-expressing tumor cells in photons per second for a defined region of interest that encompassed the left kidney. Shown are the mean (+/- SEM) for n = 5 tumor-free control mice, 11 tumor-bearing lean mice, and 14 tumor-bearing DIO mice, combined from multiple experiments. (B) Kidney weights on day 7 after IR tumor challenge for tumor-bearing (tum^+) and tumor-free contralateral (ctrl) kidneys from lean and DIO mice. Mean (+/- SEM) for 7 lean and 5 DIO mice are shown. Data for tumor-bearing (tum^+) and tumor-free contralateral (ctrl) kidneys from lean and DIO mice are shown. *$p \leq 0.05$, **$p \leq 0.01$ using student's t-test.

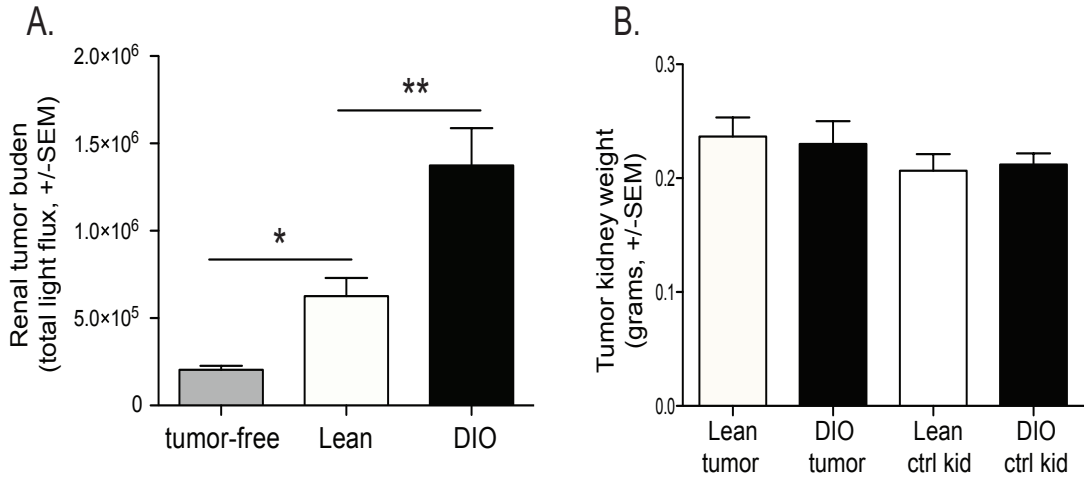

Figure 3-6: DIO mice have accelerated tumor growth

Figure 3-7: DIO mice have increased regulatory TIDC

(A) Cumulative data, illustrating the mean percentage (+/- SEM) of renal DC in tumor-bearing kidneys from lean and DIO mice at days 21– 23 posttumor challenge. (B) The mean percent inhibition (+/- SEM) of naive T cell proliferation, mediated by sort-purified renal DC from either lean or DIO tumor-bearing mice. Data are cumulative from three independent experiments where n=3-4 mice/group/experiment. *$p \leq 0.05$ using student's t-test.

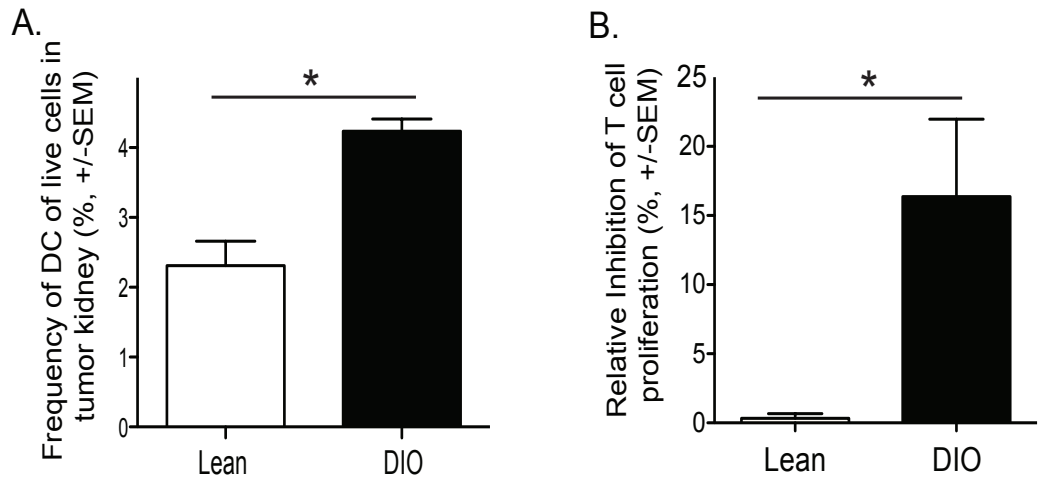

Figure 3-7: DIO mice have increased regulatory TIDC

Figure 3-8: Regulatory function is restricted to TIDC and not spDC

The mean percentages (+/- SEM) of $CD11c_{high}/CD11b_{+}$ myeloid DC are shown for lean or DIO Ad5-TRAIL/CpG treated mice, grouped by organ. Data are cumulative from two independent experiments, where n = 2 for Ad5-TRAIL/CpG LEAN c- Kid and spleen, and n = 4–8 individual mice for all other groups. The right panels illustrate naive DUC18 T cell proliferation in the presence of control spDC, with or without sort-purified renal DC (upper panel) or spDC (lower panel) from tumor bearing DIO mice that were treated with Ad5-TRAIL/CpG on day 7. x-axis numbers indicate ratios of the indicated cell populations present in culture. Combined results from three experiments are shown. c-Kid, Tumor-free contralateral kidney; spleen; tumor, tumor-bearing kidney. *$p \leq 0.05$, **$p \leq 0.001$ using student's t-test.

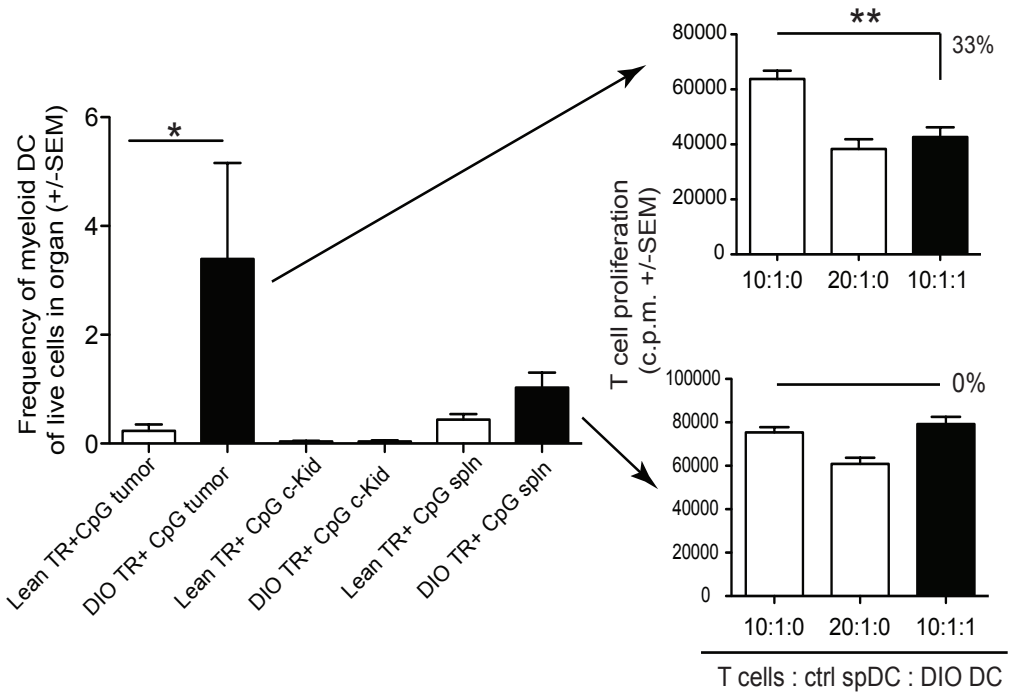

Figure 3-8: Regulatory function is restricted to TIDC and not spDC

Figure 3-9: DIO mice do not respond Ad5-TRAIL/CpG therapy

SC Renca tumor growth kinetics and survival in lean (A) and DIO (B) mice treated with either Ad5-TRAIL/CpG or PBS on day 7. Mice were imaged for bioluminescence signal for tumor-burden over time. One representative experiment shown, where n=5 mice/group/experiment. P-values determined using 2-way ANOVA analysis for kinetics, and log-rank test for survival.

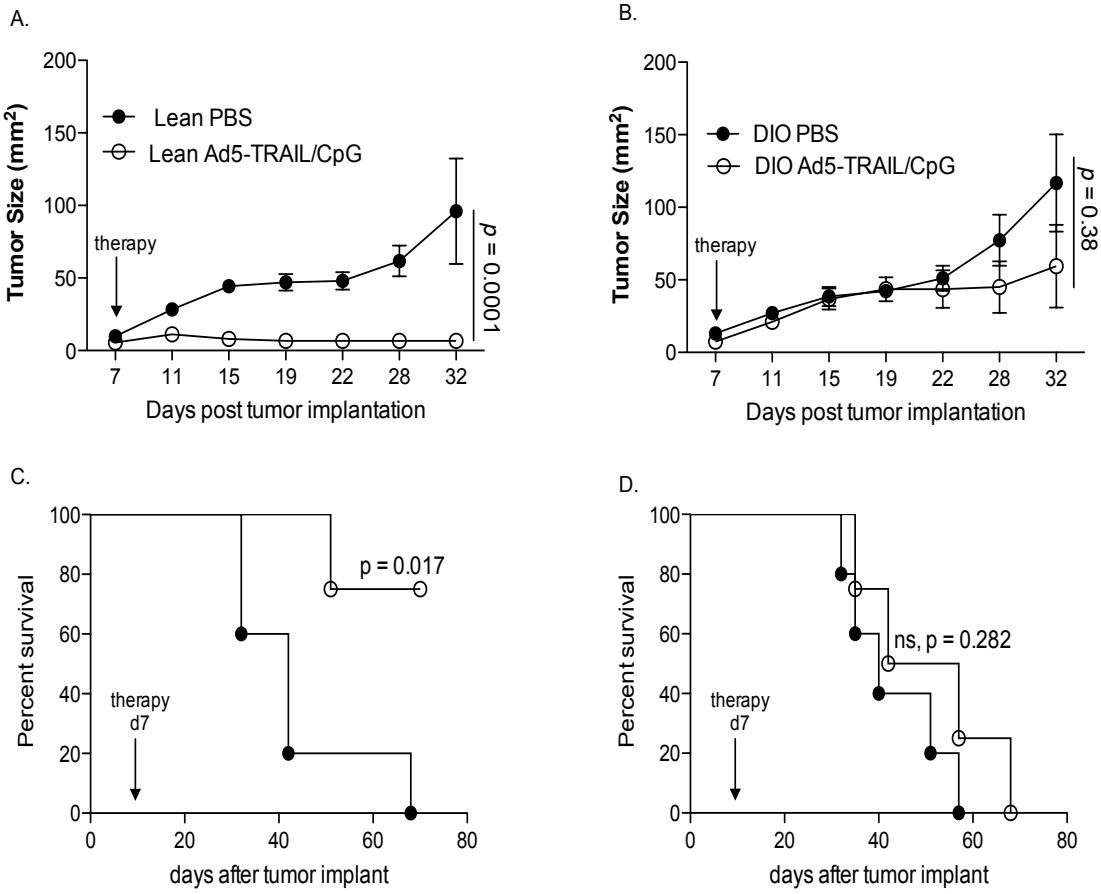

Figure 3-9: DIO mice do not respond Ad5-TRAIL/CpG therapy

Figure 3-10: DIO mice do not mount an antitumor CD8 T cell response

Lean and DIO mice were implanted IR with $2x10^5$ Renca cells, treated with either PBS or Ad5-TRAIL/CpG (Rx) on d 7, and kidneys were harvested on d 12. Prior to harvest, all mice were injected i.v. with PE-conjugated anti-CD45.2 mAb (3 μg) in PBS and sacrificed 3 min later. Single cell suspensions of tumor-bearing kidneys were prepared, and stained for flow cytometric analyses to assess immune cell infiltration. (**A-B**) Mean (+/- SEM) frequency and number of $CD3^+CD8^+CD44^{hi}$ T cells within tumor-bearing kidney tissue. Cumulative data from two independent experiments shown, where n=4 mice/group/experiment. * $p \leq 0.05$, ** $p \leq 0.01$, *** $p \leq 0.001$ using student's t-test.

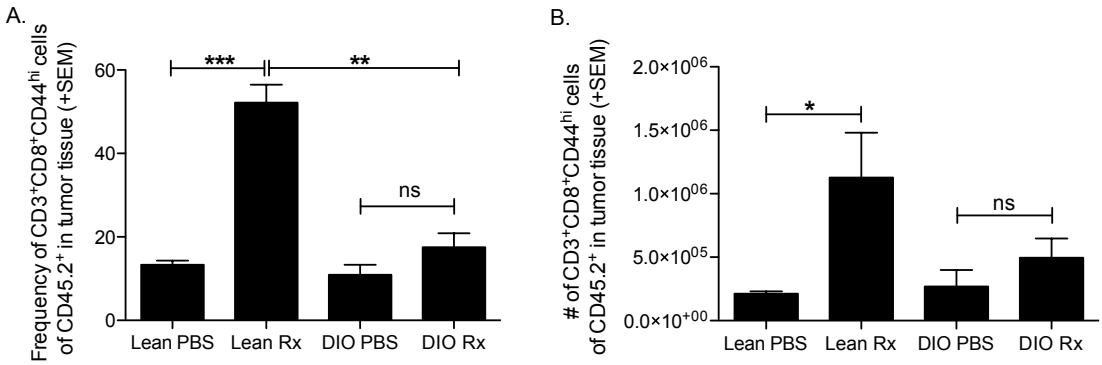

Figure 3-10: DIO mice do not mount an antitumor CD8 T cell response

Acknowledgment: The data in this chapter was generated in collaboration with Dr. Lyse Norian (University of Iowa), Tamara Kucaba (University of Minnesota) and Dr. Thomas Griffith (University of Minnesota), and was modified from "Diet-Induced Obesity Alters Dendritic Cell Function in the Presence and Absence of Tumor Growth," published in *The Journal of Immunology,* vol. 189, pp. 1311-1321, 2012.

Chapter 4: CpG- mediated modulation of MDSC contributes to the efficacy of Ad5-TRAIL/CpG therapy against renal cell carcinoma

Introduction

The limited success of cancer immunotherapies can be attributed (in part) to the existence of immune escape strategies exerted by the tumor [261, 262], including MHC modulation, antigen sequestration, and immunosuppressive cytokine production [263]. Tumors also promote the recruitment and survival of regulatory cells that suppress effector cell responses. There has been considerable interest in recent years regarding the mobilization and recruitment of immunosuppressive myeloid-derived suppressor cells (MDSC) to sites of tumor growth [264, 265]. In these contexts, MDSC accumulate rapidly during primary tumor growth and directly influence antitumor immunity by suppressing effector T cells directly or indirectly via the increased production of immunosuppressive compounds like IL-10, TGF-β, arginase, and iNOS [266-268].

In recent years, investigation into improving the efficacy of tumor immunotherapy has utilized combinations of chemotherapeutics, small molecule inhibitors, and radiation to overcome MDSC-mediated immunosuppression [269-271]. For example, metastatic RCC patients have increased frequencies of MDSC in the peripheral blood, and current therapies for RCC (e.g., sunitinib) can abrogate MDSC-mediated immune suppression [268, 271, 272]. It is posited that eliminating or modulating MDSC will restore the ability of immunotherapy to induce antitumor immunity; however, many treatments that target MDSC can have pleiotropic effects on other immune system components. Depletion of MDSC in mice using anti-Gr1 mAb [273] also depletes activated CD8 T cells [274] and plasmacytoid DC [275]. Additionally, chemotherapies such as 5-fluoruracil (5-FU), which can selectively eliminate MDSC at low doses [276], can have profound negative effects on the immune system [277, 278] potentially rendering immunotherapies ineffective. There remains great interest in the development of novel

immunotherapies that modulate MDSC function to encourage antitumor immunity with minimal side effects.

Previous work from our laboratory described the use of a replication-deficient adenovirus encoding TNF-related apoptosis-inducing ligand (Ad5-TRAIL [279]) in combination with immunostimulatory CpG-containing oligodeoxynucleotides (CpG) for the treatment of metastatic RCC in mice [19]. Given that MDSC induced by tumors potently inhibit CD8 T cell responses, we hypothesized that modulation of the number and/or function of MDSC after Ad5-TRAIL/CpG administration contributed to the overall success of this tumor immunotherapy. We found that CpG, alone or in combination with Ad5-TRAIL, altered MDSC frequency and function. Using a novel *in vivo* staining technique to discriminate cells located in tumor tissue from those in the vasculature [204], we found that Ad5-TRAIL/CpG significantly decreased the presence of MDSC specifically within the tissue of the tumor microenvironment, which correlated with an increase in activated CD8 T cell accumulation in the tumor. Interestingly, when we examined responses in a model of diet-induced obesity (DIO), Renca-bearing obese mice had more MDSC than age-matched lean controls and CpG treatment of obese mice failed to modulate MDSC frequency and function. Collectively, these data suggest that the efficacy of Ad5-TRAIL/CpG immunotherapy depends (in part) on the ability of CpG to alter MDSC frequency and function, which allows the induced antitumor T cell response to eliminate any residual tumor.

Materials and Methods

Animals and diets

Female wild-type BALB/c mice (7-8 wk old) were purchased from the National Cancer Institute (Frederick, MD), and *Batf3*$^{-/-}$ BALB/c breeder mice were purchased from Jackson Laboratories (Bar Harbor, ME). For diet-induced obesity (DIO) studies, mice were randomly assigned to either standard chow or high fat feed (HFF; Research Diets #12492, 60% kcal from fat [202]). After 20 weeks, mice in the HFF group were defined as obese if their body weight was >3 S.D. above the mean of the mice fed standard chow

("lean"). All mice were housed under pathogen-free conditions at the University of Minnesota Animal Care Facility, which is fully accredited by the Association for Accreditation of Laboratory Animal Care. All animal procedures were approved by the Institutional Animal Care and Use Committee at The University of Minnesota.

Cell lines and tumor challenge

The murine renal adenocarcinoma cell line, Renca [201], was obtained from Dr. Robert Wiltrout (National Cancer Institute, Frederick, MD), and was authenticated in 2010 by microsatellite marker analysis (Research Animal Diagnostic Laboratory, Columbia, MO). Renca cells were maintained in RPMI supplemented with 10% fetal bovine serum, penicillin, streptomycin, sodium pyruvate, non-essential amino acids, 2-mercaptoethanol, and HEPES (hereafter referred to as complete RPMI), as previously described [19].
For intrarenal (IR) tumor challenge, mice were anesthetized, a skin incision was made on the left flank, and $2x10^5$ Renca cells were injected through the intact peritoneum into the left kidney in a 100 μl volume of HBSS [19, 202]. In some cases, BALB/c mice were depleted of MDSC with 1 i.p. dose of 1 mg anti-Gr1 mAb on d 6 after tumor implantation. On d 7, mice were injected in the tumor-bearing kidney with sterile PBS alone, Ad5-TRAIL (10^9 pfu) [199], and/or the nonmethylated CpG ODN 1826 (5'-tccatgacgttcctgacgtt-3', 100 μg; IDT, Coralville, IA) with a phosphorothioate-modified backbone for nuclease resistance in a 100 μl volume.

Immunofluorescent imaging

Immunofluorescent imaging was performed as previously described [204]. Briefly, tumor-bearing and contralateral kidneys were harvested 12 d after tumor implantation. Tissues were snap frozen in OCT, cut to 7-μm thickness, and fixed in acetone for 10 min. Sections were stained using unconjugated rabbit anti-cytokeratin 8 and 18, AF488-conjugated donkey anti-rabbit secondary Ab, PE-conjugated anti-CD31, BV421-conjugated anti-CD11b, and APC-conjugated anti-Gr-1 mAb and imaged with a Leica DM5500 B microscope.

Flow cytometry

Single cell suspensions of tumor-bearing or contralateral kidneys, and spleens were prepared using a gentleMACS Dissociator (Miltenyi BioTeck Inc., Auburn, CA), and then digested for 15-30 min in HBSS containing 0.56 Wuensch units/ml of Liberase Blendzyme 3 (Roche, Branford, CT) and 0.15 mg/ml DNAse I (Sigma, St. Louis, MO). Cells were then blocked using a cocktail of anti-CD16/32 and normal mouse serum before surface staining. Cells were stained with combinations of the following mAb (eBioscience (San Diego, CA) or BioLegend (San Diego, CA)) and analyzed using multi-parameter flow cytometry on a BD LSR II (BD Biosciences, San Diego, CA) and FlowJo software (TreeStar Inc., Ashland, OR): MDSC – anti-CD3-, CD11c-, CD19-PE or PerCP/Cy5.5 (dump gate), CD11b-PE/Cy7, Ly6C (HK1.1)-APC/Cy7, Ly6G (1A8)-FITC, I-A^d-PacBlue, CD40-PE, CD86-PE/Cy5, CD80-BV650; T cells – anti-CD3-PerCP/Cy5.5, CD4-PE/Cy7, CD8-PacBlue, CD44-PE or -AF700, CD45.2-PE and -BV650. Intracellular staining for Foxp3 was done, as a dump gate, using a Foxp3 staining kit (eBioscience) per the manufacturer's protocol.

Intravascualar staining

To specifically identify leukocytes located in the tumor-bearing kidney tissue or kidney vasculature, intravascular (i.v.) staining was done as previously described [204]. Briefly, tumor-bearing mice were injected i.v. with 3 μg of PE-conjugated anti-CD45.2 mAb 3 min before sacrificing the mice and isolating single cell suspensions from organs for flow cytometric analysis as described above. Additionally, cells were stained *ex vivo* with BV650-conjugated anti-CD45.2 mAb. Dual staining of CD45.2 discriminates between cells within the vasculature (CD45.2-PE^+CD45.2-$BV650^+$) or tissue (CD45.2-PE^-CD45.2-$BV650^+$) at the time of harvest. Blood and inguinal lymph nodes served as positive and negative controls for i.v. staining, respectively.

MDSC enrichment and isolation

MDSC from tumor-bearing kidneys were enriched using Miltenyi anti-CD11b microbeads, then sort-purified on a BD Aria II or FACS DiVa based on expression of the

following markers: $CD45.2^{+}/CD11c^{low}/CD11b^{+}/ Ly6C^{+}/Ly6G^{+/-}$ after gating on live cells via Hoechst 33258 exclusion. Sorted MDSC purity was ≥ 95%. Alternatively, MDSC were purified by negative selection with Miltenyi anti-CD11c microbeads. Cells were run over two sequential columns and the negative fractions were collected. $CD11c^{-}$ enriched cells were then incubated with Miltenyi anti-CD11b microbeads and run over two sequential columns, and the bound fractions were collected. MDSC purity was ≥ 90% of live cells.

T cell proliferation assays

Ag-specific assay: T cells were harvested from naïve DUC18 TCR transgenic mice [246]. Splenic DC (spDC) from tumor-free BALB/c mice were isolated with Miltenyi anti-CD11c microbeads. T cell proliferation was assessed by culturing naive DUC18 T cells ($5x10^4$ cells/well) with tERK peptide-pulsed spDC ($5x10^3$ cells/well) with increasing numbers of sort-purified splenic or renal MDSC from tumor-bearing mice in a flat-bottom 96-well plate. [^{3}H] Thymidine was added during the final 18 h of a 72 h incubation. Relative T cell proliferation was set to 100% for control T cell/DC co-cultures not containing MDSC. The % relative proliferation was then calculated for all other culture conditions. Anti-CD3 assay: Naïve splenic BALB/c CD8 T cells and MDSC from tumor-bearing mice were MACS purified as described above. When indicated, MDSC were stimulated with 6 μg CpG for 3 h, and then washed 3x with PBS. Wells of a round-bottom 96 well plate were coated with anti-CD3 mAb (clone 500A2; 1μg/ml) overnight at 4°C. The plate was then washed with PBS and CD8 T cells ($5x10^4$ cells per well) and increasing numbers of CpG-stimulated and unstimulated MDSC were plated. [^{3}H] Thymidine was added as above, and % relative proliferation was calculated.

Quantitative real-time PCR (qPCR)

Tumor-bearing kidneys were harvested 4 h after treatment, and homogenized via gentleMACS Dissociator. Total RNA was isolated using TRIzol reagent (Invitrogen, Carlsbad, CA), and 1 μg was reverse-transcribed using Superscript III. Resulting cDNA

was used as a template for qPCR using TaqMan primer/probe sets for *arg1* and 18s rRNA (PE Applied Biosystems, Foster City, CA).

Statistical analysis

Statistical analysis between groups was determined by unpaired or paired Student's *t*-test, and 2-way ANOVA where appropriate. Data was analyzed with Prism4 GraphPad software and statistical significance is indicated in figure legends (* $p < 0.05$; ** $p < 0.001$; *** $p < 0.0001$; not significant (n. s.)).

Results

Characterization of splenic MDSC from RCC tumor-bearing mice

The Renca cell line is commonly used to model RCC in mice, where it can be injected subcutaneously to produce localized tumors or intravenously to produce experimental lung metastases [199, 266, 280, 281]. In contrast, we have developed an orthotopic model where direct implantation of Renca cells into the kidney leads to the formation of an aggressive primary intrarenal tumor as well as lung metastases [19]. Investigation of MDSC in mice bearing Renca tumors has been limited, so we initially characterized the MDSC present in mice bearing such orthotopic Renca tumors. MDSC are identified by CD11b with the concomitant expression of Ly6C and Ly6G [282] (Figure 4-1). Differential Ly6G expression defines granulocytic and monocytic MDSC, respectively, which suppress T cells by distinct mechanisms [283]. Assessment of MDSC population dynamics after tumor implantation revealed a steady increase in the number of bulk ($CD3^-CD19^-CD11c^{low}CD11b^+Ly6C^+$) MDSC in the spleen over time (Figure 4-1). Of note, both the $Ly6G^+$ granulocytic ($CD3^-CD19^-CD11c^{low}CD11b^+Ly6C^+Ly6G^+$) and $Ly6G^-$ monocytic ($CD3^-CD19^-CD11c^{low}CD11b^+Ly6C^+Ly6G^-$) MDSC populations expanded similarly in the spleen over time. To verify that the MDSC phenotype correlated with suppressive function by these populations, splenic MDSC were isolated from Renca-bearing mice and co-cultured with CD8 T cells [147]. Indeed, Ag-specific T cell proliferation was significantly suppressed when including either bulk, $Ly6G^+$ or $Ly6G^-$ MDSC in the assay

(Figure 4-1). Another hallmark of MDSC is their ability to promote tumor growth. To assess the extent to which Renca-mobilized MDSC supported tumor growth, we employed the common MDSC depletion method of administering anti-Gr1 mAb (Figure 4-2) in our RCC tumor-being mice and assessed tumor burden over time. Depletion of MDSC significantly decreased tumor burden (Figure 4-2), suggesting that the MDSC mobilized as a result of a growing Renca tumor indeed promote tumor growth. Of note, Renca cells are somewhat tumorigenic, but the immune system is unable to control the tumor burden. MDSC depletion did not induce accumulation of T cells (Figure 4-3).

CpG decreases MDSC and alters MDSC subtype distribution

Having previously described the ability of Ad5-TRAIL/CpG therapy to induce effective systemic antitumor immunity, we were interested in determining how Ad5-TRAIL/CpG was efficacious against Renca tumors in the face of an enhanced population of MDSC. Given the data in Figure 1 and 2 demonstrating the accumulation of immunosuppressive MDSC in RCC tumor-bearing mice, we hypothesized that Ad5-TRAIL/CpG therapy may modulate MDSC systemically and locally to permit the generation of an antitumor T cell response capable of clearing primary tumor within the kidney. To determine the extent to which Ad5-TRAIL/CpG therapy altered the frequency of MDSC in tumor-bearing mice, BALB/c mice were implanted IR with Renca cells and treated with PBS, Ad5-TRAIL and/or CpG on d 7. Analysis of bulk splenic MDSC on d 12 found that Ad5-TRAIL alone did not modulate the MDSC population, but CpG (alone or in combination with Ad5-TRAIL) significantly decreased the frequency of MDSC (Figure 4-4). We extended this analysis to examine the $Ly6G^+$ and $Ly6G^-$ MDSC populations, and found the $Ly6G^+$ MDSC experienced a similar decrease after administration of CpG alone or in combination with Ad5-TRAIL. Interestingly, the frequency of $Ly6G^-$ MDSC increased in the spleen after injection of Ad5-TRAIL (Figure 4-4). Together, these data suggest that local administration of CpG into tumor-bearing kidneys systemically modulates the frequency of MDSC in Renca-bearing mice.

Ad5-TRAIL/CpG alters the location of MDSC within tumor-bearing kidney

Data suggest MDSC acquire their suppressive function only after exposure to factors in the tumor microenvironment [284, 285]. Moreover, MDSC within the tumor might have the greatest effect on antitumor T cell responses [286]. Consequently, we first examined the presence and location of MDSC in Renca tumor-bearing kidneys by immunofluorescence. Structural markers for vasculature (CD31) and tumor (cytokeratins 8 and 18 [287]) were used to visualize the tumor-bearing kidney (Figure 4-5). The MDSC markers CD11b and Gr1 were used to examine the localization of MDSC in the tumor-bearing kidney. When examining the tumor margin, MDSC were primarily localized within the tumor and not in the "normal" tissue of the kidney. Further, MDSC were associated with both tumor tissue and vasculature, as seen by co-localization with cytokeratin 8 and 18^+ and $CD31^+$ cells, respectively. Subsequent analysis of MDSC within tumor-bearing and contralateral kidneys by flow cytometry demonstrated MDSC accumulation only within the tumor-bearing kidney, and both bulk MDSC and the individual subsets of MDSC isolated from tumor-bearing kidneys had the capacity to suppress T cell proliferation (Figure 4-5), similar to the splenic MDSC in this model.

Kidneys are highly vascular organs, making it likely that flow cytometric evaluation of MDSC from tumor-bearing kidneys would include both "tissue-localized" MDSC and MDSC present in the vasculature at the time of organ harvest. To clearly distinguish MDSC within the kidney tissue from MDSC within the vasculature, we used an intravascular staining technique [204] in which PE-labeled anti-CD45.2 mAb was injected i.v. prior to tumor-bearing kidney harvest. Tumor-bearing and contralateral kidneys were then processed for flow cytometry, which included *ex vivo* staining with BV650-labeled anti-CD45.2 mAb. Using this method, leukocytes in the vasculature at the time of harvest stained positive with both the PE- and BV650-labeled anti-CD45.2 mAb, whereas leukocytes truly within the kidney tissue were only stained by the *ex vivo* BV650-labeled anti-CD45.2 mAb (Figure 4-6). This technique is superior to perfusion as a substantial number of cells remain in the vasculature after perfusion, and the increased vasculature pressure that occurs during perfusion can disrupt tissue architecture [204].

When gating on the location (kidney tissue vs. vasculature) of the cells, ~15% of the CD45.2$^+$ cells specifically within the tissue ("CD45.2 i.v. negative") were Ly6G$^+$ MDSC and only ~7% were Ly6G$^-$ MDSC (Figure 4-6). Analysis of contralateral kidneys showed that the majority of MDSC were in the vasculature. Immunofluroescence microscopy was used to verify that "CD45.2 i.v. positive" cells were located within vascular endothelium or glomerular regions of the kidney (done by Dr. Kristin Anderson, University of Minnesota, MN).

Having established the utility of this intravascular staining technique to identify and quantitate the MDSC truly within the tissue of tumor-bearing kidneys, we then used this method to examine the effect of Ad5-TRAIL/CpG therapy on MDSC localization. Similar to the analyses of the whole tumor-bearing kidney that would include both tissue- and vasculature-localized cells, Ad5-TRAIL/CpG therapy decreased bulk MDSC in the kidney tissue, as well as Ly6G$^+$ MDSC (Figure 4-6). Though the Ly6G$^-$ MDSC were not significantly decreased in the kidney tissue, there was a trend towards a decrease. Importantly, the frequency of MDSC within the kidney vasculature was not altered by Ad5-TRAIL/CpG administration (Figure 4-6). These data collectively demonstrate that Ad5-TRAIL/CpG therapy decreases the frequency of MDSC specifically within the kidney tissue.

CpG significantly modulated MDSC phenotype and function

While modulating MDSC numbers can improve the efficacy of therapy, altering MDSC function can also ablate their inhibitory capacity to improve therapeutic outcomes. Consequently, much of the current research targeting MDSC is aimed at both decreasing their frequency and reducing their inhibitory capacity. To determine the extent to which CpG may also be affecting the functionality of MDSC we performed a series of *in vitro* and *in vivo* analyses of MDSC from spleens and kidneys of Renca-bearing mice. BALB/c mice were implanted with Renca tumors, and spleens and tumor-bearing kidneys were harvested 18-21 d later to allow for increased MDSC numbers. MDSC were enriched from both tumor-bearing kidneys and spleens, and then stimulated *in vitro* with CpG overnight. The CpG-stimulated MDSC exhibited a "matured" phenotype, based on

increased CD80, MHC II, CD86, and CD40 expression when compared to unstimulated MDSC from spleens (Figure 4-7), suggesting a direct effect of CpG on the MDSC population. Next, we determined the extent to which CpG stimulation affected the suppressive capacity of the MDSC. MDSC purified from tumor-bearing kidneys were stimulated with CpG for 3 h. After washing to remove any CpG from the culture, the CpG-stimulated MDSC were then added into cultures of anti-CD3 mAb-stimulated CD8 T cells to assess their ability to suppress T cell proliferation. Compared to unstimulated MDSC, the CpG-stimulated MDSC were less suppressive of T cell proliferation (Figure 4-7). These data are consistent with the idea that CpG can directly stimulate MDSC [288].

We extended the analysis *in vivo* to see the extent to which CpG administration changed MDSC within the tumor-bearing kidney. Renca-bearing mice were injected with PBS or CpG IR on d 7, and then the kidneys were harvested 4 h later and processed for qPCR analysis or 5 d later and processed for flow cytometric analysis of the MDSC. Seeing the reduction in suppressive capacity in Figure 5B, we examined the expression of mRNA for arginase 1 (*arg1*), an enzyme utilized by MDSC to suppress T cell proliferation, within tumor-bearing kidneys after PBS or CpG injection. When normalized to tumor-free kidneys, the amount of *arg1* mRNA was significantly reduced after CpG administration (Figure 4-7). These data, when coupled with the data in Figure 5B, suggest CpG can rapidly and inherently alter MDSC. When we examined the phenotype of MDSC, there were increased frequencies of MHC II^{hi}, CD86^{hi}, or CD40^{hi} MDSC from mice injected with CpG compared to PBS-injected mice (Figure 4-7) similar to the *in vitro* data. Thus, the data in Figure 4-7 suggest the potential for both direct and indirect effects of CpG on MDSC.

Diet-induced obese tumor-bearing mice have increased MDSC frequencies that are not affected by CpG

The number and suppressive function of MDSC increase with inflammation [289]. There are a variety of clinical settings marked by increased and/or chronic inflammation, and obesity is one such condition in which chronic inflammation and the increased production

of pro-inflammatory cytokines and adipokines promote immune system dysfunction [290]. We recently described how Ad5-TRAIL/CpG therapy is ineffective in clearing Renca tumors in diet-induced obese (DIO) mice [202]. Because obesity can induce significant MDSC accumulation and activation in the absence of tumors [291], we hypothesized that one explanation for the ineffectiveness of Ad5-TRAIL/CpG therapy in DIO Renca-bearing mice was exacerbated MDSC accumulation that was not modulated by CpG. Thus, we examined the frequency of MDSC in the spleens and tumor-bearing kidneys from DIO mice and age-matched mice fed standard chow ("lean" mice). There was a significant increase in frequency of bulk and $Ly6G^+$ MDSC in the spleens and bulk, $Ly6G^+$, and $Ly6G^-$ MDSC in tumor-bearing kidneys from DIO mice compared to lean mice (Figure 4-8). Utilizing the *in vivo* staining technique described in Figure 4, we examined the frequency of MDSC specifically within the tumor-bearing kidney tissue from lean and DIO mice that had been treated with either PBS or Ad5-TRAIL/CpG. In contrast to MDSC from lean mice, the MDSC frequency in the tumor-bearing kidneys of DIO mice did not change in response to Ad5-TRAIL/CpG therapy (Figure 4-8). At the same time, we quantitated the frequencies of CD8 T cells within these same tumor-bearing kidneys from lean and DIO mice. Interestingly, while analysis of tumor-bearing kidneys from lean mice showed a significant increase in the frequency of CD8 T cells within the kidney tissue, this was not seen in the tumor-bearing kidneys from DIO mice (Figure 4-8). The data in Figure 4-8 also allowed us to determine the ratio of total numbers of CD8 T cell to MDSC in the kidney tissue. Ad5-TRAIL/CpG therapy in lean mice shifted the ratio heavily in the favor of CD8 T cells, whereas the ratio of CD8 T cell:MDSC was nearly unchanged in Ad5-TRAIL/CpG-treated DIO mice compared to PBS-treated DIO mice. Finally, we examined the suppressive capacity of MDSC from lean and DIO mice directly *ex vivo* and after 3 h CpG stimulation. There was no significant difference in the ability of unstimulated and CpG-stimulated MDSC from DIO mice to suppress CD8 T cell proliferation unlike that seen for MDSC from lean mice (Figure 4-8). Together, the data in Figure 4-8 suggest that the increase in MDSC, as well

as their resistance to CpG-mediated modulation, contribute to the ineffectiveness of Ad5-TRAIL/CpG therapy in DIO mice.

Discussion

With increasing investigation into the induction of MDSC accumulation and the mechanisms of suppression used by MDSC, a paradigm shift has taken place with regard to their acceptance as a means by which tumors evade antitumor immunity. Initially, the goal of cancer immunotherapy was simply to activate the host immune response to mount a robust antitumor response, but in recent years it has become increasingly clear that cancer immunotherapy regimens must also concomitantly modulate immunosuppressive cell populations. To this end, many studies have utilized combinatorial approaches with chemotherapies and immunotherapy to modulate MDSC and induce antitumor immunity, respectively. However, there has also been increasing evidence to suggest that chemotherapy can actually dampen the antitumor immune response, specifically when given prior to an immunotherapy, and that these effects can be long lasting [269, 292]. The question then becomes, what is the optimal way to both decrease immunosuppression while still stimulating a robust immune response? The data reported herein suggest that immunostimulatory CpG-containing oligodeoxynucleotides, which have been used extensively in the last 20 years as adjuvants in a number of infection and cancer settings [230], modulate the number and function of MDSC in a mouse model of advanced RCC.

MDSC are present and promote tumor growth in humans with RCC and mouse models of RCC that use the renal adenocarcinoma cell line Renca. While MDSC depletion/modulation by a variety of therapies (e.g., sunitinib, 5-FU, and anti-Gr-1 mAb) can slow tumor progression, these therapies have not shown clear and consistent success in curing tumor-bearing animals (or humans) when given alone – especially in cases of metastatic cancer [147, 269, 276]. These reports suggest that while depletion/modulation of MDSC is certainly beneficial, altering the quantity and quality of MDSC may not be enough to lead to complete tumor eradication. We have previously described the ability of Ad5-TRAIL/CpG therapy to clear primary orthotopic and metastatic RCC tumors in

mice [19], and here we have presented data to suggest a mechanism by which Ad5-TRAIL/CpG therapy induces such a potent response. We have confirmed the increased presence of MDSC in Renca-bearing mice, and have characterized the MDSC in this model. Both $Ly6G^+$ and $Ly6G^-$ MDSC accumulate in large numbers systemically and locally during tumor challenge, and both subsets exhibit the canonical ability to suppress T cell proliferation. In spite of this large population of immunosuppressive cells at the time of treatment, Ad5-TRAIL/CpG therapy was capable of inducing a CD8 T cell response responsible for tumor eradication in RCC tumor bearing mice through MDSC modulation in a CpG-dependent manner.

Reports recently published by Zoglmeier et al. [293] and Shirota et al. [288] suggested CpG-induced modulation of MDSC can occur via indirect and direct mechanisms, respectively. MDSC express TLR9, and direct stimulation by CpG leads to their differentiation into F4/80-expressing macrophages and loss of immunosuppressive function [288]. Murine plasmacytoid DC (pDC), Mϕ, B cells, and all myeloid DC subsets identified to date express TLR9 and respond to CpG [225]. pDC are primary producers of type I IFN after CpG stimulation, and the type I IFN produced by CpG-stimulated pDC can also induce MDSC maturation [288]. Our data also suggests the potential for direct CpG effects on the MDSC mobilized by Renca tumor growth. *In vitro* stimulation of purified MDSC from Renca-bearing mice with CpG underwent phenotypic change and demonstrated less suppressive capacity, much like the data from the Shirota study. However, we see MDSC maturation *in vivo* that could be due to direct or indirect effects of CpG. Regardless of whether the CpG is acting directly or indirectly on the expanded MDSC within the tumor-bearing mice in our model, the data presented confirms the previous results from Zoglmeier et al. and Shirota et al. and extends the findings to suggest that systemic alterations in physiology during co-morbidities (in this case, obesity) can have profound effects on the mobilization of this immunosuppressive cell population and their sensitivity to immunostimulatory molecules.

Tumor growth leads to significant local and systemic changes in a number of immunological parameters. When investigating MDSC, it is common to see the analysis

of MDSC located in the spleen or blood from tumor-bearing mice or humans. These tissues are likely chosen because of convention and/or convenience (especially for humans), even when the tumor is located at a site that is not highly vascularized. While we did examine splenic MDSC in the Renca-tumor bearing mice, we were particularly interested in analyzing the MDSC in the tumor-bearing kidney. Most cells within the immune system constantly recirculate throughout the body, and usually only enter tissues when needing to exert a specific effector function. Immune cell migration from the blood into tissue is also commonly accompanied by changes in phenotype and differentiation states. As we were investigating the role of MDSC in the efficacy of Ad5-TRAIL/CpG therapy against orthotopic RCC tumors, we felt it was essential to clearly and precisely analyze those MDSC that were truly present within the tumor microenvironment within the tumor-bearing kidney compared to those that happened to be in the circulation at the time of tissue harvest. To our knowledge, this is the first report to utilize an intravascular staining technique that enabled the analysis of MDSC in a highly vascularized tumor-bearing organ before and after therapy. This approach showed its strength when we were able to determine changes in the ratio of CD8 T cells to MDSC within the same kidney tissue after therapy administration (Figure 4-8) using the appropriate flow cytometric mAb panel. Such analysis would not have been possible without this technique, and the ability to further assess differences in the phenotype and function of immune cells within the kidney tissue versus the kidney vasculature (presumably in circulation) are possible.

The number and suppressive function of MDSC increase with inflammation, and tumors are sites of unresolved inflammation. Chronic inflammation is a characteristic of obesity, and the increased production of pro-inflammatory cytokines and adipokines during obesity can promote immune system dysfunction [290]. Despite the correlation between cancer, obesity, and cytokine/adipokine-influenced inflammation, there is limited data regarding their relationship to MDSC presence and function. We previously showed that the Ad5-TRAIL/CpG therapy is ineffective in tumor-bearing DIO mice [202], and initially explored the contribution in alterations in DC function (as a result of obesity) to the lack of therapeutic efficacy. The data presented herein show the frequency of

MDSC is higher in tumor-bearing obese mice than in lean mice, and the MDSC in the obese mice persist at a high frequency after Ad5-TRAIL/CpG therapy. It remains to be determined whether the maintenance of elevated MDSC during obesity is due to intrinsic and/or environmental changes, as well as elucidating the functional mechanisms of MDSC from lean and DIO mice.

In summary, the findings presented here suggest that the efficacy of Ad5-TRAIL/CpG therapy lies in its multipronged approach of inducing tumor cell death (via Ad5-TRAIL), stimulating DC function (via CpG), and decreasing/modulating MDSC frequency and function (also via CpG). The development of MDSC-specific therapies will be important for the future investigation of how these cells develop, expand in setting of inflammation, and suppress immune effector cell function.

Figure 4-1: Characterization of MDSC from spleens of RCC tumor-bearing mice

BALB/c mice were implanted IR with 2 x 10^5 Renca. **(A-D)** Spleens were harvested from naïve and tumor-bearing mice 7, 14, and 18 d post tumor implantation. Single cell suspensions were made and cells were stained for flow cytometric analysis. **(A)** Representative flow plots showing the gating for bulk MDSC ($CD3^-CD19^-CD11c^-CD11b^+Ly6C^+$) and $Ly6G^+$ and $Ly6G^-$ MDSC subsets within spleens of a naïve and tumor-bearing (d8) animal. **(B-C)** Mean $\pm$ SEM frequency and number of bulk and subset MDSC in spleens during tumor challenge. Data are representative of three independent experiments, with at least 3 mice/group/experiment. **(D)** Spleens were harvested after 18-21 d. Bulk, $Ly6G^+$ and $Ly6G^-$ MDSC were sort-purified to $\geq$ 95% purity. MDSC were seeded in increasing numbers into DUC18 $CD8^+$ T cell and tERK-pulsed DC co-cultures for 72 h. Co-cultures were pulsed with [^{3}H] Thymidine during the last 18 h of incubation to assess proliferation. Relative mean + SEM $CD8^+$ T cell proliferation was calculated based on normalization to the 10 $CD8^+$ Tcells:1 spDC:0 MDSC control group. Data are representative of two independent experiments, and samples were each run in triplicate. Cultures containing MDSC were compared to the control group using 2-way ANOVA, *** $p \leq 0.001$.

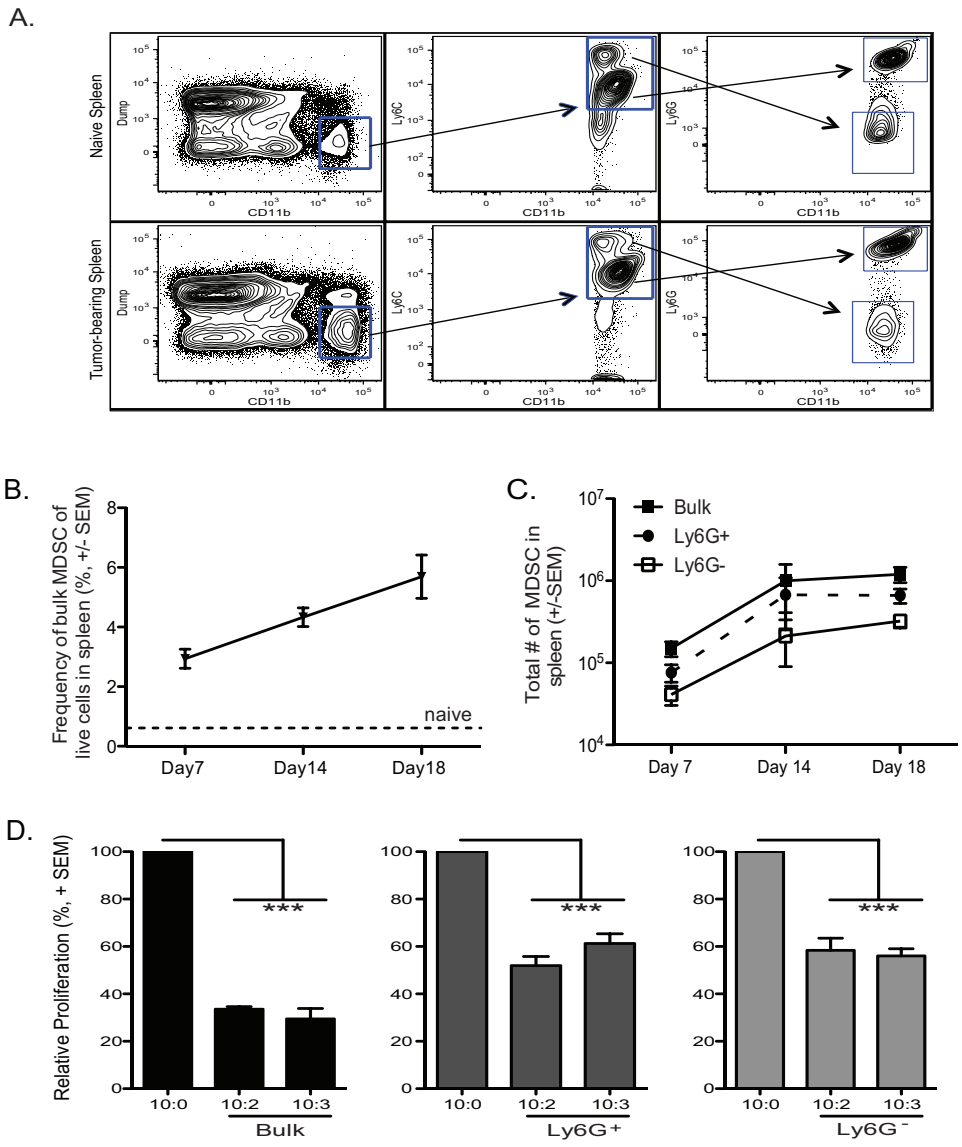

Figure 4-1: Characterization of MDSC from spleens of RCC tumor-bearing mice

Figure 4-2: MDSC promote tumor growth

(A) Mean + SEM number of $CD11c^{-}CD11b^{+}Ly6C^{+}Ly6G^{+/-}$ splenocytes in naïve mice following 1 dose of 1 mg anti-Gr1 mAb on d6. **(B)** Mean +/- SEM kidney weight (g) from tumor-bearing mice was determined on d 12. Data are representative of three independent experiments, with at least 5 mice/group/experiment. * $p \leq 0.05$ using Student's t-test.

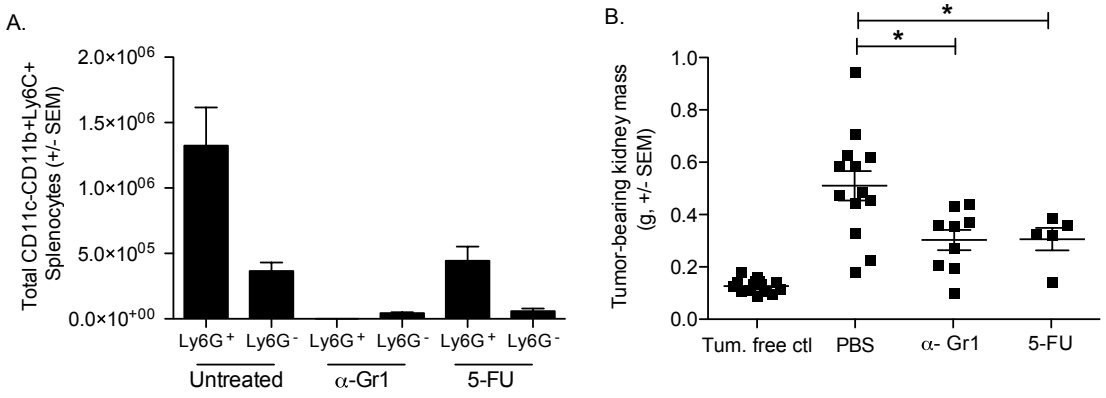

Figure 4-2: MDSC promote tumor growth

Figure 4-3: MDSC depletion does not induce a CD8 T cells response

BALB/c mice were implanted IR with $2x10^5$ Renca cells on d 0, followed by 1 dose of 1 mg anti-Gr1 mAb, or 1 dose of 1mg/20g 5-FU on d6 and Ad5-TRAIL/CpG or PBS d7. Tumor-bearing kidneys were harvested d12, homogenized, and single cell suspensions made and stained for flow cytometric analyses. Mean + SEM frequency of $CD8^+$ T cells of live cells in tumor-bearing kidneys. Data are representative of two independent experiments with at least 4 mice/group/experiment. For all experiments * $p \leq 0.05$, ** $p \leq 0.01$, *** $p \leq 0.001$ using Student's *t*-test.

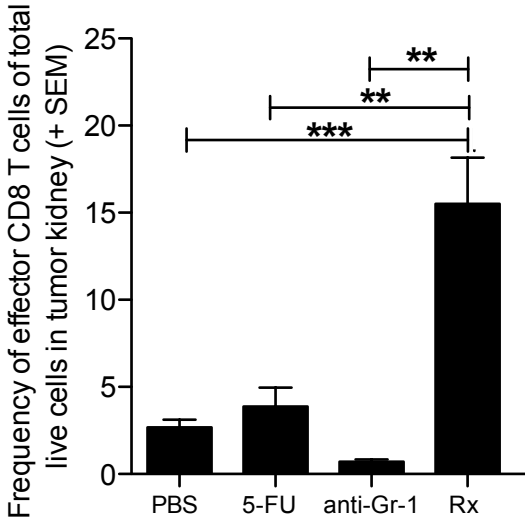

Figure 4-3: MDSC depletion does not induce a CD8 T cells response

Figure 4-4: CpG decreases MDSC in tumor-bearing mice

BALB/c mice were implanted IR with 2 x 10^5 Renca, and treated with PBS, Ad5-TRAIL alone, CpG alone or Ad5-TRAIL/CpG on d 7. Spleens were harvested on d 12 and processed for flow cytometry to determine the frequency of **(A)** bulk, **(B)** Ly6G+, or **(C)** Ly6G- $CD3^-CD19^-CD11c^-CD11b^+Ly6C^+$ MDSC. Mean + SEM frequency of splenic MDSC from tumor-bearing mice is shown, and data are representative of four independent experiments with at least mice/group/experiment. For all experiments *$p <$ 0.05, ** $p \leq 0.01$, *** $p \leq 0.001$ using Student's *t*-test.

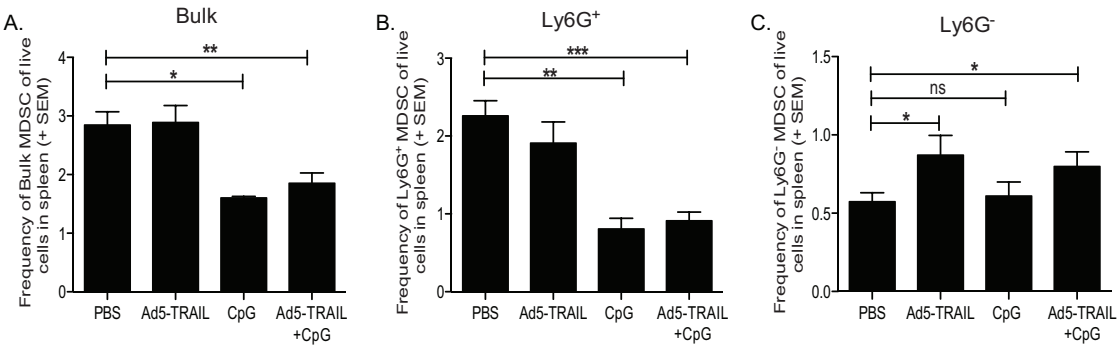

Figure 4-4: CpG decreases MDSC in tumor-bearing mice

Figure 4-5: Characterization of MDSC in tumor-bearing kidneys

BALB/c mice were implanted IR with 2 x 105 Renca. **(A)** WT tumor-bearing kidneys were harvested d 12 for IF imaging to identify MDSC. **(i-ii)** 10x images were taken and stitched together to view the entire tumor bearing kidney, and tumor margin architecture with CD31 and cytokeratins 8 and 18. The tumor margin image also includes Gr-1 and CD11b staining to visualize MDSC. **(iii)** Separate 20x images were taken to visualize Gr-1 alone, CD11b alone, and merged Gr-1+CD11b+ cells within the tumor using the structural markers to identify the regions of tumor tissue and vasculature within the kidney. Images are representative of four independent experiments totaling 8 mice. **(B-C)** Tumor-bearing and contralateral kidneys were harvested from mice 7, 14, or 18 d post tumor implantation. Single cell suspensions were made and cells were stained for flow cytometric analysis. Mean + SEM frequency and number of bulk, Ly6G+, or Ly6G- MDSC in tumor-bearing kidneys during tumor challenge. Data are representative of three independent experiments, with at least 3 mice/group/experiment. **(D)** Tumor-bearing kidneys were harvested after 18-21 d. Bulk and subset MDSC were sort-purified to > 95% purity. Co-cultures were plated and pulsed with [3H] Thymidine as described above. Relative mean + SEM CD8+ T cell proliferation was calculated based on normalization to the 10 CD8+ Tcells:1 spDC:0 MDSC control group. Data are representative of two independent experiments where samples were each run in triplicate. Cultures containing MDSC were compared to the control group using 2-way ANOVA, *** $p \leq 0.001$.

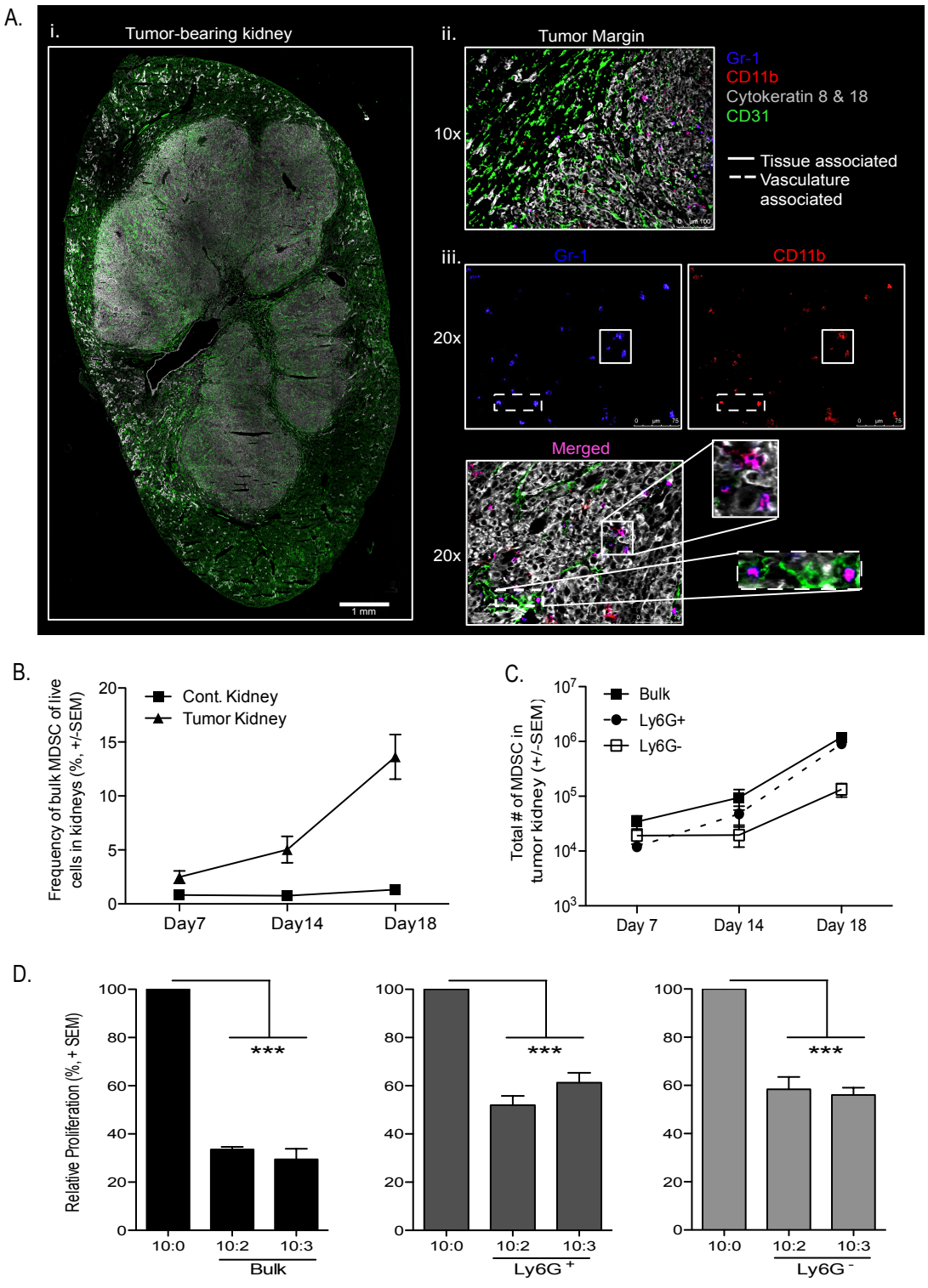

Figure 4-5: Characterization of MDSC in tumor-bearing kidneys

Figure 4-6: Ad5-TRAIL/CpG therapy alters MDSC location within the tumor-bearing kidney

BALB/c mice were implanted IR with $2x10^5$ Renca cells and treated with PBS or Ad5-TRAIL/CpG on d 7 (some mice received no injection). Tumor-bearing and contralateral kidneys were harvested on d 12. Prior to harvest, all mice were injected i.v. with PE-conjugated anti-CD45.2 mAb (3 μg) in PBS to discriminate tissue- from vasculature-associated MDSC, and sacrificed 3 min later. Single cell suspensions of tumor-bearing kidneys were prepared, and stained for flow cytometric analyses to assess MDSC cell infiltration. **(A)** Representative flow plots for tissue- or vasculature-localized MDSC in tumor-bearing and contralateral kidneys from untreated mice. **(B-C)** Mean + SEM frequency of tissue- and vasculature-localized MDSC from **(B)** tumor-bearing or **(C)** contralateral kidneys. Data are representative of three independent experiments totaling 8 mice. **(D-G)** Mean + SEM frequency of bulk MDSC, $Ly6G^+$, or $Ly6G^-$ MDSC in the tissue and vasculature of tumor-bearing kidneys from mice treated with either PBS or Ad5-TRAIL/CpG on d 7. Data are representative of four independent experiments with at least 4 mice/group/experiment. For all experiments ** $p \leq 0.01$, *** $p \leq 0.001$ using Student's *t*-test.

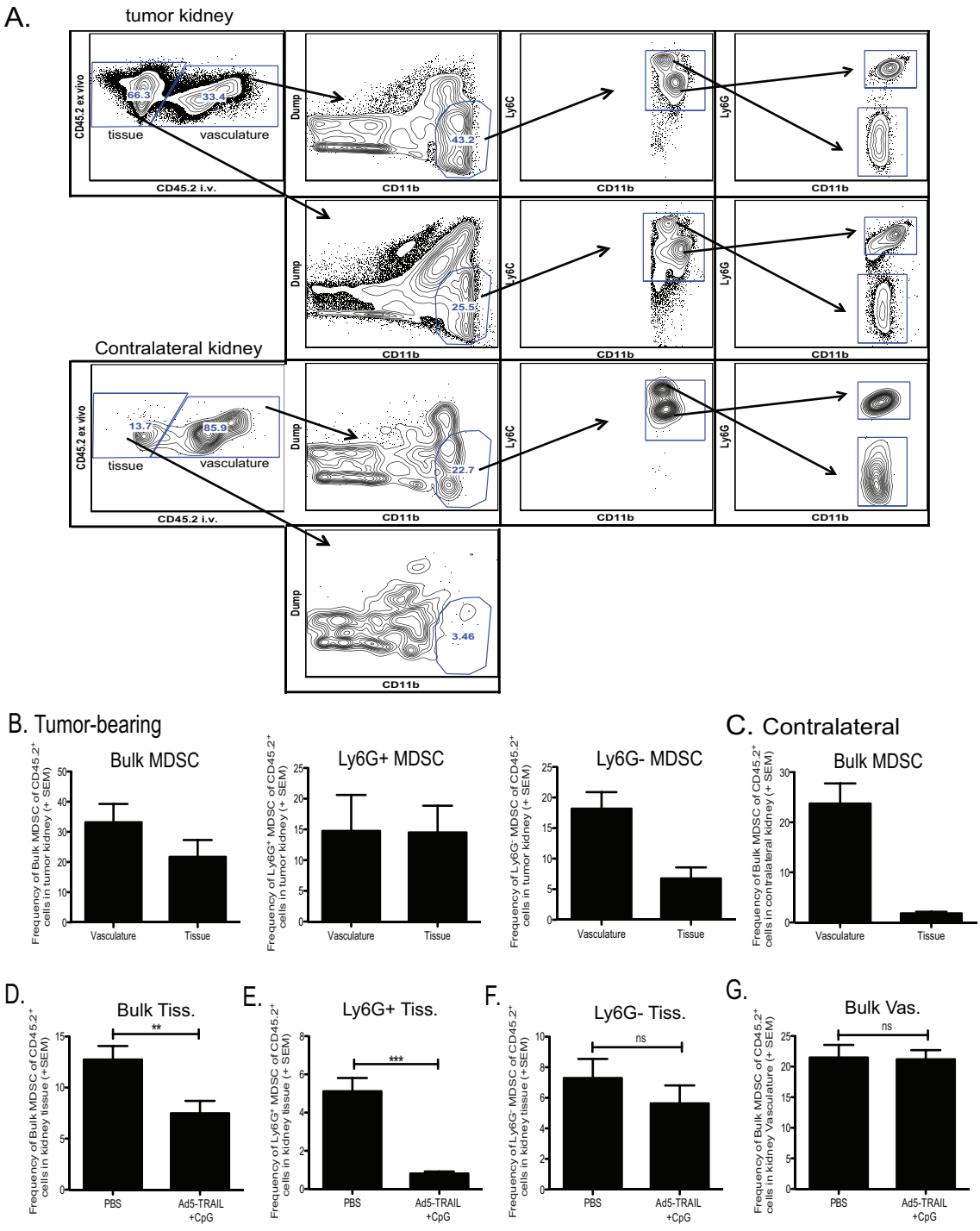

Figure 4-6: Ad5-TRAIL/CpG therapy alters MDSC location within the tumor-bearing kidney

Figure 4-7: CpG alters MDSC phenotype and function *in vitro* and *in vivo*

BALB/c mice were implanted IR with 2 x 10^5 Renca, and tumor-bearing kidneys and spleens were harvested d18-21. **(A)** Splenocytes were plated 10^6cells/well in a 24-well plate. Cells were either treated with 100U of IFN-γ or 6μg CpG overnight. Cells were harvested from plate and stained for flow cytometric analysis. **(A)** Mean + SEM frequency of MDSC expressing high levels of CD80, MHCII, CD86 and CD40. Data are representative of three independent experiments with at least 4 mice/group/experiment. **(B)** Mean +/- SEM $CD8^+$ T cell proliferation from MACs purified naïve WT BALB/c splenic $CD8^+$ T cells stimulated with 1μg/ml anti-CD3 mAb and co-cultured with +/- CpG-stimulated MACS purified bulk MDSC. Ratios represent #$CD8^+$ T cells: # MDSC. Co-cultures were pulsed with [^{3}H] Thymidine during the last 18 hours of incubation to assess proliferation. Data are representative of two independent experiments in which samples were each run in triplicate, *** $p \leq 0.001$ using 2-way ANOVA. **(C)** qPCR analysis of *arg1* expression in Renca-bearing kidneys 4 h after injection of PBS or CpG. (**D**) BALB/c mice were implanted IR with 2 x 10^5 Renca, and treated with CpG alone or PBS on d7 and tumor-bearing kidneys were harvested d 12. Single cell suspensions were made and stained for flow cytometric analysis. Mean + SEM frequency of MDSC expressing high levels of the activation markers. Data are representative of two independent experiments with at least 4 mice/group/experiment. For all experiments (except where noted) * $p \leq 0.05$, ** $p \leq 0.01$, *** $p \leq 0.001$ using Student's *t*-test.

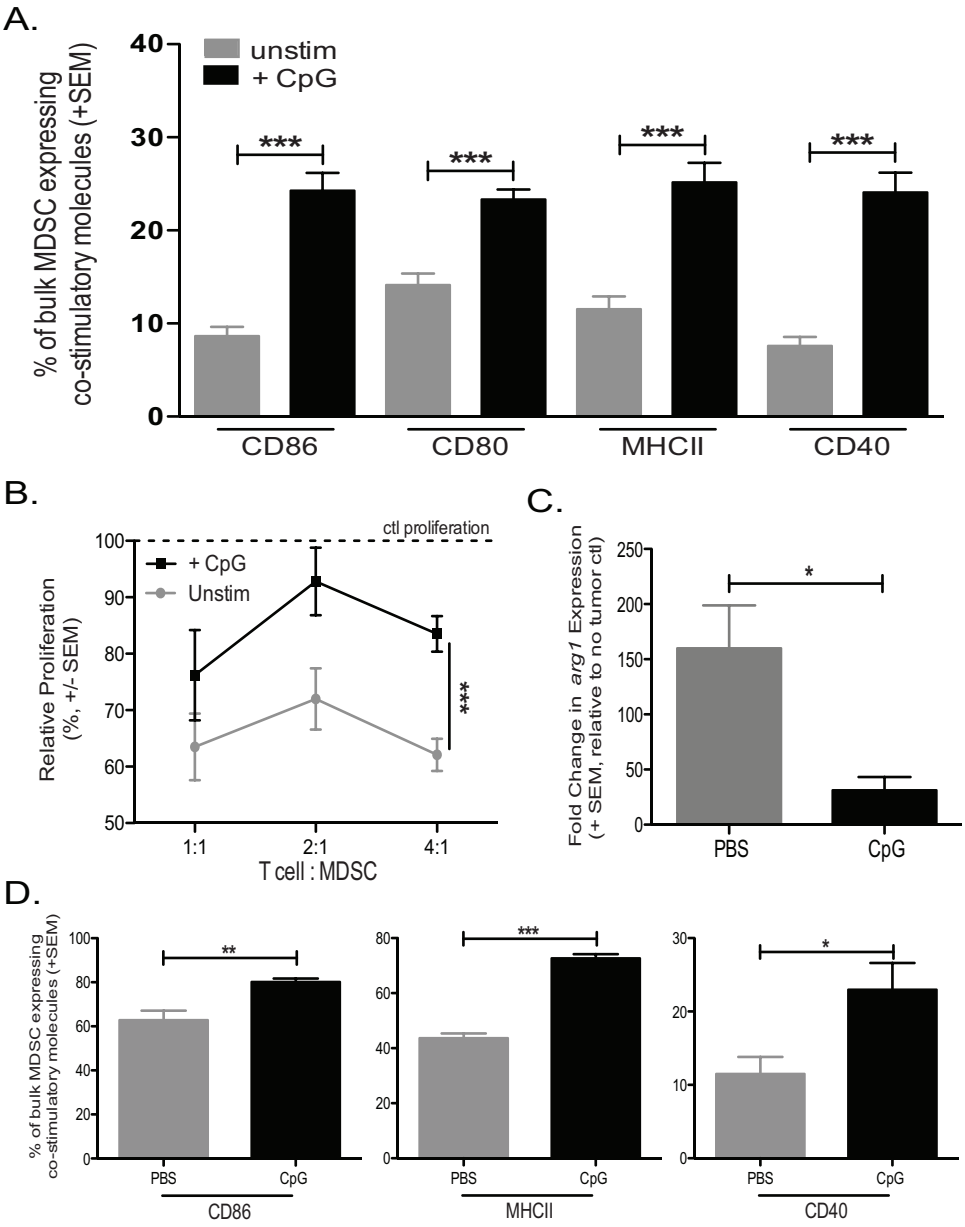

Figure 4-7: CpG alters MDSC phenotype and function *in vitro* and *in vivo*

Figure 4-8: DIO tumor-bearing mice have increased MDSC that do not respond to CpG resulting in a diminished antitumor response

Lean and DIO BALB/c mice were implanted IR with $2x10^5$ Renca cells on d 0 and either left untreated **(A-B)**, or treated with PBS or Ad5-TRAIL/CpG on d 7 **(C-E)**. Spleens and tumor-bearing kidneys were harvested d12, homogenized, and single cell suspensions made and stained for flow cytometric analyses. **(A-B)** Mean + SEM frequency of MDSC in spleens and tumor-bearing kidneys. **(C-F)** Mean + SEM frequency, using i.v. staining, of MDSC and $CD8^+$ T cells and respective ratio of the number of $CD8^+$ T cells to the number of MDSC. Data are representative of two independent experiments with at least 4 mice/group/experiment. For all experiments * $p \leq 0.05$, ** $p \leq 0.01$, *** $p \leq 0.001$ using Student's *t*-test. **(G)** Mean + SEM $CD8^+$ T cell proliferation from MACS purified naïve WT BALB/c splenic $CD8^+$ T cells stimulated with 1μg/ml anti-CD3 mAb and co-cultured with CpG-stimulated MACS purified bulk MDSC from either lean or DIO tumor-bearing kidneys. Ratios represent #$CD8^+$ T cells: # MDSC. Co-cultures were pulsed with [^{3}H] Thymidine during the last 18 hours of incubation to assess proliferation. Data are representative of two independent experiments in which samples were each run in triplicate, *** $p \leq 0.001$ using 2-way ANOVA.

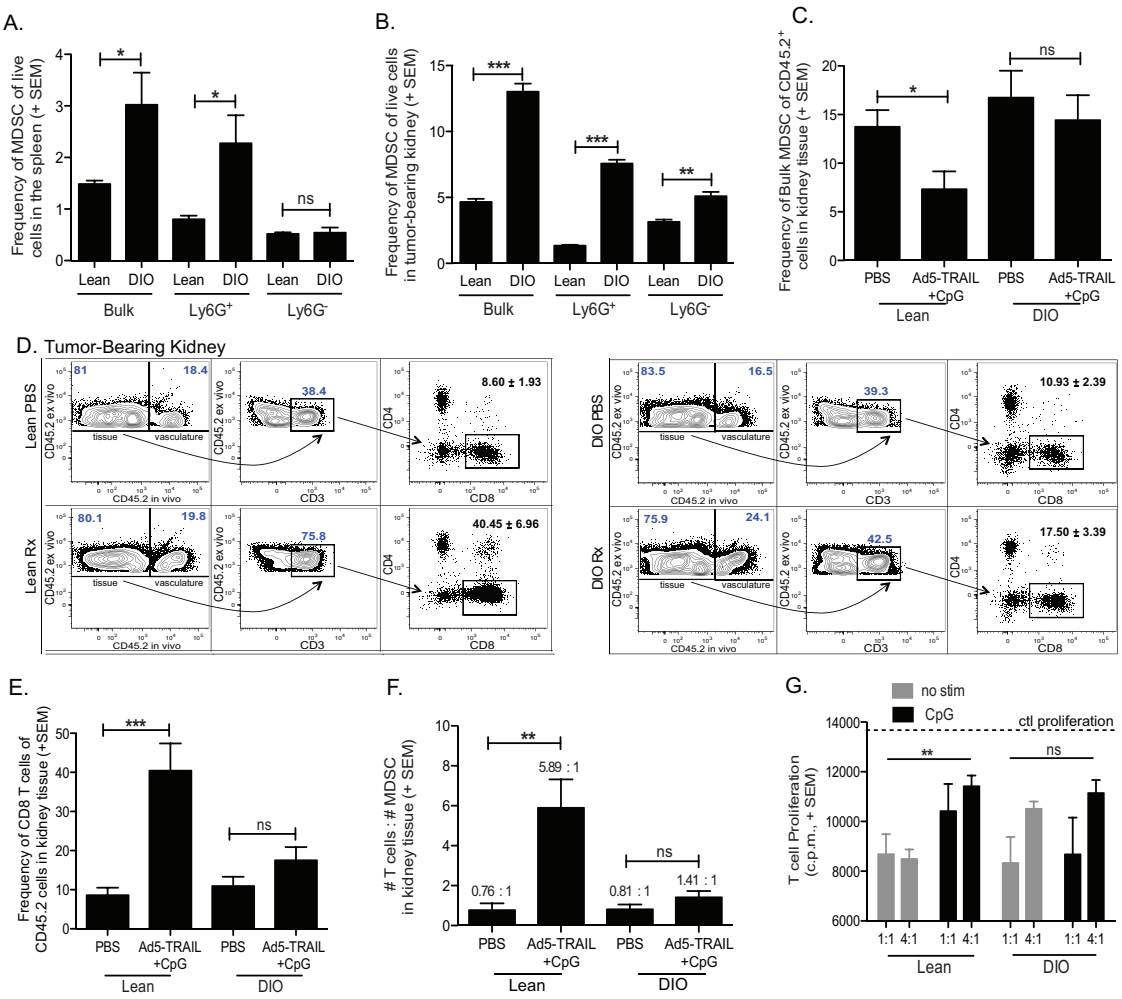

Figure 4-8: DIO tumor-bearing mice have increased MDSC that do not respond to CpG resulting in a diminished antitumor response

Acknowledgement: The work in this chapter was modified from "CpG-mediated modulation of MDSC contributes to the efficacy of Ad5-TRAIL/CpG therapy in renal cell carcinoma" submitted to *Cancer Immunology, Immunotherapy.*

Chapter 5: Discussion and Future Directions

For years cancer therapies have attempted to stimulate one's own immune system to induce an endogenous antitumor response to eradicate the primary and metastatic tumor burden. However, many of these immunotherapies failed when introduced into the clinic, even though there was evidence of tumor immunogenicity and the expansion of antigen-specific T cells. Because of these discrepancies our lab has focused on identifying the immune cells, other than T cells, at play during the induction of an antitumor immune response. We also set out to understand how immune-regulating co-morbidities can negatively impact immunotherapy efficacy, and how these may be overcome.

Both CD8αDC and pDC have been implicated in the antitumor immune response and the relationship/crosstalk between the two can be very important, making it important to understand how these two cell populations work together. For example, pDC are important in the licensing of CD8αDC to optimally uptake and present antigen. The antitumor CD8 T cell response strongly depends on efficient tumor antigen availability and presentation by CD8αDC as well as cytokine signals, presumably from CD8αDC and pDC. Our lab has previously demonstrated that Ad5-TRAIL/CpG therapy induces tumor cell death, and released tumor cell antigens are taken up and presented by conventional DC (cDC, $CD11c^{+}MHCII^{+}$)[20]. However, these previous experiments were done *in vitro* and did not demonstrate requirement of DC populations for therapy efficacy *in vivo*. To determine the necessity and function of DC populations following Ad5-TRAIL/CpG therapy we utilized depletion models to selectively deplete mice of different DC populations prior to therapy. The results from Chapter 2 indicate that both pDC and CD8αDC were necessary to induce antitumor immunity capable of clearing tumor and prolonging survival in Renca tumor-bearing animals. CD8αDC were required for optimal cytokine production, pDC activation and CD8 T cell accumulation. pDC appeared to play a minor role in cytokine production yet were necessary for CD8 T cells accumulation in tumors. These data suggest that of the two populations, CD8αDC are important early on

in the induction of antitumor immunity, and that pDC may play more of a secondary role in the response.

A surprising finding from Chapter 2 was the loss of the type I IFN response in the *Batf3-/-* mice, and the intact type I IFN response in the pDC-depleted mice. One explanation for this observation could be that CD8αDC are the primary producers of type I IFN in this system. Although pDC are historically described as the main producers of type I IFNs, many have demonstrated the ability of cDC and CD8αDC to produce IFNα/β. Sato and colleagues[294] (reviewed in[295]) have described a biphasic model of type I IFN induction that could be an explanation for the results seen in Chapter 2. The biphasic model describes an early type I IFN phase that begins with IRF-3 activation, eliciting weak production of IFNβ, specifically. This induction of IFNβ, though modest, potently signals through IFNAR and induces IRF-7. The cooperation between IRF-7 and IRF-3 leads to a very robust, late-phase production of IFNα/β. The type I IFN from either the early or late phases would have been adequate to induce upregulation of the IFN-response genes we examined. Therefore, the 4hr time point might have only captured the "early" IFNβ response, which CD8αDC are known to produce, explaining why *Batf3-/-* lacked this response. If the early IFNβ production by CD8αDC was the primary response seen at 4h, this would explain why the pDC-depleted and WT-replete mice had similar type I IFN signatures, as they both had intact CD8αDC compartments. This hypothesis would suggest that if a later time point were examined, during the second IFNα/β response (presumably involving pDC-dependent production of IFNα), we would have observed a difference between the WT-replete and pDC-depleted treatment groups. Additionally, type I IFN is necessary for optimal DC maturation and activation, explaining a possible reason why the pDC from *Batf3-/-* mice exhibited decreased levels of maturation markers.

pDC-depleted mice had normal activation of CD8αDC and production of a type I IFN but their CD8 T cell response was blunted, similar to *Batf3-/-* mice. pDC-depleted and *Batf3-/-* mice also exhibited decreased *in situ* production of IL-15/IL-15R complex. The loss of IL-15/IL-15R production could explain the decreased CD8 T cell response as

IL-15/IL15R promotes proliferation and activation of CD8 T cells, specifically in the tumor microenvironment[250]. To fully understand the extent to which the IL-15/IL-15R deficit contributed to the decreased CD8 T cell response and subsequent uncontrolled tumor growth, add-back experiments could be completed. Administration of exogenous IL-15/IL-15R complexes have been used to treat solid tumors, and have shown promising results in eliciting tumor-specific CD8 T cell responses[113, 296]. Including IL-15/IL-15R complexes in the treatment scheme prior to and/or following Ad5-TRAIL/CpG may be able to rescue the pDC-depleted and *Batf3-/-* phenotype, and would confirm the necessary role for IL-15/IL-15R in the antitumor response elicited by Ad5-TRAIL/CpG therapy.

Altered T cell trafficking is an attractive explanation for the decreased accumulation of effector CD8 T cells into tumors of DC-depleted mice. The integrin, CD11a was expressed at high levels on the WT-replete CD8 T cells, but at significantly lower levels on the CD8 T cells from the DC-depleted groups. CD11a can be used as marker of T cell activation, but functionally it can dimerize with CD18 and act as an integrin (LFA-1) that binds to ICAM-1[297], an adhesion molecule expressed on vascular endothelium needed for the trafficking of T cells into tissues[298]. If the DC-depleted mice had decreased CD11a and ICAM-1 expression on vasculature endothelium, that could explain why those groups demonstrated decreased T cell numbers in their tumors. CpG can induce ICAM-1[299] and VCAM-1 (another adhesion molecule)[300] and we have confirmed this in our tumor model. Using flow cytometric analysis and immunofluorescence imaging of tumors we found that following Ad5-TRAIL/CpG therapy in WT-replete mice, there is a rapid and sustained upregulation of ICAM-1 and VCAM-1 on vasculature endothelium ($CD31^+$ cells) within the tumor-bearing kidney (Figure 5-1). Further analysis of ICAM-1 and VCAM-1 expression on vasculature endothelium in the DC-depleted mice following therapy would be of interest. If these molecules were expressed at lower levels, coupled with the decreased CD11a on the T cells, it would suggest an overall deficit in T cells trafficking in pDC and CD8αDC deficient mice.

Chapter 3 explored the impact of diet-induced obesity on the immune system and subsequently on the efficacy of Ad5-TRAIL/CpG for the treatment of RCC. Studies demonstrated that naïve DIO mice exhibited classical signs of obesity, including increased body weight, visceral fat and serum leptin. DIO mice also presented with a low-grade level of inflammation, typical of obese hosts. While appearing to have normal DC development, the DC from naïve DIO mice had a decreased functional capacity to induce antigen-specific T cell proliferation and had an altered cytokine/chemokine profile. T cells from DIO mice also lacked in cytolytic function. Tumor growth in DIO mice was somewhat accelerated and was accompanied by a large induction of tumor-associated myeloid DC compared to lean controls. When isolated, the myeloid DC from the DIO tumors proved to be regulatory and inhibited T cell proliferation *in vitro.* These immune dysfunctions correlated with DIO mice not responding to Ad5-TRAIL/CpG therapy and ultimately succumbing to tumor. These studies demonstrated the need to account for common co-morbidities that are present in patients, when examining the efficacy of a therapy in pre-clinical studies.

Obesity is one of the main risk factors and co-morbidities for RCC and it has been documented to cause many dysregulations of the immune system. This suggests that immunotherapies that utilize the host's immune system are more likely to fail in obese hosts, as we have demonstrated. Further research into methods to modulate the immune system's ability to respond adequately to immunotherapy is needed for pre-clinical studies. One avenue of investigation has been to target leptin, a hormone secreted from adipose tissue, and highly elevated in obese individuals. Leptin can play a role in the regulation of immune function as its receptor is expressed in a variety of immune cells. Leptin signals via JAK/STAT pathways, specifically STAT3, and constitutive STAT3 signaling has been implemented in cancer progression. Leptin signaling can also induce the production of elevated proinflammatory cytokines, which can lead to altered innate and adaptive immune responses. These data suggest the elevated leptin in obese patients could be a plausible mechanism by which the obese environment negatively impacts the

immune system. Therapies aimed at modulating leptin levels/activity could potentially help restore the obese immune system.

Blocking leptin signaling could be a viable pre-treatment to immunotherapy to help allow the obese immune system to respond. Using reagents such as recombinant leptinR-Fc chimeras (leptin receptor bound to the Fc portion of an antibody) could be used to essentially "soak up" the soluble leptin present in the system, effectively decreasing the amount of leptin available to signal through endogenous receptors expressed on immune cells. This approach would allow for a "resetting" of the obese immune system in the absence of immunosuppressive leptin signaling, theoretically leading to an immune system that can respond to immunotherapy treatment. The drawback to these experiments is not knowing the amount of time needed to restore immune cell function.

Apart from the immunological effects leptin plays, it can also have direct effects on the tumor cells themselves. Leptin receptor is expressed on both murine and human RCC cell lines[301], and ligation of leptin to the receptor on the tumor cells can induce JAK/STAT and ERK signaling pathways leading to increased proliferation and mobility[302, 303]. Leptin signaling can induce anti-apoptotic signals within tumor cells[304] thereby potentially rendering tumor cells insensitive to TRAIL-induced death. Ad5-TRAIL/CpG immunotherapy relies on the availability of apoptotic tumor cell debris as the source of antigen to induce an antitumor immune response. If leptin decreases TRAIL-induced death of tumor cells in obese hosts, this would in part explain why DIO mice do not respond to Ad5-TRAIL/CpG therapy. Preliminary data examining tumor burden via bioluminescence imaging 24h post Ad5-TRAIL/CpG therapy of lean and DIO tumor-bearing mice, suggests that the initial loss of tumor cells (as seen by a decrease in bioluminescence) that occurs in lean hosts, does not occur in DIO hosts (Figure 5-2). Additionally, tumor cells that were implanted into DIO hosts and examined 7d later demonstrated a significant decrease in DR5 expression compared to lean controls (Figure 5-2). TRAIL-based therapies are also thought to work by inducing death of DR5-expressing tumor vasculature thereby cutting off the blood supply to the tumor. $CD31^+$

vasculature cells from DIO tumors also had significantly decreased expression of DR5 compared to lean tumors (Figure 5-2). These data suggest a mechanism by which the obese environment renders tumors unresponsive to Ad5-TRAIL/CpG therapy. $CD31^+$ vasculature cells in DIO tumors, also failed to upregulate ICAM-1 following Ad5-TRAIL/CpG treatment, which would lead to decreased T cell trafficking to the site of the tumor (Figure 5-1). Further investigations into the tumor microenvironment and processes taking place within the tumor following therapy in lean and DIO mice, are needed in pre-clinical studies to help understand how better to treat patients in the clinic.

Besides therapeutically blocking leptin, decreasing inflammation or key regulators of inflammation prior to immunotherapy treatment could potentially restore the obese immune system. The chronic low-grade inflammation present in obese hosts has been implemented in tumor promotion, acceleration, invasion and metastasis. Additionally the tumor, once established, also produces an inflammatory environment that the immune system must over come. Common inflammatory mediators that are over expressed within both an obese and tumor environment include prostaglandins, specifically prostaglandin E_2 (PGE_2)[305, 306]. PGE_2 is a small lipid molecule that belongs to the family of prostanoids, which mediate inflammatory effects. PGE_2 is synthesized via cyclooxygenases, COX-1 and COX-2, with COX-2 being an inducible enzyme related to inflammation (both obesity- and tumor-related)[305, 307]. PGE_2 can inhibit T cell proliferation and stimulation, bias cytokine production and inhibit DC maturation, all of which are characteristics of obesity and tumor-induced immune suppression[308]. Investigating the contribution of COX-2/ PGE_2 in either obese- or tumor-induced immunosuppression in our system would be of interest, as there are already approved COX-2 inhibitors that could be utilize to counteract these immunosuppressive effects[309].

Preliminary studies utilizing a Renca cell line that overexpresses the COX-2 (Renca GLS) enzyme and secretes large amounts of PGE_2, demonstrated that increased COX-2 led to unresponsiveness of mice to Ad5-TRAIL/CpG therapy (Figure 5-3). Kinetic analysis of tumor growth via bioluminescence imaging of mice bearing control Renca (Renca GLE) tumors or Renca GLS tumors and treated with either Ad5-

TRAIL/CpG or PBS on day 7 revealed that Renca GLS tumor-bearing mice had significantly increased tumor burden overtime compared to controls. These data suggest that over expression of COX-2/ PGE_2 can inhibit antitumor immunity elicited by Ad5-TRAIL/CpG. As stated above, overexpression of COX-2/ PGE_2 also exists in the obese environment. Further examination into the COX-2/PGE_2 axis and how it may impact immune suppression in DIO mice would be of interest. If increased levels of COX-2/ PGE_2 are found during the steady state and within the tumor microenvironment of DIO mice compared to lean controls, COX-2 inhibitors[309] may be an option to help restore the ability of DIO mice to respond to Ad5-TRAIL/CpG.

Chapter 4 characterized the MDSC population mobilized by orthotopic Renca tumors, and the modulation of the population following Ad5-TRAIL/CpG treatment. Though chemotherapy and immunotherapy approaches have shown promising pre-clinical and in some cases clinical outcomes, overall new cancer therapies have failed to improve the survival for many human cancers. It has become increasingly clear that therapies must also concomitantly block or decrease immunosuppressive and tumorigenic factors in combination with killing tumor cells directly or inducing antitumor immunity. MDSC are one of the main cell types that are both tumorigenic and immunosuppressive; therefore modulation of the population has become of increasing interest to many cancer therapy researchers.

Data in Chapter 4 demonstrated that the orthotopic Renca tumor induces the mobilization and accumulation of MDSC that are suppressive and promote tumor growth. However, following Ad5-TRAIL/CpG therapy, this population was significantly decreased and inherently altered to be less suppressive in a CpG-dependent manner. The decrease in MDSC correlated with an increase in activated CD8 T cell accumulation within the tumor tissue of Ad5-TRAIL/CpG treated animals, compared to PBS. Interestingly, decreases/alterations in MDSC and corresponding T cell accumulation was not observed in mice that were complicated with diet-induced obesity. These observations support the data in Chapter 3, demonstrating that DIO mice do not respond to therapy and ultimately succumb to the tumor.

The mechanisms by which obesity alters and induces an increased accumulation of MDSC have yet to be elucidated, though it is reasonable to hypothesize that the low-grade inflammation and altered cytokine/chemokine signature associated with obesity are to blame. Obesity is associated with increased inflammatory cytokines, such as IL-1α/β[172], which increase MDSC numbers and induce activation of MDSC[146, 310]. Similarly, obesity can increase systemic levels of other known inducers and activators of MDSC such as COX-2/PGE_2, CCL2[173, 311], S100A[154, 312] proteins and VEGF, just to name a few. Inherent changes in MDSC generation in the bone marrow could also differ in DIO and lean mice. For example, loss of the transcription factor, Irf8, increased myelopoiesis in the bone marrow. *Irf8*$^{-/-}$ mice have decreased dendritic cell development and increased neutrophil/MDSC-like cell development from common lymphoid and common myeloid progenitors (CLP and CMP)[107, 159]. Based on this, one may hypothesize that the obese environment could alter the transciptome of hematopoietic cells causing aberrant development of myeloid/neutrophil cells. Preliminary data examining *Irf8* expression in whole bone marrow from naïve lean and obese mice revealed that *Irf8* mRNA expression was not altered (Figure 5-4). Examination of other lineage-committing transcription factors, as well as isolating CLPs and CMPs specifically for analysis, would be of interest to understand if there are differences in lineage commitment between the bone marrow from lean and DIO mice. Understanding how obesity-driven factors contribute to MDSC accumulation and function will become important when testing the efficacy of therapies, as overcoming the MDSC population is one of the main hurdles for immunotherapies. Immunotherapies, that otherwise would be successful in lean hosts, will need to be combined with other drugs/inhibitors to be aid in the reduction of the over-abundant MDSC population in obese hosts.

Though the reason for the therapy not working in DIO mice could solely be due to increased numbers of MDSC, the data also suggests that the MDSC that are generated in the obese environment were non-responsive to CpG. Understanding the inherent differences between the MDSC generated in DIO vs. lean hosts would be beneficial to helping tailor therapies. Preliminary data using isolated MDSC from lean and DIO

tumor-bearing hosts suggested that the level of TLR9 mRNA is not decreased in DIO mice, which would have rendered those MDSC non-responsive to CpG (Figure 5-5). Additionally, enzyme activity and cytokine secretion did not seem to be altered in DIO MDSC as seen by similar levels of nitrite, urea and IL-10 in supernatants of isolated MDSC from DIO and lean hosts, *in vitro* (Figure 5-5). Further investigation into characterization of functional TLR9 signaling and subsequent function of MDSC from lean and DIO tumor-bearing mice following CpG stimulation will need to be done.

In summary, the research outlined in this thesis has provided multiple mechanisms by which Ad5-TRAIL/CpG therapy induces a $CD8^+$ T cell response capable of eradicating RCC tumors. These data, coupled with previous work from the lab, suggest a model whereby Ad5-TRAIL/CpG induces antitumor immunity by activating (via CpG) DC to cross-present antigen (via Ad5-TRAIL-induced tumor cell death) and secrete cytokines needed to elicit a tumor-specific $CD8^+$ T cell response in lean mice. Additionally in lean mice, Ad5-TRAIL/CpG reduces the frequency and modulates the suppressive capacity of the MDSC population. In contrast, mice complicated with diet-induced obesity to mount a $CD8^+$ T cell response following Ad5-TRAIL/CpG therapy and subsequently succumb to the tumor. Our data suggests that DIO mice do not respond to therapy due to decreased functional capacity of both the DC and T cell compartment, coupled with a significant increase in the MDSC population. These findings provide significant pre-clinical data supporting the use of Ad5-TRAIL/CpG as an immunotherapy, but also that combinatorial approaches may be necessary to counteract complications of obesity.

Figure 5-1: Ad5-TRAIL/CpG therapy induces ICAM-1 and VCAM-1 expression on CD31+ cells in tumors of lean mice but not DIO mice

BALB/c mice were implanted IR with 2 x 10^5 Renca. **(A)** Tumor-bearing kidneys were harvested d 12 for IF imaging to identify ICAM-1 expression on $CD31^+$ cells. 20x images were taken to view the tumor bearing kidney architecture with CD31 and cytokeratins 8 and 18. **(B)** Tumor-bearing kidneys were harvested d 9 for flow cytometric analysis to identify ICAM-1/VCAM-1 expression on $CD31^+$ cells. One representative experiment shown where n= 3-4mice/group. *$p \leq 0.05$, ** $p \leq 0.001$ using student's t-test.

A. IHC, 5 days post Rx

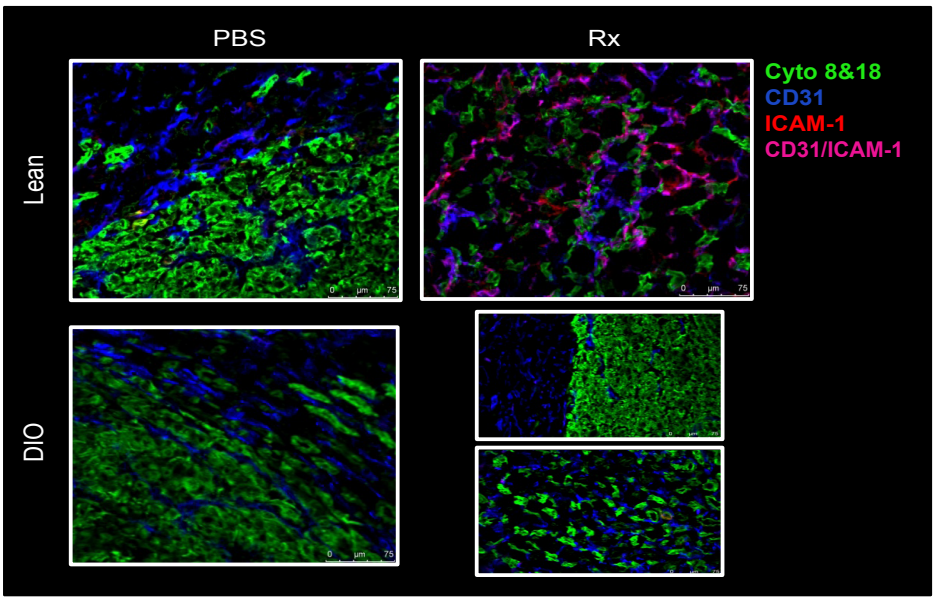

B. Flow Cytometry, 2 days post Rx

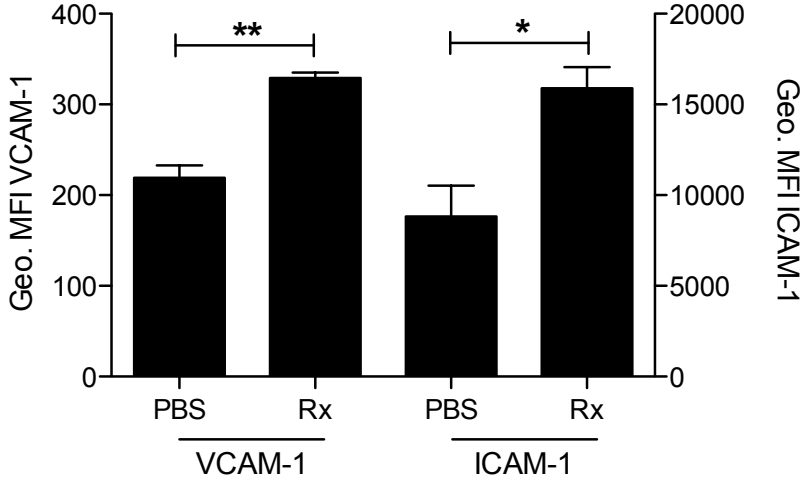

Figure 5-1: Ad5-TRAIL/CpG therapy induces ICAM-1 and VCAM-1 expression on CD31+ cells in tumors of lean mice but not DIO mice

Figure 5-2: DIO mice have reduced DR5 expression on both tumor and vasculature cells within the tumor-bearing kidney

BALB/c mice were implanted IR with 2 x 10^5 Renca. **(A)** BLI of whole body one day (d8) after Ad5-TRAIL/CpG therapy on d7. **(B)** Tumor-bearing kidneys were harvested d7 for flow cytometric analysis to identify DR5 expression on $CD31^+$ cells and tumor cells. One representative experiment shown where n= 3-4mice/group. ** $p \leq 0.001$ using student's t-test.

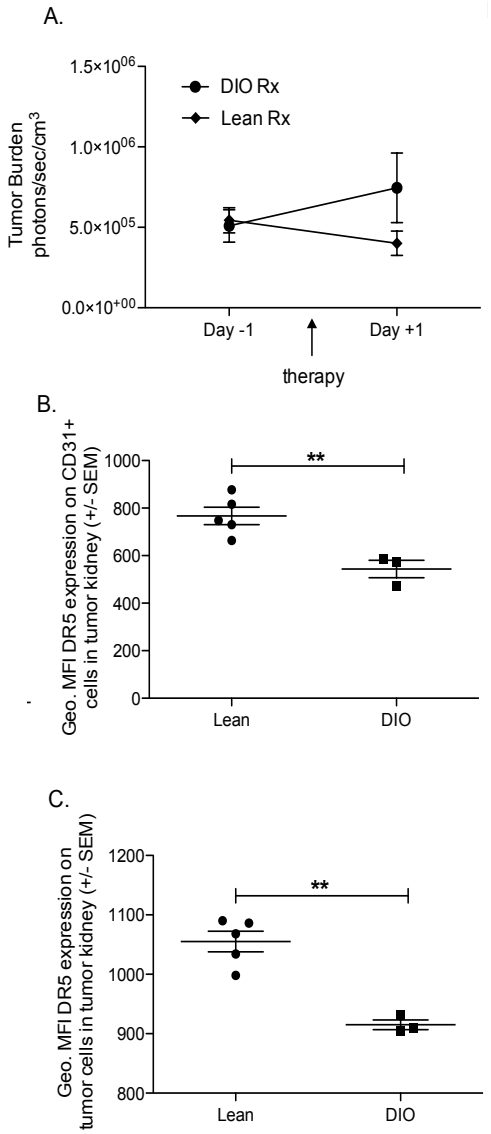

Figure 5-2: DIO mice have reduced DR5 expression on both tumor and vasculature cells within the tumor-bearing kidney

Figure 5-3: Overexpression of COX-2 by tumor cells leads decreased Ad5-TRAIL/CpG therapy efficacy

BALB/c mice were implanted IR with 2 x 10^5 Renca-GLS or Renca-GLE cells, and then treated with either PBS or Ad5-TRAIL/CpG (Rx) on d 7. (**A**-**B**) Mean +/- SEM orthotopic tumor burden in mice monitored via bioluminescence. One representative experiment shown where n= 5 mice/group. *** $p \leq 0.001$ using 2-way ANOVA.

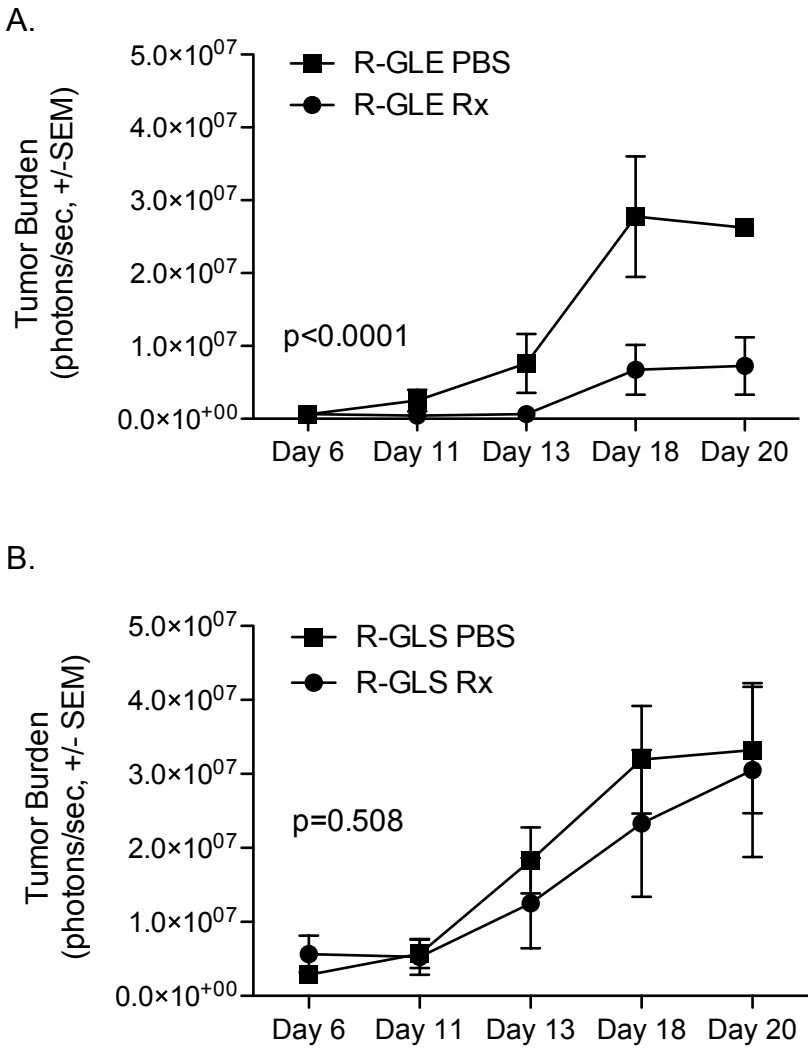

Figure 5-3: Overexpression of COX-2 by tumor cells leads decreased Ad5-TRAIL/CpG therapy efficacy

Figure 5-4: Bone marrow cells from DIO and lean mice have similar *Irf8* expression
Total RNA was isolated from whole bone marrow cells, reverse transcribed into cDNA, and analyzed by qPCR for the abundance of *Irf8* mRNA expression. Mean fold change of Irf8 mRNA expression in DIO bone marrow was determined relative to lean bone marrow. Samples were run in duplicate.

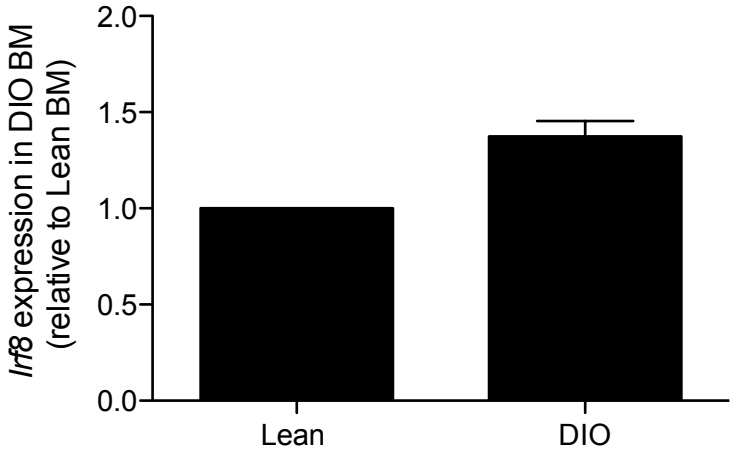

Figure 5-4: Bone marrow cells from DIO and lean mice have similar *Irf8* expression

Figure 5-5: MDSC from lean and DIO tumor-bearing mice have similar functional output

BALB/c mice were implanted IR with 2 x 10^5 Renca, and tumor-bearing kidneys were harvested d18-21. MDSC were isolated via MACs-enrichment and plated 10^6cells/well in a 24-well plate. Cells were either treated with 100U of IFN-γ or 6μg CpG overnight. Cells and supernatants were harvested from plate analyzed for **(A)** nitrite production by INOS, **(B)** urea production by arginase 1, and **(C)** IL-10 production. **(A-B)** Mean + SEM analyte production. Data are representative of 2 independent experiments with at least 4 mice/group/experiment.

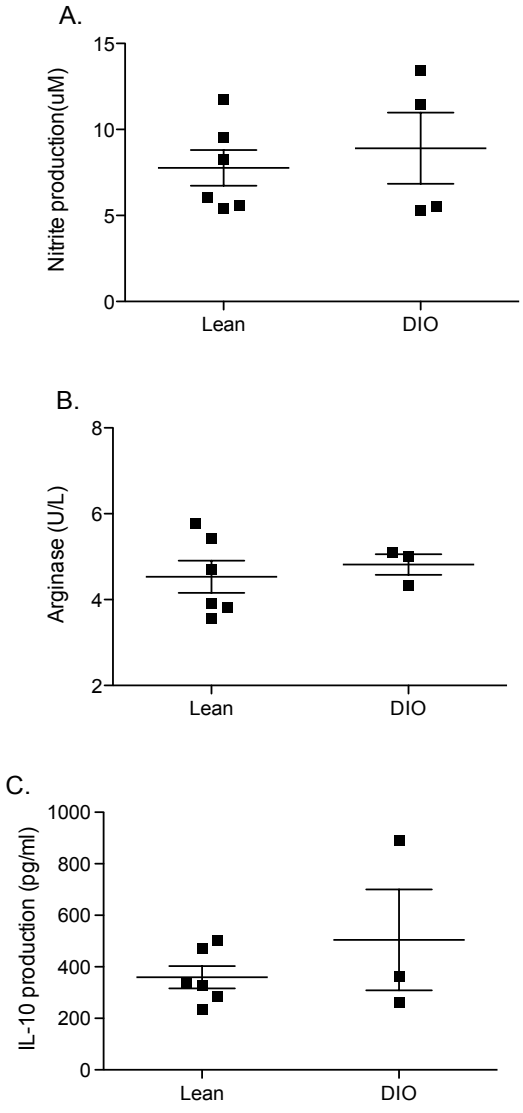

Figure 5-5: MDSC from lean and DIO tumor-bearing mice have similar functional output

References:

1. Ather, M. H., Masood, N., Siddiqui, T.: Current management of advanced and metastatic renal cell carcinoma. Urol J, **7:** 1, 2010
2. Snow, R.: Spontaneous regression of metastatic renal cell carcinoma. **20:** 177, 1982
3. McDermott, D. F.: Immunotherapy of metastatic renal cell carcinoma. Cancer, **115:** 2298, 2009
4. Dubrot, J., Palazon, A., Alfaro, C. et al.: Intratumoral injection of interferon-alpha and systemic delivery of agonist anti-CD137 monoclonal antibodies synergize for immunotherapy. Int J Cancer, **128:** 105, 2011
5. Hervas-Stubbs, S., Perez-Gracia, J. L., Rouzaut, A. et al.: Direct effects of type I interferons on cells of the immune system. Clin Cancer Res, **17:** 2619, 2011
6. Rocha, F. G., Chaves, K. C., Chammas, R. et al.: Endostatin gene therapy enhances the efficacy of IL-2 in suppressing metastatic renal cell carcinoma in mice. Cancer Immunol Immunother, **59:** 1357, 2010
7. Westwood, J. A., Darcy, P. K., Guru, P. M. et al.: Three agonist antibodies in combination with high-dose IL-2 eradicate orthotopic kidney cancer in mice. J Transl Med, **8:** 42, 2010
8. De Palma, M., Mazzieri, R., Politi, L. S. et al.: Tumor-targeted interferon-alpha delivery by Tie2-expressing monocytes inhibits tumor growth and metastasis. Cancer Cell, **14:** 299, 2008
9. Pyrhonen, S., Salminen, E., Ruutu, M. et al.: Prospective randomized trial of interferon alfa-2a plus vinblastine versus vinblastine alone in patients with advanced renal cell cancer. J Clin Oncol, **17:** 2859, 1999
10. Atkins, M. B., Sparano, J., Fisher, R. I. et al.: Randomized phase II trial of high-dose interleukin-2 either alone or in combination with interferon alfa-2b in advanced renal cell carcinoma. J Clin Oncol, **11:** 661, 1993
11. Motzer, R. J., Hutson, T. E., Tomczak, P. et al.: Overall survival and updated results for sunitinib compared with interferon alfa in patients with metastatic renal cell carcinoma. J Clin Oncol, **27:** 3584, 2009
12. Motzer, R. J., Hutson, T. E., Tomczak, P. et al.: Sunitinib versus interferon alfa in metastatic renal-cell carcinoma. N Engl J Med, **356:** 115, 2007
13. Larkin, J. M., Eisen, T.: Renal cell carcinoma and the use of sorafenib. Ther Clin Risk Manag, **2:** 87, 2006
14. Fu, L., Wang, G., Shevchuk, M. M. et al.: Generation of a mouse model of Von Hippel-Lindau kidney disease leading to renal cancers by expression of a constitutively active mutant of HIF1alpha. Cancer Res, **71:** 6848, 2011
15. Strube, A., Stepina, E., Mumberg, D. et al.: Characterization of a new renal cell carcinoma bone metastasis mouse model. Clin Exp Metastasis, **27:** 319, 2010
16. Huang, D., Ding, Y., Li, Y. et al.: Sunitinib acts primarily on tumor endothelium rather than tumor cells to inhibit the growth of renal cell carcinoma. Cancer Res, **70:** 1053, 2010

17. Hrushesky, W. J., Murphy, G. P.: Investigation of a new renal tumor model. J Surg Res, **15:** 327, 1973
18. Murphy, G. P., Hrushesky, W. J.: A murine renal cell carcinoma. J Natl Cancer Inst, **50:** 1013, 1973
19. Norian, L. A., Kresowik, T. P., Rosevear, H. M. et al.: Eradication of metastatic renal cell carcinoma after adenovirus-encoded TNF-related apoptosis-inducing ligand (TRAIL)/CpG immunotherapy. PloS One, **7:** e31085, 2012
20. VanOosten, R. L., Griffith, T. S.: Activation of tumor-specific CD8+ T Cells after intratumoral Ad5-TRAIL/CpG oligodeoxynucleotide combination therapy. Cancer Res, **67:** 11980, 2007
21. Cha, S. S., Kim, M. S., Choi, Y. H. et al.: 2.8 A resolution crystal structure of human TRAIL, a cytokine with selective antitumor activity. Immunity, **11:** 253, 1999
22. Wiley, S. R., Schooley, K., Smolak, P. J. et al.: Identification and characterization of a new member of the TNF family that induces apoptosis. Immunity, **3:** 673, 1995
23. Yang, F., Shi, P., Xi, X. et al.: Recombinant adenoviruses expressing TRAIL demonstrate antitumor effects on non-small cell lung cancer (NSCLC). Med Oncol, **23:** 191, 2006
24. Walczak, H., Miller, R. E., Ariail, K. et al.: Tumoricidal activity of tumor necrosis factor-related apoptosis-inducing ligand in vivo. Nat Med, **5:** 157, 1999
25. Ashkenazi, A., Pai, R. C., Fong, S. et al.: Safety and antitumor activity of recombinant soluble Apo2 ligand. J Clin Invest, **104:** 155, 1999
26. Lin, T., Zhang, L., Davis, J. et al.: Combination of TRAIL gene therapy and chemotherapy enhances antitumor and antimetastasis effects in chemosensitive and chemoresistant breast cancers. Mol Ther, **8:** 441, 2003
27. Huang, X., Lin, T., Gu, J. et al.: Combined TRAIL and Bax gene therapy prolonged survival in mice with ovarian cancer xenograft. Gene Ther, **9:** 1379, 2002
28. Gurung, P., Kucaba, T. A., Schoenberger, S. P. et al.: TRAIL-expressing CD8+ T cells mediate tolerance following soluble peptide-induced peripheral T cell deletion. J Leukoc Biol, 2010
29. Brincks, E. L., Katewa, A., Kucaba, T. A. et al.: CD8 T cells utilize TRAIL to control influenza virus infection. J Immunol, **181:** 4918, 2008
30. Janssen, E. M., Droin, N. M., Lemmens, E. E. et al.: CD4+ T-cell help controls CD8+ T-cell memory via TRAIL-mediated activation-induced cell death. Nature, **434:** 88, 2005
31. Holoch, P. A., Griffith, T. S.: TNF-related apoptosis-inducing ligand (TRAIL): a new path to anti-cancer therapies. Eur J Pharmacol, **625:** 63, 2009
32. Zamai, L., Ahmad, M., Bennett, I. M. et al.: Natural killer (NK) cell-mediated cytotoxicity: differential use of TRAIL and Fas ligand by immature and mature primary human NK cells. J Exp Med, **188:** 2375, 1998

33. Griffith, T. S., Wiley, S. R., Kubin, M. Z. et al.: Monocyte-mediated tumoricidal activity via the tumor necrosis factor-related cytokine, TRAIL. J Exp Med, **189:** 1343, 1999
34. Fanger, N. A., Maliszewski, C. R., Schooley, K. et al.: Human dendritic cells mediate cellular apoptosis via tumor necrosis factor-related apoptosis-inducing ligand (TRAIL). J Exp Med, **190:** 1155, 1999
35. Kemp, T. J., Moore, J. M., Griffith, T. S.: Human B cells express functional TRAIL/Apo-2 ligand after CpG-containing oligodeoxynucleotide stimulation. J Immunol, **173:** 892, 2004
36. Kemp, T. J., Ludwig, A. T., Earel, J. K. et al.: Neutrophil stimulation with Mycobacterium bovis bacillus Calmette-Guerin (BCG) results in the release of functional soluble TRAIL/Apo-2L. Blood, **106:** 3474, 2005
37. Simons, M. P., Leidal, K. G., Nauseef, W. M. et al.: TNF-related apoptosis-inducing ligand (TRAIL) is expressed throughout myeloid development, resulting in a broad distribution among neutrophil granules. J Leukoc Biol, **83:** 621, 2008
38. Marsters, S. A., Pitti, R. A., Sheridan, J. P. et al.: Control of apoptosis signaling by Apo2 ligand. Recent Prog Horm Res, **54:** 225, 1999
39. Pan, G., O'Rourke, K., Chinnaiyan, A. M. et al.: The receptor for the cytotoxic ligand TRAIL. Science, **276:** 111, 1997
40. Pan, G., Ni, J., Wei, Y. F. et al.: An antagonist decoy receptor and a death domain-containing receptor for TRAIL. Science, **277:** 815, 1997
41. Walczak, H., Degli-Esposti, M. A., Johnson, R. S. et al.: TRAIL-R2: a novel apoptosis-mediating receptor for TRAIL. EMBO J, **16:** 5386, 1997
42. Sheridan, J. P., Marsters, S. A., Pitti, R. M. et al.: Control of TRAIL-induced apoptosis by a family of signaling and decoy receptors. Science, **277:** 818, 1997
43. Degli-Esposti, M. A., Dougall, W. C., Smolak, P. J. et al.: The novel receptor TRAIL-R4 induces NF-kappaB and protects against TRAIL-mediated apoptosis, yet retains an incomplete death domain. Immunity, **7:** 813, 1997
44. Marsters, S. A., Sheridan, J. P., Pitti, R. M. et al.: A novel receptor for Apo2L/TRAIL contains a truncated death domain. Curr Biol, **7:** 1003, 1997
45. Pan, G., Ni, J., Yu, G. et al.: TRUNDD, a new member of the TRAIL receptor family that antagonizes TRAIL signalling. FEBS Lett, **424:** 41, 1998
46. Hymowitz, S. G., Christinger, H. W., Fuh, G. et al.: Triggering cell death: the crystal structure of Apo2L/TRAIL in a complex with death receptor 5. Mol Cell, **4:** 563, 1999
47. Wu, G. S., Burns, T. F., Zhan, Y. et al.: Molecular cloning and functional analysis of the mouse homologue of the KILLER/DR5 tumor necrosis factor-related apoptosis-inducing ligand (TRAIL) death receptor. Cancer Res, **59:** 2770, 1999
48. Schneider, P., Olson, D., Tardivel, A. et al.: Identification of a new murine tumor necrosis factor receptor locus that contains two novel murine receptors for tumor necrosis factor-related apoptosis-inducing ligand (TRAIL). J Biol Chem, **278:** 5444, 2003

49. Wei, M. C., Zong, W. X., Cheng, E. H. et al.: Proapoptotic BAX and BAK: a requisite gateway to mitochondrial dysfunction and death. Science, **292:** 727, 2001
50. Testa, U.: TRAIL/TRAIL-R in hematologic malignancies. J Cell Biochem, **110:** 21, 2010
51. Sprick, M. R., Weigand, M. A., Rieser, E. et al.: FADD/MORT1 and caspase-8 are recruited to TRAIL receptors 1 and 2 and are essential for apoptosis mediated by TRAIL receptor 2. Immunity, **12:** 599, 2000
52. Kischkel, F. C., Lawrence, D. A., Chuntharapai, A. et al.: Apo2L/TRAIL-dependent recruitment of endogenous FADD and caspase-8 to death receptors 4 and 5. Immunity, **12:** 611, 2000
53. Li, H., Zhu, H., Xu, C. J. et al.: Cleavage of BID by caspase 8 mediates the mitochondrial damage in the Fas pathway of apoptosis. Cell, **94:** 491, 1998
54. Barnhart, B. C., Alappat, E. C., Peter, M. E.: The CD95 type I/type II model. Semin Immunol, **15:** 185, 2003
55. Du, C., Fang, M., Li, Y. et al.: Smac, a mitochondrial protein that promotes cytochrome c-dependent caspase activation by eliminating IAP inhibition. Cell, **102:** 33, 2000
56. Verhagen, A. M., Ekert, P. G., Pakusch, M. et al.: Identification of DIABLO, a mammalian protein that promotes apoptosis by binding to and antagonizing IAP proteins. Cell, **102:** 43, 2000
57. Schulze-Osthoff, K., Ferrari, D., Los, M. et al.: Apoptosis signaling by death receptors. Eur J Biochem, **254:** 439, 1998
58. Li, P., Nijhawan, D., Budihardjo, I. et al.: Cytochrome c and dATP-dependent formation of Apaf-1/caspase-9 complex initiates an apoptotic protease cascade. Cell, **91:** 479, 1997
59. Walther, W., Stein, U.: Viral vectors for gene transfer: a review of their use in the treatment of human diseases. Drugs, **60:** 249, 2000
60. Young, L. S., Searle, P. F., Onion, D. et al.: Viral gene therapy strategies: from basic science to clinical application. J Pathol, **208:** 299, 2006
61. Lai, C. M., Lai, Y. K., Rakoczy, P. E.: Adenovirus and adeno-associated virus vectors. DNA Cell Biol, **21:** 895, 2002
62. Ginsberg, H. S., Pereira, H. G., Valentine, R. C. et al.: A proposed terminology for the adenovirus antigens and virion morphological subunits. Virology, **28:** 782, 1966
63. Ballay, A., Levrero, M., Buendia, M. A. et al.: In vitro and in vivo synthesis of the hepatitis B virus surface antigen and of the receptor for polymerized human serum albumin from recombinant human adenoviruses. EMBO J, **4:** 3861, 1985
64. Karlsson, S., Van Doren, K., Schweiger, S. G. et al.: Stable gene transfer and tissue-specific expression of a human globin gene using adenoviral vectors. EMBO J, **5:** 2377, 1986
65. Jones, N., Shenk, T.: An adenovirus type 5 early gene function regulates expression of other early viral genes. Proc Natl Acad Sci U S A, **76:** 3665, 1979

66. Bergelson, J. M., Cunningham, J. A., Droguett, G. et al.: Isolation of a common receptor for Coxsackie B viruses and adenoviruses 2 and 5. Science, **275:** 1320, 1997
67. Bergelson, J. M., Krithivas, A., Celi, L. et al.: The murine CAR homolog is a receptor for coxsackie B viruses and adenoviruses. J Virol, **72:** 415, 1998
68. Wickham, T. J., Mathias, P., Cheresh, D. A. et al.: Integrins alpha v beta 3 and alpha v beta 5 promote adenovirus internalization but not virus attachment. Cell, **73:** 309, 1993
69. Hemmi, S., Geertsen, R., Mezzacasa, A. et al.: The presence of human coxsackievirus and adenovirus receptor is associated with efficient adenovirus-mediated transgene expression in human melanoma cell cultures. Hum Gene Ther, **9:** 2363, 1998
70. Pearson, A. S., Koch, P. E., Atkinson, N. et al.: Factors limiting adenovirus-mediated gene transfer into human lung and pancreatic cancer cell lines. Clin Cancer Res, **5:** 4208, 1999
71. Griffith, T. S., Anderson, R. D., Davidson, B. L. et al.: Adenoviral-mediated transfer of the TNF-related apoptosis-inducing ligand/Apo-2 ligand gene induces tumor cell apoptosis. J Immunol, **165:** 2886, 2000
72. Griffith, T. S., Broghammer, E. L.: Suppression of tumor growth following intralesional therapy with TRAIL recombinant adenovirus. Mol Ther, **4:** 257, 2001
73. Armeanu, S., Lauer, U. M., Smirnow, I. et al.: Adenoviral gene transfer of tumor necrosis factor-related apoptosis-inducing ligand overcomes an impaired response of hepatoma cells but causes severe apoptosis in primary human hepatocytes. Cancer Res, **63:** 2369, 2003
74. Jacob, D., Bahra, M., Schumacher, G. et al.: Gene therapy in colon cancer cells with a fiber-modified adenovector expressing the TRAIL gene driven by the hTERT promoter. Anticancer Res, **24:** 3075, 2004
75. Barton, G. M., Kagan, J. C., Medzhitov, R.: Intracellular localization of Toll-like receptor 9 prevents recognition of self DNA but facilitates access to viral DNA. Nat Immunol, **7:** 49, 2006
76. Krieg, A. M., Yi, A. K., Matson, S. et al.: CpG motifs in bacterial DNA trigger direct B-cell activation. Nature, **374:** 546, 1995
77. Medzhitov, R., Preston-Hurlburt, P., Janeway, C. A., Jr.: A human homologue of the Drosophila Toll protein signals activation of adaptive immunity. Nature, **388:** 394, 1997
78. Medzhitov, R.: Toll-like receptors and innate immunity. Nat Rev Immunol, **1:** 135, 2001
79. Krieg, A. M.: Development of TLR9 agonists for cancer therapy. J Clin Invest, **117:** 1184, 2007
80. Kerkmann, M., Rothenfusser, S., Hornung, V. et al.: Activation with CpG-A and CpG-B Oligonucleotides Reveals Two Distinct Regulatory Pathways of Type I IFN Synthesis in Human Plasmacytoid Dendritic Cells. 2003

81. Gray, R. C., Kuchtey, J., Harding, C. V.: CpG-B ODNs potently induce low levels of IFN-αβ and induce IFN-αβ-dependent MHC-I cross-presentation in DCs as effectively as CpG-A and CpG-C ODNs. 2007
82. Krug, A., Rothenfusser, S., Hornung, V. et al.: Identification of CpG oligonucleotide sequences with high induction of IFN-alpha/beta in plasmacytoid dendritic cells. Eur J Immunol, **31:** 2154, 2001
83. Schreibelt, G., Tel, J., Sliepen, K. H. et al.: Toll-like receptor expression and function in human dendritic cell subsets: implications for dendritic cell-based anti-cancer immunotherapy. Cancer Immunol Immunother, **59:** 1573, 2010
84. Brito, C. d., Tomkowiak, M., Ghittoni, R. et al.: CpG Promotes Cross-Presentation of Dead Cell-Associated Antigens by Pre-CD8α+ Dendritic Cells. 2011
85. Shirota, H., NCI-Frederick, Institute, N. C. et al.: CpG-conjugated apoptotic tumor cells elicit potent tumor-specific immunity. Cancer Immunology, Immunotherapy, **60:** 659, 2011
86. Nierkens, S., den Brok, M. H., Garcia, Z. et al.: Immune adjuvant efficacy of CpG oligonucleotide in cancer treatment is founded specifically upon TLR9 function in plasmacytoid dendritic cells. Cancer Res, **71:** 6428, 2011
87. Murad, Y. M., Clay, T. M.: CpG oligodeoxynucleotides as TLR9 agonists: therapeutic applications in cancer. BioDrugs, **23:** 361, 2009
88. Cooper, C. L., Davis, H. L., Morris, M. L. et al.: CPG 7909, an immunostimulatory TLR9 agonist oligodeoxynucleotide, as adjuvant to Engerix-B HBV vaccine in healthy adults: a double-blind phase I/II study. J Clin Immunol, **24:** 693, 2004
89. Halperin, S. A., Van Nest, G., Smith, B. et al.: A phase I study of the safety and immunogenicity of recombinant hepatitis B surface antigen co-administered with an immunostimulatory phosphorothioate oligonucleotide adjuvant. Vaccine, **21:** 2461, 2003
90. Janssen, E. M., Cincinnati Children's Hospital Research Foundation, M. I., 3333 Burnet Avenue, MLS7021, Cincinnati, 45229, Ohio, USA, edith.janssen@cchmc.org et al.: Cross-Presentation of Cell-Associated Antigens by Mouse Splenic Dendritic Cell Populations. Frontiers in Immunology, **3**, 2012
91. Lorenzi, S., Mattei, F., Sistigu, A. et al.: Type I IFNs Control Antigen Retention and Survival of CD8α+ Dendritic Cells after Uptake of Tumor Apoptotic Cells Leading to Cross-Priming. 2011
92. McDonnell, A. M., School of Medicine and Pharmacology, T. U. o. W. A., Perth, Australia, Prosser, A. C. et al.: CD8α+ DC are not the sole subset cross−presenting cell−associated tumor antigens from a solid tumor. European Journal of Immunology, **40:** 1617, 2010
93. Pooley, J. L., Heath, W. R., Shortman, K.: Cutting edge: intravenous soluble antigen is presented to CD4 T cells by CD8- dendritic cells, but cross-presented to CD8 T cells by CD8+ dendritic cells. J Immunol, **166:** 5327, 2001

94. Tsujimura, H., Tamura, T., Ozato, K.: Cutting edge: IFN consensus sequence binding protein/IFN regulatory factor 8 drives the development of type I IFN-producing plasmacytoid dendritic cells. J Immunol, **170:** 1131, 2003
95. Suzuki, S., Honma, K., Matsuyama, T. et al.: Critical roles of interferon regulatory factor 4 in CD11bhighCD8alpha- dendritic cell development. Proc Natl Acad Sci U S A, **101:** 8981, 2004
96. Hildner, K., Edelson, B. T., Purtha, W. E. et al.: Batf3 deficiency reveals a critical role for CD8alpha+ dendritic cells in cytotoxic T cell immunity. Science, **322:** 1097, 2008
97. O'Keeffe, M., Hochrein, H., Vremec, D. et al.: Mouse plasmacytoid cells: long-lived cells, heterogeneous in surface phenotype and function, that differentiate into CD8(+) dendritic cells only after microbial stimulus. J Exp Med, **196:** 1307, 2002
98. Grouard, G., Rissoan, M. C., Filgueira, L. et al.: The enigmatic plasmacytoid T cells develop into dendritic cells with interleukin (IL)-3 and CD40-ligand. J Exp Med, **185:** 1101, 1997
99. Canque, B., Camus, S., Yagello, M. et al.: IL-4 and CD40 ligation affect differently the differentiation, maturation, and function of human CD34+ cell-derived CD1a+CD14- and CD1a-CD14+ dendritic cell precursors in vitro. J Leukoc Biol, **64:** 235, 1998
100. Hochrein, H., Shortman, K., Vremec, D. et al.: Differential production of IL-12, IFN-alpha, and IFN-gamma by mouse dendritic cell subsets. J Immunol, **166:** 5448, 2001
101. Shortman, K., Naik, S. H.: Steady-state and inflammatory dendritic-cell development. Nat Rev Immunol, **7:** 19, 2007
102. Naik, S. H., Sathe, P., Park, H. Y. et al.: Development of plasmacytoid and conventional dendritic cell subtypes from single precursor cells derived in vitro and in vivo. Nat Immunol, **8:** 1217, 2007
103. D'Amico, A., Wu, L.: The early progenitors of mouse dendritic cells and plasmacytoid predendritic cells are within the bone marrow hemopoietic precursors expressing Flt3. J Exp Med, **198:** 293, 2003
104. Karsunky, H., Merad, M., Cozzio, A. et al.: Flt3 ligand regulates dendritic cell development from Flt3+ lymphoid and myeloid-committed progenitors to Flt3+ dendritic cells in vivo. J Exp Med, **198:** 305, 2003
105. Brasel, K., De Smedt, T., Smith, J. L. et al.: Generation of murine dendritic cells from flt3-ligand-supplemented bone marrow cultures. Blood, **96:** 3029, 2000
106. Vremec, D., Zorbas, M., Scollay, R. et al.: The surface phenotype of dendritic cells purified from mouse thymus and spleen: investigation of the CD8 expression by a subpopulation of dendritic cells. J Exp Med, **176:** 47, 1992
107. Becker, A. M., Michael, D. G., Satpathy, A. T. et al.: IRF-8 extinguishes neutrophil production and promotes dendritic cell lineage commitment in both myeloid and lymphoid mouse progenitors. Blood, **119:** 2003, 2012

108. Dalod, M., Salazar-Mather, T. P., Malmgaard, L. et al.: Interferon alpha/beta and interleukin 12 responses to viral infections: pathways regulating dendritic cell cytokine expression in vivo. J Exp Med, **195:** 517, 2002
109. Asselin-Paturel, C., Boonstra, A., Dalod, M. et al.: Mouse type I IFN-producing cells are immature APCs with plasmacytoid morphology. Nature Immunology, **2:** 1144, 2001
110. Asselin-Paturel, C., Brizard, G., Pin, J.-J. et al.: Mouse Strain Differences in Plasmacytoid Dendritic Cell Frequency and Function Revealed by a Novel Monoclonal Antibody. 2003
111. Edwards, A. D., Diebold, S. S., Slack, E. M. et al.: Toll-like receptor expression in murine DC subsets: lack of TLR7 expression by CD8 alpha+ DC correlates with unresponsiveness to imidazoquinolines. Eur J Immunol, **33:** 827, 2003
112. Reis e Sousa, C.: Activation of dendritic cells: translating innate into adaptive immunity. Curr Opin Immunol, **16:** 21, 2004
113. Liu, R. B., Engels, B., Schreiber, K. et al.: IL-15 in tumor microenvironment causes rejection of large established tumors by T cells in a noncognate T cell receptor-dependent manner. 2013
114. Gautier, G., Humbert, M., Deauvieau, F. et al.: A type I interferon autocrine-paracrine loop is involved in Toll-like receptor-induced interleukin-12p70 secretion by dendritic cells. J Exp Med, **201:** 1435, 2005
115. Cowdery, J. S., Boerth, N. J., Norian, L. A. et al.: Differential regulation of the IL-12 p40 promoter and of p40 secretion by CpG DNA and lipopolysaccharide. J Immunol, **162:** 6770, 1999
116. Tannenbaum, C. S., Tubbs, R., Armstrong, D. et al.: The CXC chemokines IP-10 and Mig are necessary for IL-12-mediated regression of the mouse RENCA tumor. J Immunol, **161:** 927, 1998
117. Lou, Y., Liu, C., Kim, G. J. et al.: Plasmacytoid Dendritic Cells Synergize with Myeloid Dendritic Cells in the Induction of Antigen-Specific Antitumor Immune Responses. 2007
118. Fadok, V. A., Voelker, D. R., Campbell, P. A. et al.: Exposure of phosphatidylserine on the surface of apoptotic lymphocytes triggers specific recognition and removal by macrophages. J Immunol, **148:** 2207, 1992
119. Bonifaz, L., Bonnyay, D., Mahnke, K. et al.: Efficient targeting of protein antigen to the dendritic cell receptor DEC-205 in the steady state leads to antigen presentation on major histocompatibility complex class I products and peripheral CD8+ T cell tolerance. J Exp Med, **196:** 1627, 2002
120. Savina, A., Jancic, C., Hugues, S. et al.: NOX2 controls phagosomal pH to regulate antigen processing during crosspresentation by dendritic cells. Cell, **126:** 205, 2006
121. Savina, A., Peres, A., Cebrian, I. et al.: The small GTPase Rac2 controls phagosomal alkalinization and antigen crosspresentation selectively in CD8(+) dendritic cells. Immunity, **30:** 544, 2009

122. Shen, L., Sigal, L. J., Boes, M. et al.: Important role of cathepsin S in generating peptides for TAP-independent MHC class I crosspresentation in vivo. Immunity, **21:** 155, 2004
123. Mescher, M. F., Curtsinger, J. M., Agarwal, P. et al.: Signals required for programming effector and memory development by CD8+ T cells. Immunol Rev, **211:** 81, 2006
124. Fujii, S., Liu, K., Smith, C. et al.: The linkage of innate to adaptive immunity via maturing dendritic cells in vivo requires CD40 ligation in addition to antigen presentation and CD80/86 costimulation. J Exp Med, **199:** 1607, 2004
125. Curtsinger, J. M., Lins, D. C., Mescher, M. F.: Signal 3 determines tolerance versus full activation of naive CD8 T cells: dissociating proliferation and development of effector function. J Exp Med, **197:** 1141, 2003
126. Curtsinger, J. M., Valenzuela, J. O., Agarwal, P. et al.: Type I IFNs provide a third signal to CD8 T cells to stimulate clonal expansion and differentiation. J Immunol, **174:** 4465, 2005
127. Spiotto, M. T., Rowley, D. A., Schreiber, H.: Bystander elimination of antigen loss variants in established tumors. Nat Med, **10:** 294, 2004
128. Sayers, T. J., Brooks, A. D., Seki, N. et al.: T cell lysis of murine renal cancer: multiple signaling pathways for cell death via Fas. J Leukoc Biol, **68:** 81, 2000
129. Seki, N., Brooks, A. D., Carter, C. R. et al.: Tumor-specific CTL kill murine renal cancer cells using both perforin and Fas ligand-mediated lysis in vitro, but cause tumor regression in vivo in the absence of perforin. J Immunol, **168:** 3484, 2002
130. Qin, Z., Schwartzkopff, J., Pradera, F. et al.: A critical requirement of interferon gamma-mediated angiostasis for tumor rejection by CD8+ T cells. Cancer Res, **63:** 4095, 2003
131. Shresta, S., Pham, C. T., Thomas, D. A. et al.: How do cytotoxic lymphocytes kill their targets? Curr Opin Immunol, **10:** 581, 1998
132. Zhang, B., Karrison, T., Rowley, D. A. et al.: IFN-gamma- and TNF-dependent bystander eradication of antigen-loss variants in established mouse cancers. J Clin Invest, **118:** 1398, 2008
133. Drake, C. G., Jaffee, E., Pardoll, D. M.: Mechanisms of immune evasion by tumors. Adv Immunol, **90:** 51, 2006
134. Algarra, I., Cabrera, T., Garrido, F.: The HLA crossroad in tumor immunology. Hum Immunol, **61:** 65, 2000
135. Spranger, S., Koblish, H. K., Horton, B. et al.: Mechanism of tumor rejection with doublets of CTLA-4, PD-1/PD-L1, or IDO blockade involves restored IL-2 production and proliferation of CD8(+) T cells directly within the tumor microenvironment. J Immunother Cancer, **2:** 3, 2014
136. Spranger, S., Spaapen, R. M., Zha, Y. et al.: Up-regulation of PD-L1, IDO, and T(regs) in the melanoma tumor microenvironment is driven by CD8(+) T cells. Sci Transl Med, **5:** 200ra116, 2013
137. Sonnenfeld, A.: Leukamische reaktiones bei carcinoma. Klin. Med., **111**, 1929

138. Duwe, A. K., Singhal, S. K.: The immunoregulatory role of bone marrow. I. Suppression of the induction of antibody responses to T-dependent and T-independent antigens by cells in the bone marrow. Cell Immunol, **43:** 362, 1979
139. Serafini, P., Borrello, I., Bronte, V.: Myeloid suppressor cells in cancer: recruitment, phenotype, properties, and mechanisms of immune suppression. Semin Cancer Biol, **16:** 53, 2006
140. Gabrilovich, D. I., Nagaraj, S.: Myeloid-derived suppressor cells as regulators of the immune system. Nat Rev Immunol, **9:** 162, 2009
141. Kusmartsev, S., Cheng, F., Yu, B. et al.: All-trans-retinoic acid eliminates immature myeloid cells from tumor-bearing mice and improves the effect of vaccination. Cancer Res, **63:** 4441, 2003
142. Shirota, Y., Shirota, H., Klinman, D. M.: Intratumoral Injection of CpG Oligonucleotides Induces the Differentiation and Reduces the Immunosuppressive Activity of Myeloid-Derived Suppressor Cells. The Journal of Immunology, **188:** 1592, 2012
143. Obermajer, N., Muthuswamy, R., Lesnock, J. et al.: Positive feedback between PGE2 and COX2 redirects the differentiation of human dendritic cells toward stable myeloid-derived suppressor cells. Blood, **118:** 5498, 2011
144. Fleming, T. J., Fleming, M. L., Malek, T. R.: Selective expression of Ly-6G on myeloid lineage cells in mouse bone marrow. RB6-8C5 mAb to granulocyte-differentiation antigen (Gr-1) detects members of the Ly-6 family. J Immunol, **151:** 2399, 1993
145. Youn, J.-I., Nagaraj, S., Collazo, M. et al.: Subsets of Myeloid-Derived Suppressor Cells in Tumor-Bearing Mice. 2008
146. Elkabets, M., Ribeiro, V. S., Dinarello, C. A. et al.: IL-1beta regulates a novel myeloid-derived suppressor cell subset that impairs NK cell development and function. Eur J Immunol, **40:** 3347, 2010
147. Movahedi, K., Guilliams, M., Van den Bossche, J. et al.: Identification of discrete tumor-induced myeloid-derived suppressor cell subpopulations with distinct T cell-suppressive activity. Blood, **111:** 4233, 2008
148. Haverkamp, J. M., Crist, S. A., Elzey, B. D. et al.: In vivo suppressive function of myeloid-derived suppressor cells is limited to the inflammatory site. European Journal of Immunology, **41:** 749, 2011
149. Eruslanov, E., Daurkin, I., Ortiz, J. et al.: Pivotal Advance: Tumor-mediated induction of myeloid-derived suppressor cells and M2-polarized macrophages by altering intracellular PGE catabolism in myeloid cells. J Leukoc Biol, **88:** 839, 2010
150. Bunt, S. K., Yang, L., Sinha, P. et al.: Reduced inflammation in the tumor microenvironment delays the accumulation of myeloid-derived suppressor cells and limits tumor progression. Cancer Res, **67:** 10019, 2007
151. Obermajer, N., Wong, J. L., Edwards, R. P. et al.: PGE2-Driven Induction and Maintenance of Cancer-Associated Myeloid-Derived Suppressor Cells. Immunological Investigations, **41:** 635, 2012

152. Geary, S. M., Lemke, C. D., Lubaroff, D. M. et al.: The combination of a low-dose chemotherapeutic agent, 5-fluorouracil, and an adenoviral tumor vaccine has a synergistic benefit on survival in a tumor model system. PLoS One, **8:** e67904, 2013
153. Cheng, P., Corzo, C. A., Luetteke, N. et al.: Inhibition of dendritic cell differentiation and accumulation of myeloid-derived suppressor cells in cancer is regulated by S100A9 protein. J Exp Med, **205:** 2235, 2008
154. Sinha, P., Okoro, C., Foell, D. et al.: Proinflammatory S100 proteins regulate the accumulation of myeloid-derived suppressor cells. In: J Immunol. United States, vol. 181, pp. 4666, 2008
155. Chell, S. D., Witherden, I. R., Dobson, R. R. et al.: Increased EP4 receptor expression in colorectal cancer progression promotes cell growth and anchorage independence. Cancer Res, **66:** 3106, 2006
156. Wang, T., Niu, G., Kortylewski, M. et al.: Regulation of the innate and adaptive immune responses by Stat-3 signaling in tumor cells. Nat Med, **10:** 48, 2004
157. Xin, H., Zhang, C., Herrmann, A. et al.: Sunitinib inhibition of Stat3 induces renal cell carcinoma tumor cell apoptosis and reduces immunosuppressive cells. Cancer Res, **69:** 2506, 2009
158. Corzo, C. A., Cotter, M. J., Cheng, P. et al.: Mechanism regulating reactive oxygen species in tumor-induced myeloid-derived suppressor cells. J Immunol, **182:** 5693, 2009
159. Waight, J. D., Netherby, C., Hensen, M. L. et al.: Myeloid-derived suppressor cell development is regulated by a STAT/IRF-8 axis. J Clin Invest, **123:** 4464, 2013
160. Bronte, V., Serafini, P., De Santo, C. et al.: IL-4-induced arginase 1 suppresses alloreactive T cells in tumor-bearing mice. J Immunol, **170:** 270, 2003
161. Rodriguez, P. C., Ochoa, A. C.: Arginine regulation by myeloid derived suppressor cells and tolerance in cancer: mechanisms and therapeutic perspectives. Immunol Rev, **222:** 180, 2008
162. Rodriguez, P. C.: Arginase I Production in the Tumor Microenvironment by Mature Myeloid Cells Inhibits T-Cell Receptor Expression and Antigen-Specific T-Cell Responses. Cancer Research, **64:** 5839, 2004
163. Zea, A. H., Rodriguez, P. C., Atkins, M. B. et al.: Arginase-producing myeloid suppressor cells in renal cell carcinoma patients: a mechanism of tumor evasion. Cancer Res, **65:** 3044, 2005
164. Qu, X., Felder, M. A., Perez Horta, Z. et al.: Antitumor effects of anti-CD40/CpG immunotherapy combined with gemcitabine or 5-fluorouracil chemotherapy in the B16 melanoma model. Int Immunopharmacol, **17:** 1141, 2013
165. Najjar, Y. G., Finke, J. H.: Clinical perspectives on targeting of myeloid derived suppressor cells in the treatment of cancer. Front Oncol, **3:** 49, 2013
166. Ko, J. S., Rayman, P., Ireland, J. et al.: Direct and Differential Suppression of Myeloid-Derived Suppressor Cell Subsets by Sunitinib Is Compartmentally Constrained. 2010

167. Gati, A., Kouidhi, S., Marrakchi, R. et al.: Obesity and renal cancer: Role of adipokines in the tumor-immune system conflict. In: Oncoimmunology, vol. 3, p. e27810, 2014
168. Klinghoffer, Z., Yang, B., Kapoor, A. et al.: Obesity and renal cell carcinoma: epidemiology, underlying mechanisms and management considerations. Expert Rev Anticancer Ther, **9:** 975, 2009
169. Calle, E. E., Thun, M. J.: Obesity and cancer. Oncogene, **23:** 6365, 2004
170. Calle, E. E., Kaaks, R.: Overweight, obesity and cancer: epidemiological evidence and proposed mechanisms. Nat Rev Cancer, **4:** 579, 2004
171. Balkwill, F., Mantovani, A.: Inflammation and cancer: back to Virchow? Lancet, **357:** 539, 2001
172. Lee, I. S., Shin, G., Choue, R.: Shifts in diet from high fat to high carbohydrate improved levels of adipokines and pro-inflammatory cytokines in mice fed a high-fat diet. Endocr J, **57:** 39, 2010
173. Lumeng, C. N., DelProposto, J. B., Westcott, D. J. et al.: Phenotypic switching of adipose tissue macrophages with obesity is generated by spatiotemporal differences in macrophage subtypes. Diabetes, **57:** 3239, 2008
174. Fontana, L., Eagon, J. C., Trujillo, M. E. et al.: Visceral fat adipokine secretion is associated with systemic inflammation in obese humans. Diabetes, **56:** 1010, 2007
175. Lumeng, C. N., Bodzin, J. L., Saltiel, A. R.: Obesity induces a phenotypic switch in adipose tissue macrophage polarization. J Clin Invest, **117:** 175, 2007
176. Deng, Z. B., Liu, Y., Liu, C. et al.: Immature myeloid cells induced by a high-fat diet contribute to liver inflammation. Hepatology, **50:** 1412, 2009
177. Xia, S., Sha, H., Yang, L. et al.: Gr-1+ CD11b+ Myeloid-derived Suppressor Cells Suppress Inflammation and Promote Insulin Sensitivity in Obesity. Journal of Biological Chemistry, **286:** 23591, 2011
178. James, B. R., Tomanek-Chalkley, A., Askeland, E. J. et al.: Diet-induced obesity alters dendritic cell function in the presence and absence of tumor growth. J Immunol, **189:** 1311, 2012
179. Karlsson, E. A., Sheridan, P. A., Beck, M. A.: Diet-induced obesity impairs the T cell memory response to influenza virus infection. J Immunol, **184:** 3127, 2010
180. Smith, A. G., Sheridan, P. A., Tseng, R. J. et al.: Selective impairment in dendritic cell function and altered antigen-specific CD8+ T-cell responses in diet-induced obese mice infected with influenza virus. Immunology, **126:** 268, 2009
181. Yaqoob, P.: Monounsaturated fatty acids and immune function. Eur J Clin Nutr, **56 Suppl 3:** S9, 2002
182. Yaqoob, P., Knapper, J. A., Webb, D. H. et al.: Effect of olive oil on immune function in middle-aged men. Am J Clin Nutr, **67:** 129, 1998
183. Matarese, G., Procaccini, C., De Rosa, V. et al.: Regulatory T cells in obesity: the leptin connection. Trends Mol Med, **16:** 247, 2010
184. Lang, K., Ratke, J.: Leptin and Adiponectin: new players in the field of tumor cell and leukocyte migration. Cell Commun Signal, **7:** 27, 2009

185. Restifo, N. P., Dudley, M. E., Rosenberg, S. A.: Adoptive immunotherapy for cancer: Harnessing the T cell response. Nature Rev. Immunol., **12:** 269, 2012
186. van Mierlo, G. J., Boonman, Z. F., Dumortier, H. M. et al.: Activation of dendritic cells that cross-present tumor-derived antigen licenses CD8+ CTL to cause tumor eradication. J. Immunol., **173:** 6753, 2004
187. de Brito, C., Tomkowiak, M., Ghittoni, R. et al.: CpG promotes cross-presentation of dead cell-associated antigens by pre-CD8alpha+ dendritic cells [corrected]. J. Immunol., **186:** 1503, 2011
188. Shirota, H., Klinman, D. M.: CpG-conjugated apoptotic tumor cells elicit potent tumor-specific immunity. Cancer Immunol. Immunother., **60:** 659, 2011
189. Liu, C., Lou, Y., Lizee, G. et al.: Plasmacytoid dendritic cells induce NK cell-dependent, tumor antigen-specific T cell cross-priming and tumor regression in mice. J. Clin. Invest., **118:** 1165, 2008
190. Nierkens, S., den Brok, M. H., Sutmuller, R. P. et al.: In vivo colocalization of antigen and CpG within dendritic cells is associated with the efficacy of cancer immunotherapy. Cancer Res., **68:** 5390, 2008
191. Drobits, B., Holcmann, M., Amberg, N. et al.: Imiquimod clears tumors in mice independent of adaptive immunity by converting pDCs into tumor-killing effector cells. J. Clin. Invest., **122:** 575, 2012
192. den Haan, J. M., Lehar, S. M., Bevan, M. J.: CD8(+) but not CD8(-) dendritic cells cross-prime cytotoxic T cells in vivo. J. Exp. Med., **192:** 1685, 2000
193. Schulz, O., Reis e Sousa, C.: Cross-presentation of cell-associated antigens by CD8alpha+ dendritic cells is attributable to their ability to internalize dead cells. Immunology, **107:** 183, 2002
194. Wiley, S. R., Schooley, K., Smolak, P. J. et al.: Identification and characterization of a new member of the TNF family that induces apoptosis. Immunity, **3:** 673, 1995
195. Walczak, H., Miller, R. E., Ariail, K. et al.: Tumoricidal activity of tumor necrosis factor-related apoptosis-inducing ligand in vivo. Nat. Med., **5:** 157, 1999
196. den Hollander, M. W., Gietema, J. A., de Jong, S. et al.: Translating TRAIL-receptor targeting agents to the clinic. Cancer Lett., **332:** 194, 2013
197. Griffith, T. S., Anderson, R. D., Davidson, B. L. et al.: Adenoviral-mediated transfer of the TNF-related apoptosis-inducing ligand/Apo-2 ligand gene induces tumor cell apoptosis. J. Immunol., **165:** 2886, 2000
198. Griffith, T. S., Broghammer, E. L.: Suppression of tumor growth following intralesional therapy with TRAIL recombinant adenovirus. Mol. Ther., **4:** 257, 2001
199. VanOosten, R. L., Griffith, T. S.: Activation of tumor-specific $CD8^+$ T Cells after intratumoral Ad5-TRAIL/CpG oligodeoxynucleotide combination therapy. Cancer Res., **67:** 11980, 2007
200. Nierkens, S., den Brok, M. H., Garcia, Z. et al.: Immune adjuvant efficacy of CpG oligonucleotide in cancer treatment is founded specifically upon TLR9 function in plasmacytoid dendritic cells. Cancer Res., **71:** 6428, 2011

201. Hrushesky, W. J., Murphy, G. P.: Investigation of a new renal tumor model. J. Surg. Res., **15:** 327, 1973
202. James, B. R., Tomanek-Chalkley, A., Askeland, E. J. et al.: Diet-induced obesity alters dendritic cell function in the presence and absence of tumor growth. J. Immunol., **189:** 1311, 2012
203. Asselin-Paturel, C., Brizard, G., Pin, J. J. et al.: Mouse strain differences in plasmacytoid dendritic cell frequency and function revealed by a novel monoclonal antibody. J. Immunol., **171:** 6466, 2003
204. Anderson, K. G., Mayer-Barber, K., Sung, H. et al.: Intravascular staining for discrimination of vascular and tissue leukocytes. Nat. Protocols, **9:** 209, 2014
205. Lou, Y., Liu, C., Kim, G. J. et al.: Plasmacytoid dendritic cells synergize with myeloid dendritic cells in the induction of antigen-specific antitumor immune responses. J. Immunol., **178:** 1534, 2007
206. Kuwajima, S., Sato, T., Ishida, K. et al.: Interleukin 15-dependent crosstalk between conventional and plasmacytoid dendritic cells is essential for CpG-induced immune activation. Nat. Immunol., **7:** 740, 2006
207. Salup, R. R., Wiltrout, R. H.: Adjuvant immunotherapy of established murine renal cancer by interleukin 2-stimulated cytotoxic lymphocytes. Cancer Res, **46:** 3358, 1986
208. Blasius, A. L., Giurisato, E., Cella, M. et al.: Bone marrow stromal cell antigen 2 is a specific marker of type I IFN-producing cells in the naive mouse, but a promiscuous cell surface antigen following IFN stimulation. J. Immunol., **177:** 3260, 2006
209. Vinay, D. S., Lee, S. J., Kim, C. H. et al.: Exposure of a distinct PDCA-1+ (CD317) B cell population to agonistic anti-4-1BB (CD137) inhibits T and B cell responses both in vitro and in vivo. PloS One, **7:** e50272, 2012
210. Bao, Y., Han, Y., Chen, Z. et al.: IFN-alpha-producing PDCA-1+ Siglec-H- B cells mediate innate immune defense by activating NK cells. Eur. J. Immunol., **41:** 657, 2011
211. Asselin-Paturel, C., Boonstra, A., Dalod, M. et al.: Mouse type I IFN-producing cells are immature APCs with plasmacytoid morphology. Nat. Immunol., **2:** 1144, 2001
212. Fuertes, M. B., Kacha, A. K., Kline, J. et al.: Host type I IFN signals are required for antitumor CD8+ T cell responses through CD8{alpha}+ dendritic cells. J. Exp. Med., **208:** 2005, 2011
213. Basner-Tschakarjan, E., Gaffal, E., O'Keeffe, M. et al.: Adenovirus efficiently transduces plasmacytoid dendritic cells resulting in TLR9-dependent maturation and IFN-alpha production. J. Gene Med., **8:** 1300, 2006
214. Mattei, F., Schiavoni, G., Belardelli, F. et al.: IL-15 is expressed by dendritic cells in response to type I IFN, double-stranded RNA, or lipopolysaccharide and promotes dendritic cell activation. J. Immunol., **167:** 1179, 2001

215. Epardaud, M., Elpek, K. G., Rubinstein, M. P. et al.: Interleukin-15/interleukin-15R alpha complexes promote destruction of established tumors by reviving tumor-resident CD8+ T cells. Cancer Res., **68:** 2972, 2008
216. Rai, D., Pham, N. L., Harty, J. T. et al.: Tracking the total CD8 T cell response to infection reveals substantial discordance in magnitude and kinetics between inbred and outbred hosts. J. Immunol., **183:** 7672, 2009
217. Gonzalvez, F., Ashkenazi, A.: New insights into apoptosis signaling by Apo2L/TRAIL. Oncogene, **29:** 4752, 2010
218. Le, D. T., Pardoll, D. M., Jaffee, E. M.: Cellular vaccine approaches. Cancer J., **16:** 304, 2010
219. Fanger, N. A., Maliszewski, C. R., Schooley, K. et al.: Human dendritic cells mediate cellular apoptosis via tumor necrosis factor-related apoptosis-inducing ligand (TRAIL). J. Exp. Med., **190:** 1155, 1999
220. Anguille, S., Lion, E., Tel, J. et al.: Interleukin-15-induced CD56(+) myeloid dendritic cells combine potent tumor antigen presentation with direct tumoricidal potential. PloS One, **7:** e51851, 2012
221. Tel, J., Smits, E. L., Anguille, S. et al.: Human plasmacytoid dendritic cells are equipped with antigen-presenting and tumoricidal capacities. Blood, **120:** 3936, 2012
222. Griffith, T. S., Ferguson, T. A.: Cell death in the maintenance and abrogation of tolerance: the five Ws of dying cells. Immunity, **35:** 456, 2011
223. Krieg, A., Kline, J.: Immune effects and therapeutic applications of CpG motifs in bacterial DNA. Immunopharmacology, **48:** 303, 2000
224. Gilliet, M., Boonstra, A., Paturel, C. et al.: The development of murine plasmacytoid dendritic cell precursors is differentially regulated by FLT3-ligand and granulocyte/macrophage colony-stimulating factor. J. Exp. Med., **195:** 953, 2002
225. Suzuki, K., Suda, T., Naito, T. et al.: Impaired toll-like receptor 9 expression in alveolar macrophages with no sensitivity to CpG DNA. Am. J. Respir. Crit. Care Med., **171:** 707, 2005
226. Salio, M., Palmowski, M. J., Atzberger, A. et al.: CpG-matured murine plasmacytoid dendritic cells are capable of in vivo priming of functional CD8 T cell responses to endogenous but not exogenous antigens. J. Exp. Med., **199:** 567, 2004
227. Yoneyama, H., Matsuno, K., Toda, E. et al.: Plasmacytoid DCs help lymph node DCs to induce anti-HSV CTLs. J. Exp. Med., **202:** 425, 2005
228. Lorenzi, S., Mattei, F., Sistigu, A. et al.: Type I IFNs control antigen retention and survival of CD8alpha(+) dendritic cells after uptake of tumor apoptotic cells leading to cross-priming. J. Immunol., **186:** 5142, 2011
229. Chu, K. F., Dupuy, D. E.: Thermal ablation of tumours: biological mechanisms and advances in therapy. Nat. Rev. Cancer, **14:** 199, 2014
230. Krieg, A. M.: CpG still rocks! Update on an accidental drug. Nucleic Acid Ther., **22:** 77, 2012

231. Holoch, P. A., Griffith, T. S.: TNF-related apoptosis-inducing ligand (TRAIL): a new path to anti-cancer therapies. Eur. J. Pharmacol., **625:** 63, 2009
232. Micheau, O., Shirley, S., Dufour, F.: Death receptors as targets in cancer. Br. J. Pharmacol., **169:** 1723, 2013
233. Laber, D. A.: Risk factors, classification, and staging of renal cell cancer. Med Oncol, **23:** 443, 2006
234. Hjartaker, A., Langseth, H., Weiderpass, E.: Obesity and diabetes epidemics: cancer repercussions. Adv Exp Med Biol, **630:** 72, 2008
235. Maya-Monteiro, C. M., Bozza, P. T.: Leptin and mTOR: partners in metabolism and inflammation. Cell Cycle, **7:** 1713, 2008
236. Hotamisligil, G. S.: Inflammation and metabolic disorders. Nature, **444:** 860, 2006
237. Wisse, B. E.: The inflammatory syndrome: the role of adipose tissue cytokines in metabolic disorders linked to obesity. J Am Soc Nephrol, **15:** 2792, 2004
238. Gregor, M. F., Hotamisligil, G. S.: Inflammatory mechanisms in obesity. Annu Rev Immunol, **29:** 415, 2011
239. Xu, H., Barnes, G. T., Yang, Q. et al.: Chronic inflammation in fat plays a crucial role in the development of obesity-related insulin resistance. J Clin Invest, **112:** 1821, 2003
240. Lee, I. S., Shin, G., Choue, R.: Shifts in diet from high fat to high carbohydrate improved levels of adipokines and pro-inflammatory cytokines in mice fed a high-fat diet. Endocr J, **57:** 39, 2009
241. Fenton, J. I., Nunez, N. P., Yakar, S. et al.: Diet-induced adiposity alters the serum profile of inflammation in C57BL/6N mice as measured by antibody array. Diabetes Obes Metab, **11:** 343, 2009
242. Macia, L., Delacre, M., Abboud, G. et al.: Impairment of dendritic cell functionality and steady-state number in obese mice. J Immunol, **177:** 5997, 2006
243. Verwaerde, C., Delanoye, A., Macia, L. et al.: Influence of high-fat feeding on both naive and antigen-experienced T-cell immune response in DO10.11 mice. Scand J Immunol, **64:** 457, 2006
244. Fuertes, M. B., Kacha, A. K., Kline, J. et al.: Host type I IFN signals are required for antitumor CD8+ T cell responses through CD8α+ dendritic cells. 2011
245. Norian, L. A., Rodriguez, P. C., O'Mara, L. A. et al.: Tumor-infiltrating regulatory dendritic cells inhibit CD8+ T cell function via L-arginine metabolism. Cancer Res, **69:** 3086, 2009
246. Hanson, H. L., Donermeyer, D. L., Ikeda, H. et al.: Eradication of established tumors by CD8+ T cell adoptive immunotherapy. Immunity, **13:** 265, 2000
247. He, D., Department of Dermatology, U. o. A. a. B., Birmingham, Alabama, United States of America, Li, H. et al.: IL-17 Mediated Inflammation Promotes Tumor Growth and Progression in the Skin. PLOS ONE, **7**, 2012
248. Begley, L. A., Kasina, S., Mehra, R. et al.: CXCL5 promotes prostate cancer progression. Neoplasia, **10:** 244, 2008

249. Acharyya, S., Oskarsson, T., Vanharanta, S. et al.: A CXCL1 paracrine network links cancer chemoresistance and metastasis. Cell, **150:** 165, 2012
250. Klebanoff, C. A., Finkelstein, S. E., Surman, D. R. et al.: IL-15 enhances the in vivo antitumor activity of tumor-reactive CD8+ T Cells. 2004
251. James, B. R., Brincks, E. L., Kucaba, T. A. et al.: Effective TRAIL-based immunotherapy requires both plasmacytoid and CD8alpha dendritic cells. Cancer Immunol Immunother, 2014
252. Anderson, K. G., Mayer-Barber, K., Sung, H. et al.: Intravascular staining for discrimination of vascular and tissue leukocytes. Nat Protoc, **9:** 209, 2014
253. Cleary, M. P., Grande, J. P., Juneja, S. C. et al.: Diet-induced obesity and mammary tumor development in MMTV-neu female mice. Nutr Cancer, **50:** 174, 2004
254. Rose, D. P., Connolly, J. M.: Regulation of tumor angiogenesis by dietary fatty acids and eicosanoids. Nutr Cancer, **37:** 119, 2000
255. Ratke, J., Entschladen, F., Niggemann, B. et al.: Leptin stimulates the migration of colon carcinoma cells by multiple signalling pathways. Endocr Relat Cancer, 2009
256. Allavena, P., Garlanda, C., Borrello, M. G. et al.: Pathways connecting inflammation and cancer. Curr Opin Genet Dev, **18:** 3, 2008
257. Mantovani, A., Pierotti, M. A.: Cancer and inflammation: a complex relationship. Cancer Lett, **267:** 180, 2008
258. Lin, W. W., Karin, M.: A cytokine-mediated link between innate immunity, inflammation, and cancer. J Clin Invest, **117:** 1175, 2007
259. Restifo, N. P., Dudley, M. E., Rosenberg, S. A.: Adoptive immunotherapy for cancer: harnessing the T cell response. Nature Reviews Immunology, **12:** 269, 2012
260. Palucka, K., Banchereau, J.: Cancer immunotherapy via dendritic cells. Nat Rev Cancer, **12:** 265, 2012
261. Kusmartsev, S., Gabrilovich, D. I.: Role of immature myeloid cells in mechanisms of immune evasion in cancer. Cancer Immunol. Immunother., **55:** 237, 2006
262. Drake, C. G., Jaffee, E., Pardoll, D. M.: Mechanisms of immune evasion by tumors. Adv. Immunol., **90:** 51, 2006
263. Mittal, D., Gubin, M. M., Schreiber, R. D. et al.: New insights into cancer immunoediting and its three component phases-elimination, equilibrium and escape. Curr. Op. Immunol., **27C:** 16, 2014
264. Ostrand-Rosenberg, S.: Myeloid-derived suppressor cells: more mechanisms for inhibiting antitumor immunity. Cancer Immunol. Immunother., **59:** 1593, 2010
265. Ostrand-Rosenberg, S., Sinha, P., Beury, D. W. et al.: Cross-talk between myeloid-derived suppressor cells (MDSC), macrophages, and dendritic cells enhances tumor-induced immune suppression. Sem. Cancer Biol., **22:** 275, 2012

266. Ko, J. S., Rayman, P., Ireland, J. et al.: Direct and differential suppression of myeloid-derived suppressor cell subsets by sunitinib is compartmentally constrained. Cancer Res., **70:** 3526, 2010
267. Rodriguez, P. C., Ernstoff, M. S., Hernandez, C. et al.: Arginase I-producing myeloid-derived suppressor cells in renal cell carcinoma are a subpopulation of activated granulocytes. Cancer Res., **69:** 1553, 2009
268. Ochoa, A. C., Zea, A. H., Hernandez, C. et al.: Arginase, prostaglandins, and myeloid-derived suppressor cells in renal cell carcinoma. Clin. Cancer Res., **13:** 721s, 2007
269. Fridlender, Z. G., Sun, J., Singhal, S. et al.: Chemotherapy delivered after viral immunogene therapy augments antitumor efficacy via multiple immune-mediated mechanisms. Mol. Ther., **18:** 1947, 2010
270. Kao, J., Ko, E. C., Eisenstein, S. et al.: Targeting immune suppressing myeloid-derived suppressor cells in oncology. Crit. Rev. Oncol. Hematol., **77:** 12, 2011
271. Ko, J. S., Zea, A. H., Rini, B. I. et al.: Sunitinib mediates reversal of myeloid-derived suppressor cell accumulation in renal cell carcinoma patients. Clin. Cancer Res., **15:** 2148, 2009
272. Najjar, Y. G., Finke, J. H.: Clinical perspectives on targeting of myeloid derived suppressor cells in the treatment of cancer. Front. Oncol., **3:** 49, 2013
273. Xia, S., Sha, H., Yang, L. et al.: Gr-1+ CD11b+ myeloid-derived suppressor cells suppress inflammation and promote insulin sensitivity in obesity. J. Biol. Chem., **286:** 23591, 2011
274. Matsuzaki, J., Tsuji, T., Chamoto, K. et al.: Successful elimination of memory-type CD8+ T cell subsets by the administration of anti-Gr-1 monoclonal antibody in vivo. Cell. Immunol., **224:** 98, 2003
275. Dalod, M., Salazar-Mather, T. P., Malmgaard, L. et al.: Interferon alpha/beta and interleukin 12 responses to viral infections: pathways regulating dendritic cell cytokine expression in vivo. J. Exp. Med., **195:** 517, 2002
276. Vincent, J., Mignot, G., Chalmin, F. et al.: 5-Fluorouracil selectively kills tumor-associated myeloid-derived suppressor cells resulting in enhanced T cell-dependent antitumor immunity. Cancer Res., **70:** 3052, 2010
277. Mozaffari, F., Lindemalm, C., Choudhury, A. et al.: Systemic immune effects of adjuvant chemotherapy with 5-fluorouracil, epirubicin and cyclophosphamide and/or radiotherapy in breast cancer: a longitudinal study. Cancer Immunol. Immunother., **58:** 111, 2009
278. Mozaffari, F., Lindemalm, C., Choudhury, A. et al.: NK-cell and T-cell functions in patients with breast cancer: effects of surgery and adjuvant chemo- and radiotherapy. Br. J. Cancer, **97:** 105, 2007
279. Griffith, T. S., Stokes, B., Kucaba, T. A. et al.: TRAIL gene therapy: from preclinical development to clinical application. Current gene therapy, **9:** 9, 2009
280. Kusmartsev, S., Eruslanov, E., Kubler, H. et al.: Oxidative stress regulates expression of VEGFR1 in myeloid cells: link to tumor-induced immune suppression in renal cell carcinoma. J. Immunol., **181:** 346, 2008

281. Rocha, F. G., Chaves, K. C., Chammas, R. et al.: Endostatin gene therapy enhances the efficacy of IL-2 in suppressing metastatic renal cell carcinoma in mice. Cancer Immunol. Immunother., **59:** 1357, 2010
282. Gabrilovich, D. I., Bronte, V., Chen, S. H. et al.: The terminology issue for myeloid-derived suppressor cells. Cancer Res., **67:** 425; author reply 426, 2007
283. Youn, J. I., Nagaraj, S., Collazo, M. et al.: Subsets of myeloid-derived suppressor cells in tumor-bearing mice. J. Immunol., **181:** 5791, 2008
284. Kusmartsev, S., Gabrilovich, D. I.: STAT1 signaling regulates tumor-associated macrophage-mediated T cell deletion. J. Immunol., **174:** 4880, 2005
285. Greifenberg, V., Ribechini, E., Rossner, S. et al.: Myeloid-derived suppressor cell activation by combined LPS and IFN-gamma treatment impairs DC development. Eur. J. Immunol., **39:** 2865, 2009
286. Ueha, S., Shand, F. H., Matsushima, K.: Myeloid cell population dynamics in healthy and tumor-bearing mice. Int. Immunopharmacol., **11:** 783, 2011
287. Messai, Y., Noman, M. Z., Derouiche, A. et al.: Cytokeratin 18 expression pattern correlates with renal cell carcinoma progression: relationship with Snail. Int. J. Oncol., **36:** 1145, 2010
288. Shirota, Y., Shirota, H., Klinman, D. M.: Intratumoral injection of CpG oligonucleotides induces the differentiation and reduces the immunosuppressive activity of myeloid-derived suppressor cells. J. Immunol., **188:** 1592, 2012
289. Bunt, S. K., Yang, L., Sinha, P. et al.: Reduced inflammation in the tumor microenvironment delays the accumulation of myeloid-derived suppressor cells and limits tumor progression. Cancer Res., **67:** 10019, 2007
290. Ouchi, N., Parker, J. L., Lugus, J. J. et al.: Adipokines in inflammation and metabolic disease. Nature Rev. Immunol., **11:** 85, 2011
291. Okwan-Duodu, D., Umpierrez, G. E., Brawley, O. W. et al.: Obesity-driven inflammation and cancer risk: role of myeloid derived suppressor cells and alternately activated macrophages. Am. J. Cancer Res., **3:** 21, 2013
292. Litterman, A. J., Zellmer, D. M., Grinnen, K. L. et al.: Profound impairment of adaptive immune responses by alkylating chemotherapy. J. Immunol., **190:** 6259, 2013
293. Zoglmeier, C., Bauer, H., Norenberg, D. et al.: CpG blocks immunosuppression by myeloid-derived suppressor cells in tumor-bearing mice. Clin. Cancer Res., **17:** 1765, 2011
294. Sato, M., Suemori, H., Hata, N. et al.: Distinct and essential roles of transcription factors IRF-3 and IRF-7 in response to viruses for IFN-alpha/beta gene induction. Immunity, **13:** 539, 2000
295. Taniguchi, T., Ogasawara, K., Takaoka, A. et al.: IRF family of transcription factors as regulators of host defense. Annu Rev Immunol, **19:** 623, 2001
296. Epardaud, M., Elpek, K. G., Rubinstein, M. P. et al.: Interleukin-15/Interleukin-15Rα Complexes Promote Destruction of Established Tumors by Reviving Tumor-Resident CD8+ T Cells. 2008

297. Staunton, D. E., Dustin, M. L., Springer, T. A.: Functional cloning of ICAM-2, a cell adhesion ligand for LFA-1 homologous to ICAM-1. Nature, **339:** 61, 1989
298. Oppenheimer-Marks, N., Davis, L. S., Bogue, D. T. et al.: Differential utilization of ICAM-1 and VCAM-1 during the adhesion and transendothelial migration of human T lymphocytes. J Immunol, **147:** 2913, 1991
299. El Kebir, D., Jozsef, L., Pan, W. et al.: Bacterial DNA activates endothelial cells and promotes neutrophil adherence through TLR9 signaling. J Immunol, **182:** 4386, 2009
300. Zhu, P., Liu, X., Treml, L. S. et al.: Mechanism and regulatory function of CpG signaling via scavenger receptor B1 in primary B cells. J Biol Chem, **284:** 22878, 2009
301. Horiguchi, A., Sumitomo, M., Asakuma, J. et al.: Increased serum leptin levels and over expression of leptin receptors are associated with the invasion and progression of renal cell carcinoma. J Urol, **176:** 1631, 2006
302. Horiguchi, A., Sumitomo, M., Asakuma, J. et al.: Leptin promotes invasiveness of murine renal cancer cells via extracellular signal-regulated kinases and rho dependent pathway. J Urol, **176:** 1636, 2006
303. Li, L., Gao, Y., Zhang, L. L. et al.: Concomitant activation of the JAK/STAT3 and ERK1/2 signaling is involved in leptin-mediated proliferation of renal cell carcinoma Caki-2 cells. Cancer Biol Ther, **7:** 1787, 2008
304. Chen, C., Chang, Y. C., Liu, C. L. et al.: Leptin induces proliferation and anti-apoptosis in human hepatocarcinoma cells by up-regulating cyclin D1 and down-regulating Bax via a Janus kinase 2-linked pathway. Endocr Relat Cancer, **14:** 513, 2007
305. Jaworski, K., Ahmadian, M., Duncan, R. E. et al.: AdPLA ablation increases lipolysis and prevents obesity induced by high-fat feeding or leptin deficiency. Nature Medicine, **15:** 159, 2009
306. Chell, S., Kaidi, A., Williams, A. C. et al.: Mediators of PGE2 synthesis and signalling downstream of COX-2 represent potential targets for the prevention/treatment of colorectal cancer. Biochim Biophys Acta, **1766:** 104, 2006
307. Greenhough, A., Smartt, H. J., Moore, A. E. et al.: The COX-2/PGE2 pathway: key roles in the hallmarks of cancer and adaptation to the tumour microenvironment. Carcinogenesis, **30:** 377, 2009
308. Sinha, P., Clements, V. K., Fulton, A. M. et al.: Prostaglandin E2 promotes tumor progression by inducing myeloid-derived suppressor cells. Cancer Res, **67:** 4507, 2007
309. Hsieh, P. S., Lu, K. C., Chiang, C. F. et al.: Suppressive effect of COX2 inhibitor on the progression of adipose inflammation in high-fat-induced obese rats. European Journal of Clinical Investigation, **40:** 164, 2010
310. Tu, S., Bhagat, G., Cui, G. et al.: Overexpression of Interleukin-1β Induces Gastric Inflammation and Cancer and Mobilizes Myeloid-Derived Suppressor Cells in Mice. Cancer Cell, **14:** 408, 2008

311. Fridlender, Z. G., Buchlis, G., Kapoor, V. et al.: CCL2 blockade augments cancer immunotherapy. Cancer Res, **70:** 109
312. Ostrand-Rosenberg, S., Sinha, P.: Myeloid-derived suppressor cells: linking inflammation and cancer. J Immunol, **182:** 4499, 2009